POLITECNICO
MILANO 1863

SCUOLA DI INGEGNERIA INDUSTRIALE
E DELL'INFORMAZIONE

EXECUTIVE SUMMARY OF THE THESIS

Analysis of Somatosensory Evoked Potentials in simultaneous EEG and SEEG recordings

TESI MAGISTRALE IN BIOMEDICAL ENGINEERING – INGEGNERIA BIOMEDICA

AUTHOR: ANGELOS THEOCHARIS

ADVISOR: PROF ANNA MARIA BIANCHI

ACADEMIC YEAR: 2020-2021

1. Introduction

The somatosensory system is a complex system that allows us to perceive changes in the internal or external environment by employing several structures in the peripheral and central nervous system. A successful non-invasive method to study the functional characteristics of the somatosensory system with millisecond precision is the Electroencephalography (EEG). To date, EEG has been successfully used in various applications such as diagnosis of brain diseases including Parkinson, Alzheimer's and epilepsy. Despite the high-temporal precision and the non-invasiveness of EEG, the signals picked by the EEG cap placed on the scalp of the subject typically suffer from a spatial blurring effect due to the propagation of the cortical activity through several layers of the outer brain and scalp [1]. As a consequence, the low spatial resolution of EEG prevents clinicians from obtaining a holistic picture of somatosensory processing. On the other hand, cortical and subcortical activity can be directly recorded using invasive methods such as stereotactic EEG (SEEG) where intracerebral electrodes are implanted in the brain. However, SEEG recordigns are only available when subjects are undergoing pre-surgical evaluation for identifying an ictal zone [2].

In this project, simultaneous high-density EEG (HD-EEG) and SEEG recordings from eight drug-resistant epileptic patients following median nerve stimulation were used to enhance our understanding about somatosensory processing. To the best of our knowledge, an analysis on simultaneous HD-EEG and SEEG recordings of somatosensory evoked responses has never been performed. Since intracranial recordings are rarely available, the ultimate goal of this project is to reveal a mapping between the intracranial (SEEG) and the extracranial space (EEG) which is typically the only available diagnostic tool for clinicians.

Recent research on SEEG recordings from median nerve stimulation showed that certain areas involved in the distributed somatosensory processing exhibit distinct behaviour, namely early/short (i.e., phasic) and late/long (i.e., tonic) responses [3]. In this thesis we show that similar phasic and tonic behaviour is reflected in scalp EEG recordings, thus, enhancing our understanding of somatosensory processing. The findings of this thesis could assist practitioners to infer information about the intracranial activity without the need of intracranial recordings, advancing clinical practice in diagnosis and treatment of conditions related to somatosensory processing including epilepsy, Parkinson's disease and dystonia.

Subject	Age	Sex	Laterality of electrodes	Epileptic zone	Pharmacology
sub-01	31	F	left	n/a	brivaracetam, perampanel
sub-02	25	F	right	right operculum	levetiracetam, topiramate
sub-03	44	M	left	left supramarginal, opercular	lacosamide, valproate, topiramate
sub-04	39	F	left	left mesial temporal	carbamazepine, clobazam, levetiracetam
sub-05	31	F	left	left parietal cingulum	carbamazepine, lamotrigine
sub-06	35	M	left	left mesial temporal	levetiracetam, carbamazepine, lacosamide
sub-07	23	F	right	right operculum	valproate, lacosamide
sub-08	37	M	right	right operculum, insula	lacosamide, oxcarbazepine

Table 1.Demographic and clinical information of the patients.

2. Experimental Setup

2.1 Participants

Simultaneous EEG and SEEG recordings were obtained from 8 patients in the Niguarda Hospital, Milan, Italy. All subjects were patients undergoing intracranial monitoring for pre-surgical evaluation of drug-resistant epilepsy and provided their Informed Consent before participating (Table 1). The study was approved by the local Ethical Committee (protocol number: 463-092018, Niguarda Hospital, Milan, Italy) and it was carried out in accordance with the Declaration of Helsinki.

2.2 Median nerve stimulation

The median nerve was stimulated opposite to the hemisphere with the implanted electrodes at the wrist, using constant-current pulses of 0.2 ms duration at a rate of 1 Hz. The intensity and the exact location of the stimulation was determined when an observable thumb twitch was obtained. The motor threshold ranged from 3.2 to 5.8 mA while the stimulation intensity was set to 10% above the motor threshold [3]. More information about the number of trials and the intensity of the stimulation for each session is given in Table 2. Figure 1 illustrates the experimental setup with the co-registered HD-EEG and SEEG acquisition system as well as the trigger signal used to synchronize the recording systems. The localization of the intracranial and extracranial electrodes was also performed to enable spatial co-registration.

2.3 Electrode Localization

The location of implanted SEEG electrodes was solely determined by the clinical necessity for identifying the epileptogenic zone. The SEEG planning was supported by individual brain MRI (Achieva 1.5 T, Philips Healthcare) and CT (O-arm 1000 system, Medtronic) recordings. The investigated hemisphere/s as well as the location and number of explored sites were determined based on non-invasive clinical assessment while the duration of the SEEG investigation was determined only by the clinical needs. Placement of the SEEG electrodes was carried out under general anaesthesia using a robotized passive tool-holder (Neuromate, Renishaw Mayfield SA). The implanted electrode location was assessed using pre-implant MRI and post-implant CT (O-arm 1000 system, Medtronic).
The single lead position was further assessed with respect to the MRI using Freesurfer, 3D Slicer and SEEG assistant software. In cases of mismatch between the pre-implant MRI and the EEG digitization MRI, the contacts position were transformed from the SEEG to the EEG space using affine transformation in the ANTs software.

Session	Subject	Stimulation side	Stimulation intensity (mA)	No. SEEG/ HD-EEG channels	No. of trials
ses-01	sub-01	right	7	195/256	1000
ses-02		left	4		500
ses-03	sub-02	left	8	239/256	974
ses-04	sub-03	right	7	214/256	960
ses-05	sub-04	right	9	201/256	1000
ses-06		left	9		500
ses-07	sub-05	right	8	214/256	998
ses-08	sub-06	right	5	157/256	1140
ses-09	sub-07	right	8	182/256	214
ses-10		left	8		363
ses-11	sub-08	left	7	178/256	1000

Table 2. Information about the individual sessions.

2.4 Simultaneous Recordings

The simultaneous recordings were performed using a 256-channel EEG cap (Geodesic Sensor Net; HydroCel CleanLeads). The whole procedure was carried out using the sterile technique to minimize and prevent infections. The EEG signals were sampled at 1000 Hz with an EGI NA-400 amplifier (Electrical Geodesics, Inc; Oregon, USA). A SofTaxicOptic system (EMS s.r.l., Bologna, Italy) was used to digitize the spatial locations of the EEG electrodes and anatomical fiducials, coregistered with a pre-implant MRI (Achieva 1.5T, Philips Healthcare). The recorded signals were referenced to the Cz electrode and were downsampled to 500 Hz to improve computational efficiency while still retaining enough samples to capture the signal dynamics.
At the same time, the SEEG recordings were performed using a variable number of platinum–iridium semi flexible multi-contact intracranial electrodes (Microdeep intracerebral electrodes, D08, Dixi Medical, or Depth Electrodes Range 2069, Alcis). The SEEG signals were acquired with a Neurofax EEG-1100 (Nihon Kohden System), sampled at 1000 Hz sampling frequency. The SEEG recordings were then downsampled to 500 Hz to reduce the computational cost. The intracranial reference was selected by clinicians using both patient-specific anatomical and functional criteria and was computed as the average of two adjacent white matter leads. The implanted electrodes had a diameter of 0.8 mm and contact length of 2 mm. The number of contacts ranged from 8-18 per electrode with an intercontact distance of 1.5 mm. The implantations for all 8 subjects were unilateral since clinical evidence generally indicates which hemisphere is responsible for generating the seizures. More information about the number of EEG and SEEG channels, trials and laterality of the stimulation of the simultaneous recordings can be found in Table 2.

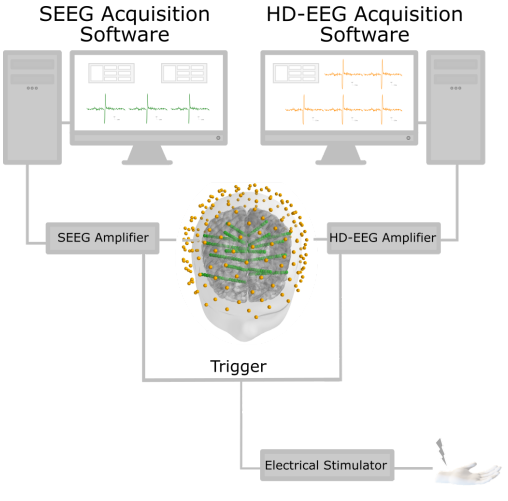

Figure 1. The simultaneous HD-EEG and SEEG acquisition system to record somatosensory evoked responses following median nerve stimulation (adjusted from [4]).

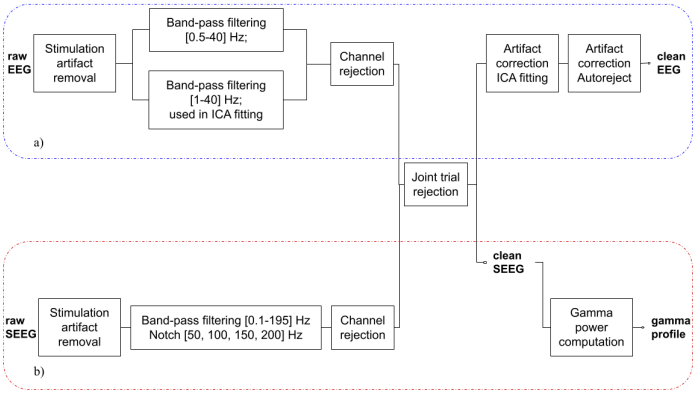

Figure 2. Proposed preprocessing pipeline for a) EEG and b) SEEG signals. The trial rejection step was performed through a joint analysis of the synchronized EEG and SEEG trials.

3. Method

The simultaneous HD-EEG and SEEG data was processed using custom-built functions in Python using the MNE package [5]. The proposed pre-processing pipeline (Fig. 2) involved both automatic and manual processing blocks to ensure minimum bias while at the same time visual inspection ensured that the automatic processes did not corrupt or distort the data. The stages of the pre-processing workflow consisted of stimulation artifact removal, band-pass filtering, bad channel/ trial rejection and artifact correction through Independent Component Analysis (ICA) and Autoreject.

The synchronization of the simultaneous recordings was achieved using information from the stimulation trigger signal. This trigger signal allows epoching and averaging to obtain evoked potentials (EPs) from the synchronized HD-EEG and SEEG recordings. One-minute long epochs were generated and split into -300 ms pre-stimulus and 700 ms post-stimulus intervals. The epochs were then baseline corrected using the mean of the pre-stimulus activity to remove DC offsets.

Following preprocessing, the HD-EEG signals were used for source reconstruction to reveal the location, and intensities of the current sources that produced the recorded activity. Popular distributed inverse modelling approaches (i.e., where the number of sources exceeds the number of EEG sensors) were investigated including minimum norm estimate (MNE), standardized and exact low-resolution electromagnetic tomography (sLORETA/eLORETA) as well as dynamic statistical parametric mapping (dSPM). These methods were considered first due to their wide and successful use in the scientific literature but also due to the fact that the somatosensory processing is performed by distributed neural networks. The optimal source modelling approach for the given data was selected using a grid search optimization of the explained variance and visual inspection of the time-course of the estimated sources. Time-frequency analysis using short-time Fourier Transform (STFT) of the activity of the estimated sources was performed to reveal the spectrotemporal dynamics of the estimated activity.

Given the potential similarities between intra- and extracranial EPs following median nerve stimulation, the possibility to find a mapping between intracranial and extracranial space was investigated. Since intracranial recordings are rarely available, obtaining a mapping from extracranial to intracranial space can enable better diagnosis and treatment of diseases related to somatosensation even in cases where intracranial invasive recordings are not possible. Therefore, the multivariate temporal response function (mTFR) was used to predict the intracranial activity based on HD-EEG recordings. The acquired mapping allowed us to predict the neural response at the SEEG level given the HD-EEG enabling the analysis of the underlying decoding and encoding mechanisms, respectively.

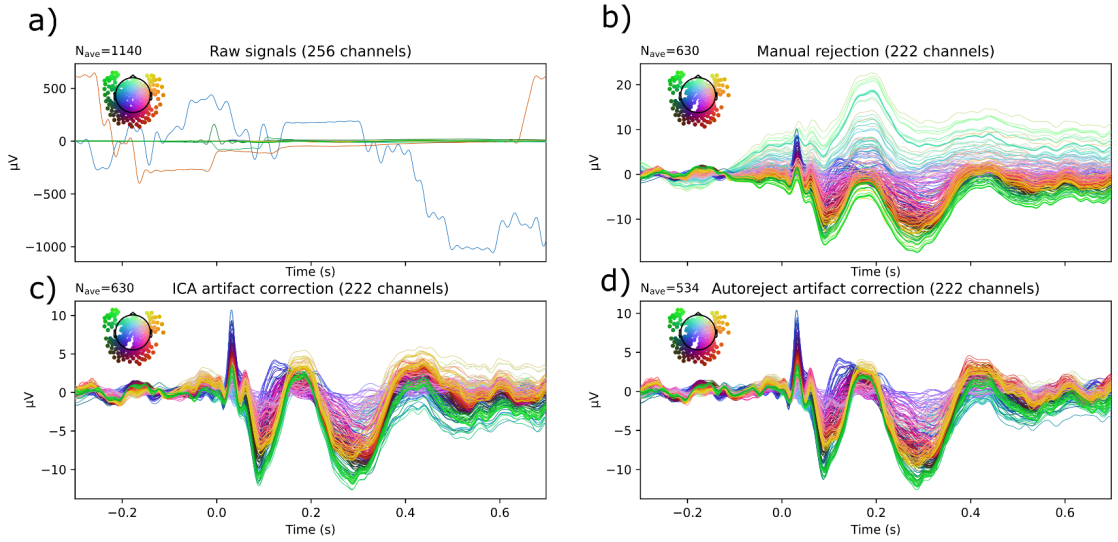

Figure 3. Output of each preprocessing stage for EEG signals of sub-06; (a) raw EEG signals, (b) after filtering and manual rejection, (c) after ICA-based artifact correction, and (d) after Autoreject-based trial correction.

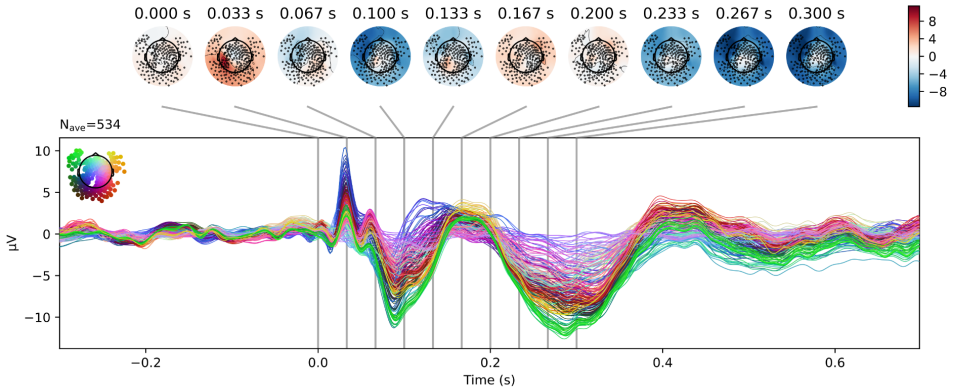

Figure 4. Topographic map of the somatosensory evoked potentials after preprocessing from patient sub-06.

4. Results and Discussion

In summary, the following hypotheses were tested as part of this thesis:

- Reconstructed signals from source modelling on the EEG recordings exhibit phasic and tonic behaviour depending on the location of the source (e.g., SI vs SII).
- Intracranial tonic activity can be predicted by extracranial recordings. The predicted intracranial activity is compared against the groundtruth activity provided by the SEEG recordings.

4.1 Preprocessing pipeline for simultaneous EEG and SEEG signals

The proposed preprocessing pipeline can effectively improve the SNR of the SEPs and intracranial SEPs as it can be shown in Fig. 3 where the output of the major processing stages are presented for two patients. Regarding the EEG signals, the first stage, i.e., manual removal of bad channels and filtering successfully revealed the typical SEP waveform that was before hindered due to broken or noisy channels. Artifacts such as the high voltage eye blink contributions were then corrected by ICA and Autoreject. Figure 4 shows a topographic map of the activation arising from the median nerve stimulation as recorded from the EEG channels for a patient in the first 300 ms after the stimulation. The arrival of the somatosensory signal to the contralateral SI area is visible at around 30 ms, while the bilateral activation of the posterior parietal cortex and the primary somatosensory cortex (SMI) was observed after 50 ms.

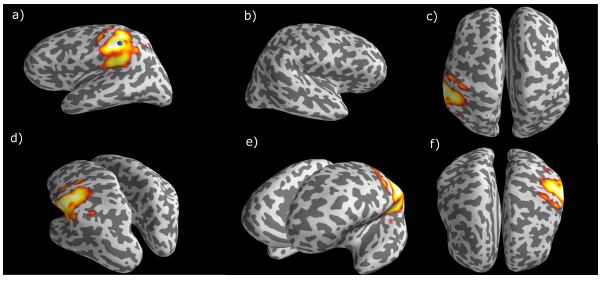

Figure 5. Different views of the activation maps at around 30 ms following right median nerve stimulation: a) right and b) left lateral, c) axial, d) parietal, e) frontal, and f) dorsal.

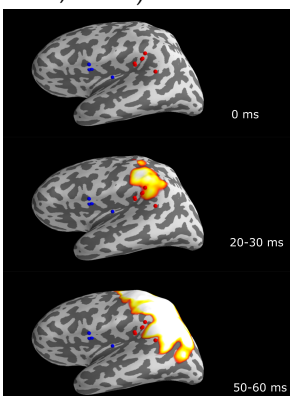

Figure 6. Activation maps following right median nerve stimulation at time instances: 0 ms, 20-30 ms and 50-60 ms.

4.2 Localization of somatosensory processing

Figure 5 shows the activation maps from different views of the brain. Since right median nerve stimulation was performed for this subject, the source modelling accurately reconstructs activity on the left hemisphere near the somatosensory cortex at around 30ms. The graphical user interface (GUI) in Fig 6 provides the source modelling results with superimposed phasic and tonic electrodes, color-coded with red and blue, respectively.

4.3 Reconstructed sources exhibit distinct characteristics

Figure 7 shows the results of the TF analysis which proves that somatosensory areas exhibit phasic and tonic, respectively, as seen from the EEG recordings. This finding of the thesis suggests that EEG contains information about intracranial activity and may assist practitioners to infer information about the neural dynamics which up to date were only observable with intracranial EEG. On the one hand the intracranial signals were clustered into phasic and tonic to be used as ground truth to support our hypothesis based on the algorithm in [3]. On the other hand, TF analysis of the EEG-based reconstructed sources were computed for the locations of the phasic and tonic sources. The TF analysis results agreed with the groundtruth SEEG data

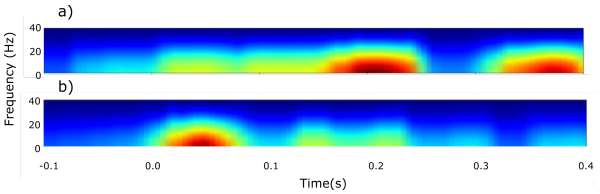

Figure 7. Time-frequency analysis of a) tonic and b) phasic reconstructed sources.

4.4 Prediction of intracranial activity

After having shown that the time-frequency distribution of the reconstructed sources share similarities with the SEEG ground truth signals, the intracranial tonic activity was predicted using the multivariate temporal response function (mTFR) based on extracranial HD-EEG recordings. Figure 8 shows the preliminary results of the prediction for 4 patients and 4 different tonic electrodes.

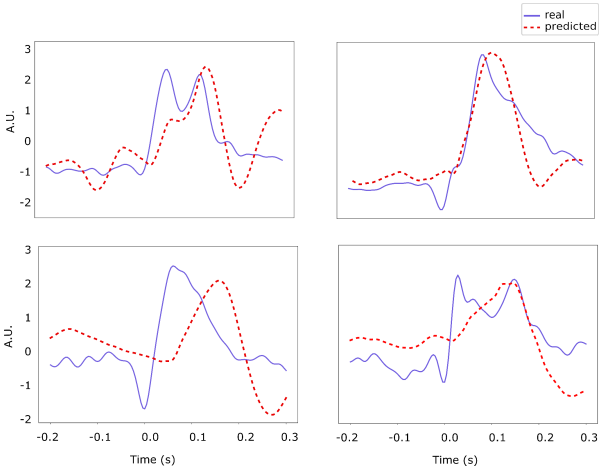

Figure 8. Prediction of intracranial tonic activity based on EEG recordings from 4 subjects.

5. Conclusion

In this thesis, an extensive literature review on state-of-the art findings related to somatosensory evoked responses following median nerve stimulation was performed (*see* Chapter 3 of thesis). Recommendations for future SEP studies using simultaneous EEG and SEEG recordings were provided (*see* Section 5.1 of thesis). A custom-designed preprocessing pipeline was developed to clean the simultaneous HD-EEG and SEEG recordings from 8 epileptic patients (*see* Section 4.6 and Section 5.2 of thesis). Given the clean HD-EEG data, source modelling was implemented to reconstruct the sources (*see* Section 5.4 of thesis). Custom-built scripts were developed to evaluate results of the source modeling and showcase that reconstructed sources from EEG recordings exhibit distinct

phasic and tonic behaviour which is area-dependent (*see* Section 5.3-5.5 of thesis). Lastly, preliminary results show that intracranial activity can be predicted based on HD-EEG recordings (*see* Section 5.6)

The results of this work have led to a scientific poster, titled '*Scalp EEG prediction of intracranial high-frequency responses to median nerve stimulation: insights from simultaneous recordings*', Ezequiel Mikulan, Angelos Theocharis, Simone Russo, Flavia Maria Zauli, Ivana Sartori, Sara Parmigiani, Simone Sarasso, Maria Del Vecchio, Pietro Avanzini, Andrea Pigorini, Poster presented at the 4th International Brain Stimulation Conference. Charleston, USA.

6. Reference

[1] G. Buzsáki, C. A. Anastassiou, and C. Koch, "The origin of extracellular fields and currents — EEG, ECoG, LFP and spikes," *Nat. Rev. Neurosci.*, vol. 13, no. 6, pp. 407–420, Jun. 2012, doi: 10.1038/nrn3241.

[2] F. Cardinale *et al.*, "Stereoelectroencephalography: Surgical methodology, safety, and stereotactic application accuracy in 500 procedures," *Neurosurgery*, vol. 72, no. 3, pp. 353–366, Mar. 2013, doi: 10.1227/NEU.0b013e31827d1161.

[3] P. Avanzini *et al.*, "Four-dimensional maps of the human somatosensory system," *Proc. Natl. Acad. Sci.*, vol. 113, no. 13, p. E1936, Mar. 2016, doi: 10.1073/pnas.1601889113.

[4] E. Mikulan *et al.*, "Simultaneous human intracerebral stimulation and HD-EEG, ground-truth for source localization methods," *Sci. Data*, vol. 7, no. 1, pp. 1–8, Dec. 2020, doi: 10.1038/s41597-020-0467-x.

[5] A. Gramfort *et al.*, "MNE software for processing MEG and EEG data," *NeuroImage*, vol. 86, pp. 446–460, 2014.

POLITECNICO
MILANO 1863

SCUOLA DI INGEGNERIA INDUSTRIALE
E DELL'INFORMAZIONE

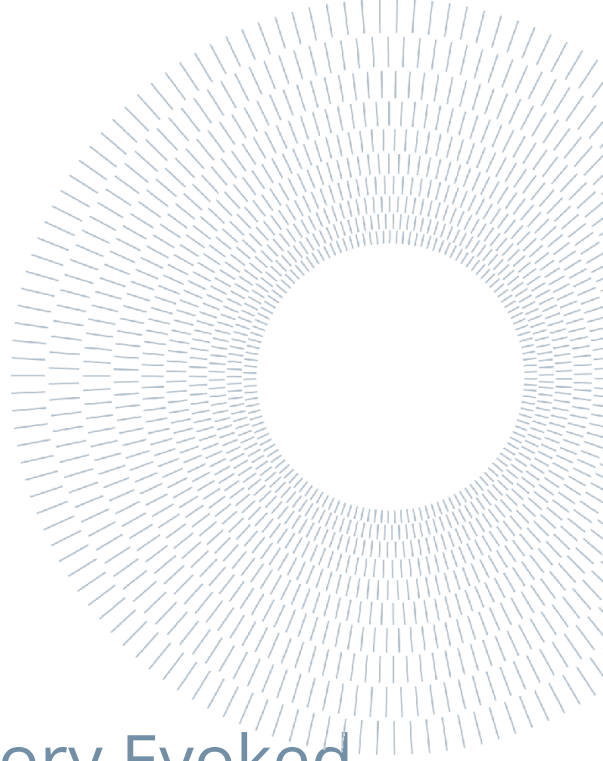

Analysis of Somatosensory Evoked Potentials in simultaneous EEG and SEEG recordings

TESI DI LAUREA MAGISTRALE IN

BIOMEDICAL ENGINEERING-INGEGNERIA BIOMEDICA

Author: **Angelos Theocharis**

Student ID:	942317
Advisor:	Prof. Anna Maria Bianchi; Dr. Andrea Pigorini
Co-advisor:	Dr. Ezequiel Mikulan, Dr. Stefania Coelli
Academic Year:	2020-2021 AA

Abstract

The somatosensory system is a complex system that allows us to perceive changes in the internal or external environment by employing several structures in the peripheral and central nervous system. A successful non-invasive method to study the functional characteristics of the somatosensory system with millisecond precision is the Electroencephalography (EEG). To date, EEG has been successfully used in various applications such as diagnosis of brain diseases including Parkinson, Alzheimer's and epilepsy. Despite the high-temporal precision and the non-invasiveness of EEG, the signals picked by the EEG cap placed on the scalp of the subject typically suffer from a spatial blurring effect due to the propagation of the cortical activity through several layers of the outer brain and scalp. As a consequence, the low spatial resolution of EEG prevents clinicians from obtaining a holistic picture of somatosensory processing. On the other hand, cortical and subcortical activity can be directly recorded using invasive methods such as stereotactic EEG (SEEG) where intracerebral electrodes are implanted in the brain. However, SEEG recordigns are only available when subjects are undergoing pre-surgical evaluation for identifying an ictal zone.

In this project, simultaneous high-density EEG (HD-EEG) and SEEG recordings from eight drug-resistant epileptic patients following median nerve stimulation protocol were used to enhance our understanding about somatosensory processing. To the best of our knowledge, an analysis on simultaneous HD-EEG and SEEG recordings of somatosensory evoked responses has never been performed. Since intracranial recordings are rarely available, the ultimate goal of this project is to reveal a mapping between the intracranial (SEEG) and the extracranial space (EEG) which is typically the only available diagnostic tool for clinicians.

Recent research on SEEG recordings from median nerve stimulation showed that certain areas involved in the distributed somatosensory processing exhibit distinct behaviour, namely early/short (i.e., phasic) and late/long (i.e., tonic) responses. In this thesis we show that the similar phasic and tonic behaviour is reflected in scalp EEG recordings, thus, enhancing our understanding about somatosensory processing. The findings of this thesis could assist practitioners to infer information about the neural dynamics which up to date were only observable with intracranial EEG, advancing clinical practice in diagnosis and treatment of conditions related to somatosensory processing including epilepsy, Parkinson's disease and dystonia.

Key words: somatosensory evoked potentials, EEG, SEEG, simultaneous analysis

Abstract (IT)

Il sistema somatosensoriale è un sistema complesso che ci permette di percepire i cambiamenti nell'ambiente interno o esterno utilizzando diverse strutture del sistema nervoso periferico e centrale. Un metodo non invasivo di successo per studiare le caratteristiche funzionali del sistema somatosensoriale con precisione al millisecondo è l'elettroencefalografia (EEG). Ad oggi, l'EEG è stato utilizzato con successo in varie applicazioni come la diagnosi di malattie cerebrali tra cui Parkinson, Alzheimer ed epilessia. Nonostante l'alta precisione temporale e la non invasività dell'EEG, i segnali raccolti dalla cuffia EEG posta sul cuoio capelluto del soggetto soffrono tipicamente di un effetto di sfocatura spaziale dovuto alla propagazione dell'attività corticale attraverso diversi strati del cervello esterno e del cuoio capelluto. Di conseguenza, la bassa risoluzione spaziale dell'EEG impedisce ai clinici di ottenere un quadro olistico dell'elaborazione somatosensoriale. D'altra parte, l'attività corticale e sottocorticale può essere registrata direttamente utilizzando metodi invasivi come l'EEG stereotassico (SEEG), dove gli elettrodi intracerebrali sono impiantati nel cervello. Tuttavia, le registrazioni SEEG sono disponibili solo quando i soggetti sono sottoposti a valutazione pre-chirurgica per identificare una zona ictale.

In questo progetto, le registrazioni simultanee ad alta densità EEG (HD-EEG) e SEEG da otto pazienti epilettici resistenti ai farmaci dopo il protocollo di stimolazione del nervo mediano sono stati utilizzati per migliorare la nostra comprensione circa l'elaborazione somatosensoriale. Per quanto ne sappiamo, non è mai stata eseguita un'analisi sulle registrazioni HD-EEG e SEEG simultanee delle risposte evocate somatosensoriali. Poiché le registrazioni intracraniche sono raramente disponibili, l'obiettivo finale di questo progetto è quello di rivelare una

mappatura tra lo spazio intracranico (SEEG) e quello extracranico (EEG) che è tipicamente l'unico strumento diagnostico disponibile per i clinici.

Una recente ricerca sulle registrazioni SEEG dalla stimolazione del nervo mediano ha mostrato che alcune aree coinvolte nell'elaborazione somatosensoriale distribuita esibiscono un comportamento distinto, ovvero risposte precoci/brevi (cioè fasiche) e tardive/lunghe (cioè toniche). In questa tesi dimostriamo che il simile comportamento fasico e tonico si riflette nelle registrazioni EEG del cuoio capelluto, migliorando così la nostra comprensione dell'elaborazione somatosensoriale. I risultati di questa tesi potrebbero aiutare i professionisti a dedurre informazioni sull'attività intracranica senza la necessità di registrazioni intracraniche, facendo progredire la pratica clinica nella diagnosi e nel trattamento delle condizioni legate all'elaborazione somatosensoriale, tra cui l'epilessia, il morbo di Parkinson e la distonia.

Parole chiave: potenziali evocati somatosensoriali, EEG, SEEG, analisi simultanea

My Contribution

- Extensive literature review on state-of-the art findings related to somatosensory evoked responses following median nerve stimulation (*see* Chapter 3).
- Recommendation for future somatosensory evoked potentials studies using simultaneous EEG and SEEG recordings (*see* Section 5.1)
- Development of a preprocessing pipeline to clean simultaneous EEG and SEEG recordings from 8 epileptic patients (*see* Section 4.6 and Section 5.2).
- Source modelling implementation to reconstruct signal sources from HD-EEG signals for the available data (*see* Section 5.4).
- Development of custom-built scripts to evaluate results of source modelling (*see* Section 5.3-5.5).
- Showcase that reconstructed sources from EEG recordings exhibit distinct phasic and tonic behaviour which is area-dependent (*see* Section 5.5).
- Prediction of intracranial activity based on EEG recordings (*see* Section 5.6)
- Publication: '*Scalp EEG prediction of intracranial high-frequency responses to median nerve stimulation: insights from simultaneous recordings'* (2021). Ezequiel Mikulan, Angelos Theocharis, Simone Russo, Flavia Maria Zauli, Ivana Sartori, Sara Parmigiani, Simone Sarasso, Maria Del Vecchio, Pietro Avanzini, Andrea Pigorini. Poster presented at the 4th International Brain Stimulation Conference. Charleston, USA

Acknowledgments

I would like to thank Prof Anna Maria Bianchi and Dr Stefania Coelli from the Department of Electronics, Information and Bioengineering of the Politecnico di Milano for their guidance and supervision throughout my master thesis. I would also like to express my gratitude to Dr Ezequiel Mikulan and Dr Andrea Pigorini from the Department of Biomedical and Clinical Sciences "L.Sacco" for their constant guidance, support and advice. Their knowledge and passion about neuroelectrophysiology have inspired me to pursue high-standard research with an inquiring mindset. Last but not least, I would like to thank my family for putting up with me during these years.

Table of Contents

1. Aim and Structure

Human sensation is at the core of life as it enables the experience of internal and external disturbances and establishes the communication channel between the environment and the human body. Among the complex sensory systems, somatosensation serves the conscious perception of changes in muscles, joints and the skin. These changes allow to quantify and localize touch, vibration, pain, and pressure by employing distributed neural networks in the brain [1]. Despite being a well studied system, there has been a continued interest in the clinical and scientific community to reveal the exact underlying mechanisms of the somatosensory system.

A successful method to study the functional characteristics of the somatosensory system at the millisecond scale has been the Electroencephalography (EEG). By placing electrodes on the scalp and along the processing pathway of somatic information one can study the temporal variations of neural processing when a somatosensory stimulus is presented. The ongoing brain activity tends to overmask the neural response due to the presented stimulus. To this end, multiple stimulations are typically performed to obtain evoked potentials. The advantage of repeated stimulations and multiple trials lies in the reduction of background neural activity through the averaging process. Despite early studies in the 1960s focusing on evoked responses originating from the healthy and diseased nervous system [2], there are still efforts to exploit the information provided by somatosensory evoked potentials in characterizing the different states of somatosensory neural processing.

More recently, stereotactic EEG (SEEG) has been used to study the underlying neural mechanisms involved in various conditions, such as epilepsy, and has also recently gained momentum in Brain-Computer Interface (BCI) applications.

Stereotactic surgery involves implanting electrodes in cortical and subcortical structures of the brain for the presurgical evaluation of epileptogenic areas in drug-resistant epileptic patients. This factor makes the SEEG recordings very rare and valuable as they provide information about the activity of cortical and subcortical areas with very precise spatial accuracy [3]. A recent SEEG study showed that some cortical and subcortical areas have an early and short response (i.e., phasic components) while others have a late and prolonged response (i.e., tonic components) following median nerve stimulation [4].

In this thesis project, simultaneous SEEG and high density EEG recordings are used to examine whether tonic and phasic responses can be observed from the extracranial electrodes and potentially reveal a mapping between the intra- and extracranial space.

1.1. Thesis Aim

The scope of this thesis is to investigate the relationship between brain activity recorded from intracranial and surface electrodes elicited by somatosensory stimuli. Scalp EEG has been extensively used to study the functional properties of the brain and has been successfully applied in early diagnosis of challenging brain diseases such as Alzheimer [5], [6], Parkinson [7], [8] and epilepsy [9], [10]. In addition, EEG research has shed light on mechanisms related to sleep, anaesthesia and sensory processing [11]. More specifically, EEG was used early in brain research to characterize the injuries in the somatosensory afferent signals through the use of evoked potentials (EPs). By stimulating specific areas of the human body in a systematic and controlled manner, evoked responses can be recorded from the brain that are reproducible across many trials. ERPs have also been used for characterizing the cognitive processes and assessing vigilance of patients [12].

Traditionally, EP studies involve recordings on the surface level through EEG, or less frequently intracranial recordings such as SEEG and Electrocorticography

(ECoG). Examining separately intracranial or extracranial recordings limits the integration of information that could potentially reveal a more complete picture of the somatosensory processing. To this end, this project aims at combining simultaneous recordings of high density EEG (HD-EEG) and SEEG to investigate the correlates of intra- and extracranial activity elicited by median nerve stimulation. To the best of our knowledge, somatosensory evoked potentials of median nerve stimulation have not been explored in simultaneous HD-EEG and SEEG modalities.

Somatosensory evoked potentials (SEPs) can be used to characterize lesions in the somatosensory pathway involving the spinal cord, brainstem, thalamus and cerebral cortex [13], and also the peripheral nerve functionality from thestimulatin site, to spinal cord. Electrodes placed on the scalp can capture changes in the electric field caused by synchronized postsynaptic potentials at the apical dendrites of pyramidal neurons [1]. At the same time, the availability of cortical and subcortical electrodes sampling somatosensory-related areas can provide precise temporal and spatial information about the arrival of brain signals from peripheral nerves. Studying EPs from two simultaneous and arguably complementary perspectives we expect that valuable insights can be gained in terms of the neural correlates of the somatosensory perception. Since intracranial recordings are rarely available, the ultimate goal of this project is to reveal a mapping between the intracranial (SEEG) and the extracranial space (EEG) which is typically the only available diagnostic tool for clinicians. The findings of this thesis will assist practitioners to infer information about the intracranial activity without the need of intracranial recordings, advancing clinical practice in diagnosis and treatment of conditions related to somatosensory processing including epilepsy, Parkinson's disease and dystonia.

1.2. Proposed methodology

Median nerve stimulation can be used to elicit a somatosensory response, which is traditionally recorded using EEG electrodes. Since EEG recordings have high temporal resolution but suffer from low spatial resolution, high density EEG (HD-EEG) can be used to enable a finer spatial resolution. Despite the improved spatial resolution of HD-EEG over EEG, the recorded activity reflects intracranial signals that have been propagated through the brain volume and the scalp thus limiting the achievable spatial resolution of extracranial recordings. On the other hand, SEEG can directly record signals from specific neural structures and offer high temporal precision with very good localization of the activity. Simultaneous HD-EEG and SEEG recordings, following median nerve stimulation, enable both recording the overall brain activity with high temporal precision and obtaining recordings from specific well-localized brain structures that are known to be involved in the somatosensory processing.

Preprocessing of the recordings is necessary to improve the quality and ensure synchronisation of the simultaneous recordings. Following preprocessing, EEG source modelling can be performed to reconstruct the intracranial sources of the activity recorded at the surface level [14], [15]. Source modelling involves modelling of the locations and intensities of signal generators, namely the inverse solution as well as how the generated signals propagate through the brain volume to the surface electrodes, namely the forward solution. By estimating the location and intensity of the signal generators (i.e. sources) that gave rise to the surface recordings, researchers have extensively used source modelling to associate active neural structures to a given mental state or experimental protocol (e.g. median nerve stimulation). Time-frequency analysis of the reconstructed source activity allows to further pinpoint the spectral characteristics of the neural activity in well-defined time windows [16].

Since intracranial recordings are rarely available, obtaining a mapping from extracranial to intracranial space can enhance clinical information related to somatosensation even in cases where intracranial invasive recordings are not available. Based on the extracranial recordings the intracranial activity can be reconstructed using the receptive field approach [17]. The acquired mapping allows to predict the neural response at the SEEG level given the EEG activity and vice versa, enabling the analysis of the underlying decoding and encoding mechanisms, respectively.

1.3. Thesis structure

The remainder of this thesis is organized as follows. Chapter 2 provides the theoretical framework on which the proposed methodology is based. The fundamental principles of EEG, SEEG and the known underlying mechanisms of somatosensory pathways are described. An overview of recent findings on somatosensory processing neural structures and characteristics is presented in Chapter 3. Chapter 4 provides a detailed description of the proposed methodology, documenting the methods employed to perform the experimental work. This chapter covers the pre-processing workflow designed for the simultaneous EEG and SEEG recordings as well as the implemented source modelling and intracranial activity prediction approach. In Chapter 5, the results are presented and discussed to provide insight on the neural correlates between intracranial and extracranial recordings. Important connections are drawn with the existing literature to position our findings in the most recent scientific context. Chapter 6 summarizes the outcomes of the thesis and provides recommendations for improvement and continuation of the work.

2. Introduction

This section provides information about the basic principles behind neurophysiological recordings, the somatosensory processing mechanisms and the state-of-the-art findings in median nerve stimulation studies. Firstly, electrophysiological recordings techniques such as EEG and SEEG are presented, followed by a review on the somatosensory pathways, involved areas and characteristics of somatosensory evoked potentials (SEPs). Lastly, the importance of SEPs in clinical practice is outlined and an extensive review on studies in median nerve-evoked somatosensory responses is provided.

2.1. Electrophysiological recordings

Recording neuronal activity is of great interest in clinical practice to assess brain activity, abnormalities and diagnose certain brain disorders. Various recording approaches have been proposed depending on the desirable level of analysis, starting from the intracellular ionic level to the broader extracranial level.

To begin with, the voltage clamp technique has been used in the seminal work by Hodgkin and Huxley to measure the conductance of the membrane and ionic currents [18]. In addition, the patch clamp technique can be used to characterize a single or a set of ionic channels [19]. The ability to measure neural activity at the cell level helps to understand the nature of ionic current, operation of ion channels and as a result the generation of action potentials. Importantly, the recording from patch electrodes allows for a high signal-to-noise ratio (SNR) and the most timely information on the intra-cellular processes. However, the required expertise and invasiveness of the method makes this technique very challenging.

Neuronal population activity measurements have been explored through the use of Electrocorticography (ECoG) and intracerebral electrodes [20]. ECoG provides

very good spatial resolution as the electrodes can be placed directly on small neuronal population or small neural networks. However, intracranial electrodes or cortical arrays have poor spatial sampling as they are refined to measure activity from the surrounding neural structures. To overcome the invasiveness of these approaches, one can focus on extracranial recording techniques such as Electroencephalography (EEG). EEG can be used to measure brain activity and obtain functional characteristics about the brain. One should note that extracranial recordings also suffer from poor spatial resolution as the brain signals have to propagate through several layers of tissue surrounding the cortex and are subjected to severe attenuations [21].

It is also worth mentioning that despite the advent of electrophysiological techniques, several neuroimaging approaches including Magnetoencephalography (MEG) and functional Magnetic Resonance Imaging (fMRI), have been decisive in understanding the structural and functional properties of the brain [22], [23].

2.1.1. Electroencephalography

Nerve cells comprise the dendrites, the nucleus and the axon while they are spatially confined in the extracellular space by the cell membrane. Although this lipid bi-layer structure acts as a protective shield, neurons need to communicate with their environment, thus, requiring the existence of certain channel structures that make the membrane semi-permeable. The neurons in the brain are constantly processing information from the environment and the homeostatic state of the body through these channels. The flow of information is achieved through complex electrochemical processes. More specifically, the intra- and extracellular space is abundant with ions including potassium, sodium, chloride and calcium. An arriving signal from other neurons will cause a cascade of ion movement while the preference of the ions to move between the intra and extracellular space is

dictated by balancing the effect of two mechanisms, namely, diffusion and electric field. Following the arrival of an incoming signal, high-frequency signals termed action potentials are generated. The high-frequency nature of these potentials imply that action potentials are very short signals (1-3 ms) that are rapidly dissipated in the extracellular space.

On the contrary, postsynaptic currents are relatively larger amplitude, longer-lasting signals (>5 ms) allowing for a stronger summation in the extracellular field, which makes them more visible in extracellular recordings [21]. Therefore, electrodes placed on the scalp can capture the changes in electric field caused by synchronized postsynaptic potentials at the apical dendrites of pyramidal neurons with millisecond precision [24]. Thanks to its non-invasive nature, EEG is widely applied in many clinical scenarios. However, EEG recordings typically suffer from low SNR caused by contributions of signals from different brain areas. Consequently, the spatial resolution of EEG is low but depends greatly on the available number of electrodes. In the 1950s, the 10-20 system was introduced to standardize the placement of the EEG cap with 21 electrodes. Three decades later, the standard was extended to the 10-10 system, increasing the number of electrodes to 74. In the early 2000s, the 10-5 system, which defines the positions and nomenclature of 345 locations on the head, was introduced. Nowadays, EEG studies widely use 64, 128 or even 256 electrodes to address the inherent low spatial sampling of extracranial recordings [25]. In fact, in this thesis work, a montage with 256 EEG electrodes is employed, also termed as High Density EEG (HD-EEG) [26].

Moreover, there are many practical considerations when recording EEG signals and have been studied in the literature. These considerations range from the electrode material and impedances, the cap placement and amplifiers to the referencing method. A very important aspect for clinicians is the reference method as it directly affects the polarity of the signals and the field localization [1]. EEG

interpretation is a very challenging task and the choice of reference can provide different interpretations in different scales. Depending on whether the clinician aims to determine a well localized field or a more widespread one, several available montages can be used including the monopolar, bipolar, common reference, average reference and laplacian [1], [27].

Electrophysiological recordings provide measurement of electrical activity through the use of "active" and "inactive" electrodes. Essentially, the readings given by the recording system convey information about the relative activity of the electrodes i.e. there is no recorded activity in an absolute sense. In fact, the principle behind voltages is the potential difference or the charge difference between two points. Referencing, thus, determines the amplitude and the phase of the recorded signals. With the advent of digital signal processing, it has been possible to record the brain signals with a given reference choice and then re-reference the signals off-line [27], [28], [29].

In practical terms, the choice of reference varies a lot between different research and clinical groups, but certain factors may be considered when choosing the referencing site. Firstly, given that truly neutral "inactive" electrodes do not exist, one can choose a convenient and comfortable site depending on the nature of the experimental procedure. Factors that need to be taken into account are the duration of recordings, the type of protocol (e.g. cognitive-intensive/ passive experiments) and the preference of the subject (e.g. discomfort of earclips during long recordings). In addition, the reference site choice must not be biased towards one hemisphere. Popular online referencing choices are the Cz, Fz, Oz, FCz electrodes, the earlobe, mastoid, or other body surface electrodes [27], [21].

On the other hand, offline techniques can be used to re-reference the recorded signals as long as certain conditions are satisfied. The advantage that offline re-referencing offers lies in the ability to enhance specific local/distributed and near/far field distributions by using existing or virtual channels. Some of the most

popular techniques are the unipolar montages, i.e., the use of a single reference channel (real or virtual). Such methods include the monopolar, common average, and the linked mastoid reference. The most appropriate referencing method depends on several factors, namely, the electrode density and coverage, as well as the individual physio-anatomical parameters of the subject (e.g. head shape, inner conductivity). The uni-polar montages have been successfully used to capture the neural activity of near and far field sources. This is achievable when the reference electrode is relatively distant and neutral. However, the data quality can also affect the interpretation of the recorded signals in unipolar montage. As an example, one can consider that if the reference electrode Oz is considered as reference and is highly contaminated with noise, then the recorded signal (e.g. difference between electrode activity and Oz activity) will also be contaminated. For this reason, common reference is recommended after extrinsic noise and artifacts have been minimized [27], [21].

Alternatively, one may use other reference montages such as the bipolar or the Laplacian. The bipolar referencing approach is based on calculating the electrode activity as a function of the neighbouring electrodes activity, thus, removing the dependence of the recorded signals on the quality of the reference electrode. Nonetheless, limitations still exist and are linked to the spatial sampling requirements. In fact, bipolar reference must have a small interelectrode distance to provide accurate readings of the local activity. The Laplacian referencing is based on a transformation of the recorded voltage to current source density using a spatial high pass filter, thus reducing the volume conduction effect [27]. In practise, the non-unipolar montages have been used to inspect near field sources as the bipolar montage can effectively reduce non-cerebral artifacts.

Summarizing, in EP studies, single electrodes from the EEG cap or facial/body electrodes have been used in online referencing. Further processing and re-referencing can be done in an offline fashion and depends on the nature of the

experiment. If focal cortical activity is of interest, one may use the bipolar or Laplace referencing, assuming a sufficient electrode coverage. On the contrary, if near field sources or broad fields are the subject of study, unipolar techniques, such as the common reference or common average reference are recommended [29].

Despite the advances in extracranial recording methods such as EEG and MEG which can provide information about near and far fields, investigating local subcortical fields with high spatial resolution proves to be a challenge. To date, such information can be provided through invasive techniques, most notable, ECoG and SEEG.

2.1.2. Stereotactic electroencephalography

Stereotactic electroencephalography (SEEG) enables the placement of stereo-tactically arranged intracranial electrodes and allows measuring potentials in various depths from the outer layers of the cortex. Originally developed to assist in the definition of the epileptogenic zones [30], SEEG has been used in sleep studies of K-complexes [31], in research of cortico-cortical and somatosensory evoked potentials [4], [32], and as a guide for radiofrequency thermocoagulation in treating nonoperative epilepsies [33]. However, SEEG recordings are still only available when patients are undergoing presurgical clinical evaluation. An extensive clinical study on 500 procedures and 6496 implanted electrodes has demonstrated the increased accuracy in target point localization and safety of SEEG. This has been possible through the advances of imaging technologies and robots. Typically, an SEEG procedure requires pre-operative 3D angiography, MRI and X-ray to ensure the correct placement and trajectory planning of the implanted electrode. The use of robot-assisted implantation has further minimized implications and the target point localization error [34], [35].

Furthermore, several challenges are still present in this invasive recording method. To start with, the implanted electrodes are mostly orthogonal (although oblique insertion is also possible) to the skull, limiting the flexibility and the available intracranial sampling [35]. However, the electrodes trajectories have been shown to successfully interrogate the mesial temporal region strongly associated with epilepsy [36] and subcortical structures such as the basal ganglia that play a role in Parkinson's disease [37]. In addition, the potential to sample bilateral and obscured areas, such as the insula, makes SEEG more advantageous compared to subdural electrodes. At this point, it is worth mentioning that SEEG procedures are facilitated in refractory focal epilepsy cases where the electrodes are used for presurgical evaluation and localization of the epileptogenic zone. Thus, it is more common to implant electrodes on a single brain hemisphere as dictated by the preoperative evaluation.

The spatial resolution along the collinear sensors of the electrodes is typically very good as it is customary to place 4-18 contacts along the same electrode shaft allowing a spatial resolution of a few millimeters [35]. Another advantage of SEEG over surface EEG is that it has a significantly higher SNR as it can access deeper structures of the brain and avoids attenuation attributed to brain signals passing through the skull. Lastly, conversely to EEG, SEEG electrodes have a local coverage due to its limited ability to record contiguous cortical regions.

Similar to EEG, the referencing choice can provide different perspectives of the intracranial recorded signals [38], [39]. The common reference has been used in SEEG procedures, where the common reference is the average of two or more white matter contacts located remotely from the region of interest [4], [38]. In SEEG, special care is required to place these references distantly from the epileptogenic foci as brain activity due to epileptic seizures can provide incorrect reference signals. The common average and the electrode shaft reference have also been used as unipolar referencing methods. In a clinical and research context, one

can also use bipolar re-referencing to focus on local activity [38]. More recently, alternatives to these widely-used montages have been proposed. The reference virtual electrode can be obtained by using low-variance signals while ICA-derived reference has also been used [39].

2.1.3. Challenges of simultaneous HD-EEG and SEEG recordings

In this thesis, unipolar online reference Cz has been used during recordings and pre-processing of HD-EEG. The average re-reference is also computed for the whitening and source localization stage as will be more thoroughly presented in Chapter 3 [29], [40], [41]. For SEEG, the average of two adjacent white matter electrodes was chosen as reference by clinicians using both anatomical and functional criteria. The selection of the leads was performed time-by-time to ensure no response was present due to the evoked potential protocols (i.e., median nerve electrical stimulation) and the stimulation of the reference electrodes did not evoke any sensory and/or motor activity. Simultaneous studies on EEG and SEEG recordings have been limited, specifically, due to the increased experimental complexity derived from potential interfering of the two recording modalities and practical difficulties of the simultaneous placement of the EEG cap and SEEG implanted electrodes [42]. To the best of our knowledge, somatosensory evoked potentials of median nerve stimulation have not been explored with simultaneous HD-EEG and SEEG modality.

2.2. Somatosensory Evoked Potentials

Somatosensory Evoked Potentials (SEPs) are signals generated from neural mechanisms involved in the perception and processing of sensory input. Typically, SEPs are induced by stimulating nerves in the upper and lower extremities such as median, ulnar and tibial, and peroneal nerves, respectively

[43]. The signal-to-noise (SNR) ratio of the SEPs depends on the quality of the recorded signals as well as on the number of available trials. In addition, SEPs depend not only on the stimulation protocols [44] but also on many other factors such as the fatigue and stress of the subject as well as inherent characteristics of the stimulation site including the number of receptors and their receptive field. Interpreting the recorded evoked responses after somatosensory stimulation requires an understanding of the neural pathways and structures involved in translating stimulation into sensation.

2.2.1. Somatosensory Processing Pathway

There are two basic types of stimulation that are typically used to induce a SEP, namely mechanical and electrical stimulation. When external mechanical stimuli are presented on the mechanosensory subsystem, skin deformations cause changes in ionic permeability of the underlying neural structure. This phenomenon is called sensory transduction and gives rise to an afferent depolarizing current which will be decoded in the brain and translated into sensation. On the other hand, electrical stimulation activates large diameter, fast conducting group Ia muscle and group II cutaneous afferent fibres bypassing the mechanotransduction mechanisms [45]. This results in SEPs with different latencies between mechanical and electrical stimulations mainly due to a) skin indentation and mechanoelectrical transduction in skin receptors and b) slower conduction velocity of cutaneous afferents for mechanical stimulation [46].

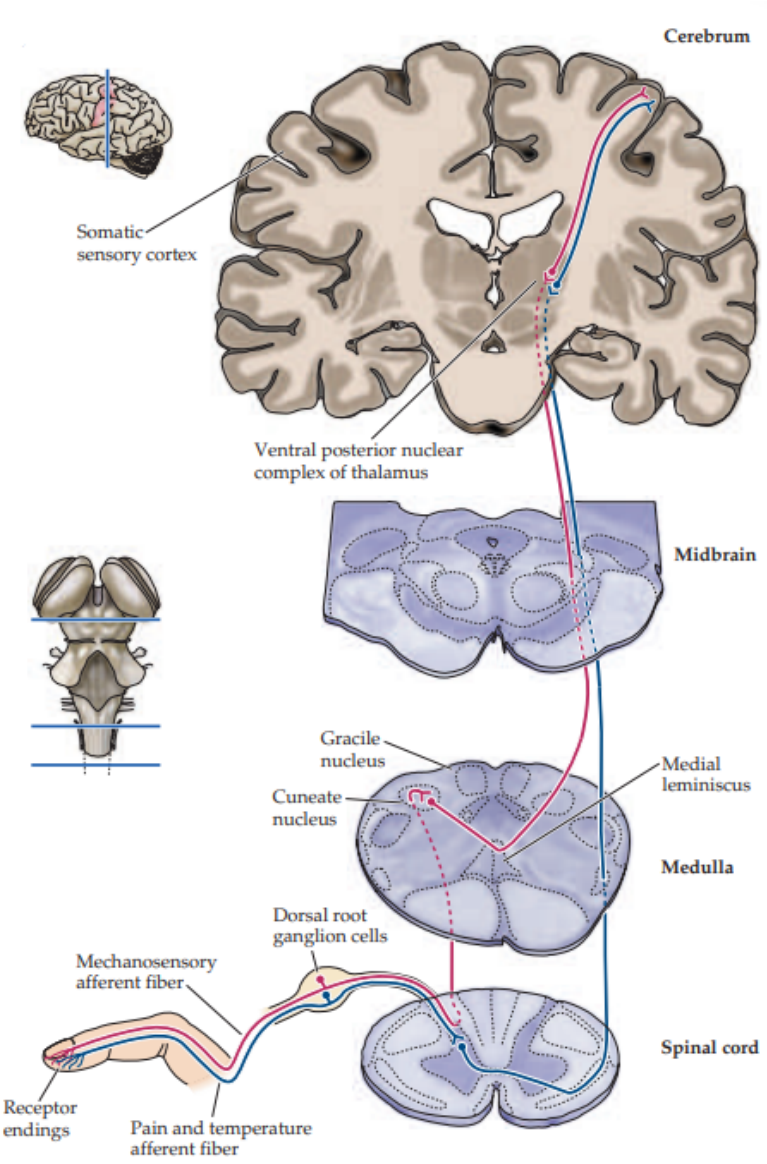

Figure 2.1. The somatosensory pathway [47].

The somatic sensory system is based on 3 neuron relays as illustrated in Fig. 2.1. The afferent signals from the stimulated area are first relayed at the dorsal root ganglion cell. The dorsal root ganglion cells project their axons through the dorsal root of the cervical spinal cord and form synapses with the brainstem nuclei at the caudal medulla. Following, the brainstem nuclei project through the medial lemniscus to the ventral posterior nucleus (VPN) of the thalamus which then sends its axons to the primary somatosensory cortex (SI) at the postcentral gyrus

and the secondary somatosensory area (SII) in the parietal operculum [48]. Although our understanding of the somatosensory processing has been mainly based on studies of nonhuman primates, the advent of brain recording techniques in the last 20 years including positron emission tomography (PET), electroencephalography (EEG), and functional magnetic resonance (fMRI) imaging have shed new light on the human somatosensory processing mechanisms [49].

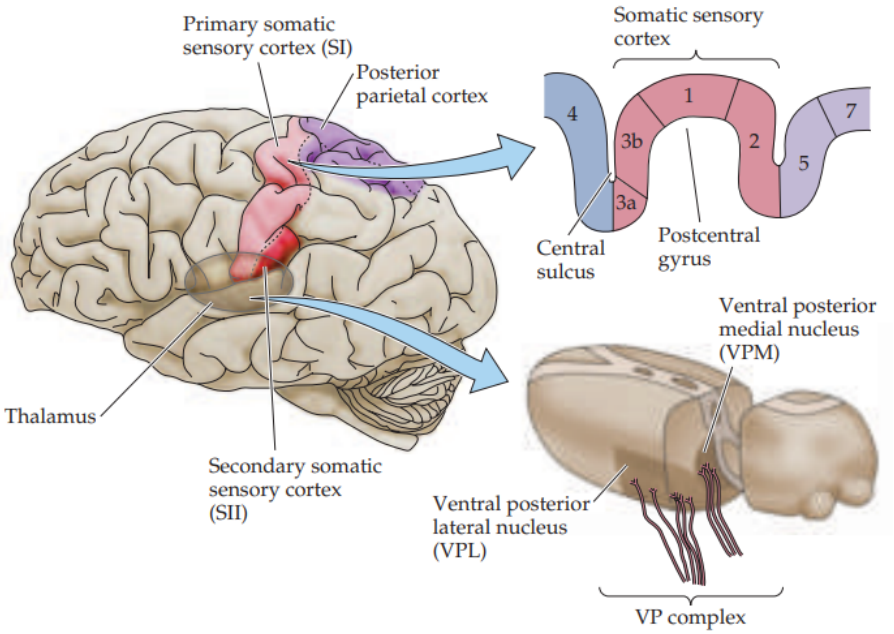

Figure 2.2. Somatotopic organization of somatosensory areas [47].

The SI consists of 4 neural structures, namely, Broadman areas 3a, 3b, 1 and 2 as shown in Fig. 2.2 that are discriminated by differences in histology [50], [51] and neurotransmitter binding sites [52]. It has been shown that each of these 4 structures possess a separate and complete representation of the body. These somatotopic maps represent the foot, leg, trunk, and forelimbs in medial to lateral arrangement. However, the functions of each structure differ; areas 3b and 1 respond to cutaneous stimuli; area 3a is more involved with proprioception; area 2 processes tactile and proprioceptive information [47].

Furthermore, the information travels to other cortical and subcortical structures such the secondary somatosensory area SII at the parietal operculum (OP) [53], namely Broadman areas 40 and 43 to perform higher order processing. This area comprises 4 subregions OP1, OP2, OP3 and OP4 with cytoarchitectural differences. Surrounding areas are also involved in the secondary somatosensory processing, such as the ventral parietal area, insula, and supramarginal gyrus [4], [54]–[56]. These substructures located deep within the Slyvian fissure are responsible for sensorimotor integration and bilateral processing of somatosensory information [57]. The processed information is then relayed to several limbic system structures such as amygdala and hippocampus which contribute to tactile learning and memory.

Despite the main processing centers in SI and SII, it is known that a wide network of cortical and subcortical structures is involved in decoding somatic information. More specifically, the medial and lateral VPN project on SI while the medial VPN projects to SII enabling parallel processing of ascending information. Subareas 3a, 3b,1 and 2 of SI are also interconnected and extend their connections to areas 5, and 7 in the parietal cortex as well as motor and premotor areas (Broadman 4 and 6, respectively) in the frontal lobe. More importantly, SI also projects back to the spinal cord enabling modulation of the ascending somatosensory signals. Lastly, both SI and SII form connections with the insula [58] while some portions of SII project to the amygdala and hippocampus [47].

Somatosensory evoked responses provide a standard methodology to reveal the neural pathways and structures involved as well as highlight malfunctioning. Interestingly, SEP across different subjects exhibit a prototypical waveform with certain peaks and troughs that are associated with ascending information reaching a specific neural structure.

2.2.2. Characteristic Components

Evoked Potentials are stimulus-locked responses with typically less than 5 μV amplitude. In clinical practise it is often of great importance to examine the somatosensory processing upon external stimulations of upper or lower extremities. Studying the somatosensory evoked response (SEP) of upper extremities can be done by stimulating the median or ulnar nerve, while for lower extremities, the tibial and peroneal nerves are preferred. Throughout many studies, it has been shown that the somatosensory system has a prototypical response composed of short, middle and long latency components as is generally the case in evoked responses [43], [59]–[64]. The occurrence of certain components depends on the nature of the clinical protocol. It has been postulated that short-latency components are present in various cognitive states and are stable. On the other hand, experiments involving some vigilance and cognitive functions by the subjects give rise to larger amplitude middle and long latency components [12], [43], [60].

Another important differentiation between characteristic components is the dynamics of the generated response and the corresponding generating neural mechanism. Early components have high-frequency content and represent ascending information arriving sequentially in the dorsal root entry zone, the medial lemniscus as well as the postcentral gyrus (SI). The recorded changes in the electric field are primarily due to changes in surrounding volume conduction and relay nuclei activation. Later components are characterized by low frequency content and are associated with further processing of the stimulation in the upper bank of the sylvian fissure [64], [65]. An important underlying mechanism associated with long latency components is that the generating neural structures have longer refractory periods. Thus, a low stimulation frequency around 1Hz is

recommended as high stimulus frequencies do not allow the unfolding of the long latency components [43], [59], [64]. One should note that the normative values presented in Table 1 are dependent on many factors such as the sleep stage, the age, the medication and the mental state of the subject [64]. Admittedly, the richness of information contained within the recorded SEPs and their components can provide information about clinical conditions of the somatosensory pathways and brain structures.

Component name	**Generator**
P9	Distal brachial plexus
P11	Dorsal root entry zone
P13/14	Medial lemniscus
N16 [66]	Thalamus
P18	Pons/Medulla
P20/N20	Pre/post central gyrus
P22	Supplementary motor cortex
P40-N60 [67]	Thalamocortical projections
P45 [59]	Parietal region
N60 [59]	Parietal region
P65,P100 (frontally) [59]	Myogenic origin
P100 [63]	Upper wall of SS in SII (i.e. parietal operculum)
N125-P200 [63]	Surface cortex above SII.
N140-P200 [59], [64]	Corpus callosum/ somatosensory associative cortex/orbitofrontal cortex

Table 1. Summary of well-studied components and their respective neural sources.

2.2.3. Clinical Application and Challenges

All the aforementioned somatosensory evoked potentials (SEPs) characteristics, namely, the latency, amplitude and frequency greatly depend on physiological and pharmacological factors such as blood pressure [68], oxygenation and temperature as well as anaesthetic agents, propofol and midazolam [69]. Thus, alterations in SEP latency, amplitude and waveform might reveal clinical information about the perception and reaction of the human body to such factors. In addition, the absence of cortical components such as the N20, may infer death prediction or persistence of the vegetative state in comatose patients in the ICU [70]. The SEP recordings can also be employed for predicting outcome after a cardiac arrest or during a spinal cord surgery to provide information about the blood supply to the dorsal column [13]. In clinical practise, SEPs are also used to examine patients with multiple sclerosis, myoclonus and as a guide to prevent cerebral ischaemia in the ICU [71], [72]. Despite SEP monitoring having exhibited a reduction in neurologic deficits in postoperative paraplegia by more than 50% [73], the abnormalities of SEP do not always imply pathology and therefore it may be used complementary with other monitoring modalities [70].

3. State-of-the-Art

In the past two decades there has been a plethora of studies where hand median nerve stimulation has been mapped to the cortical and subcortical neural correlates. Attempts to characterize and localize the neural areas involved in somatosensory processing have been done using neurophysiological recording methods as well as imaging approaches. More specifically, techniques such as EEG [59], [60], MEG [74], SEEG [66], ECoG [62], [63] and fMRI [71], [75] as well as a combination [76] of them have been widely explored to pin down regions crucial in the somatosensory perception and categorization. A summary of some of the existing body of work covering the last 35 years of research on passive non painful hand area stimulation with a focus on median nerve stimulation is presented in Table 2.

Short-latency (i.e., 20-40ms) components have been investigated following median nerve stimulation. P20-30 was found anterior to the central sulcus (CS), while N20-P30 was localized in posterior CS supporting the hypothesis of a tangentially-oriented generator in the posterior wall of CS which acts vertically to the central sulcus. P25-N35 appeared close, and on both sides of CS suggesting the presence of a radial generator in area 1. Later components originated over the central and lateral hand area of SI [62]. A distinct feature used to classify responses as cortically-generated near field potentials is the inversion and sharpness in polarity passing from surface to white matter. On the contrary, lack of polarity inversion as well as similar and shallow gradients between surface and white matter might indicate the generation of potentials at distant sites.

The same research group also investigated long-latency of 40-250ms components [63]. The complex P45-N80-P180 presented a similar nature to N20-P30 located anterior to CS, while N45-P80-N180 was measured posteriorly to CS and was

attributed to a generator in 3b. At the same time, the P50-N90-P190 complex resembled the characteristics of the short-latency P25-N35, suggesting its generation in area 1. Interestingly, recordings from the perisylvian area exhibited P100 and N100 components, measured above and below the sylvian sulcus (SS), respectively, thus implying a tangential generator in the upper wall of SS in SII. On the contrary, the N125 and P200 recorded on both sides of SS suggest a radial generator in SII near the surface cortex [63]. A key difference between CS and SS-located generators is the laterality as only perisylvian potentials were evoked by both ipsilateral and contralateral stimulations [67]. Despite the analgesic and anesthetic agents used in this study known to change the characteristics of late SEPs, the findings of this research are in agreement with other works [4], [56].

A following study revealed the presence of a long-latency ipsilateral activation of the primary sensorimotor cortex (SMI). The results from 122-channel MEG recordings of 10 healthy subjects verified the existence of four widely accepted sources after median nerve stimulation, such as the contralateral SMI, the bilateral SII and the contralateral posterior parietal cortex (PPC) [77]. Synthetic aperture magnetometry has also been used to investigate the role and differences between low (40-60 Hz) and high (70-100) gamma oscillations following median nerve stimulation. Using MEG recordings, a gamma power increase was observed in all bands at the contralateral SI. In middle latencies, the temporal distribution of power changed between low and high gamma in contralateral SI while results from ipsilateral SI were not consistent in all subjects. It is worth noting that an increase in high gamma power at 80-180ms was observed simultaneously in both SI and SII. Given that alpha and beta might be very slow oscillation that are unable to carry higher processing level signals and that very high frequency oscillations may be unsuitable to allow for establishment of synchrony, the authors proposed the high gamma band as a good candidate for being a mediator in functional cortico-cortical connections (i.e. transferring information from SI to SII).

Whitehead *et al.* [78] studied the emergence of hierarchical somatosensory processing in late prematurity by performing experiments on infants with tactile stimulation of the palm area. Using EEG and source localization analysis, possible generators to SEPs were hypothesized to be SI, SII, supplementary motor area (SMA) and PPC [78]. In a different study, the feasibility to use dipole source localization (DSL) and co-registered fMRI was investigated for studying the somatosensory processing following medina nerve stimulation [76]. After the registration of the EPs, five dipoles were sequentially fitted (i.e., determination of the location/orientation/moment of the neural generators) that gave rise to the EEG signals. The fMRI showed certain clusters of activation while the superimposed activation sites of DSL and fMRI were found to be the contralateral SI, contralateraal SII, contralateral and ipsilateral anterior insula as well as the medial wall. It is worth mentioning that activation in the primary motor cortex, posterior parietal cortex and thalamus were present to a smaller extent. On the contrary, stereotaxic surgery allowed recording of thalamic SEPs, contralateral to the median nerve stimulation site and found a subcortical generator giving rise to N16 which was firstly picked by scalp electrodes and was verified by the direct recording from the intracranial electrode in the thalamus [66].

An fMRI study revealed activation of contralateral SI, bilateral SII and bilateral insula upon median nerve stimulation. Interestingly, the stronger activation contralateral SII can shed light in the hierarchical somatosensory processing suggesting that (a) the information is compressed along the callosal pathway or (b) the delayed arrival to the ipsilateral region reduces the synchronization and thus the evoked cortical response. The findings of this study are different to existing EEG and MEG studies due to the different underlying generating mechanism of the recordings (i.e., hemodynamic and electrochemical processes) [71]. The effect of varying stimulation rate (i.e. 1-10 Hz) on the activation of the somatosensory cortex following median nerve stimulation has also been explored [79]. Although

not all subjects in this fMRI study showed consistent activations across the different stimulation rates, key activated areas included contralateral SI and bilateral SII and insula. By increasing the stimulation rate, fMRI showed higher activation in various cortical areas including SI, SII and insula. Unlike previous neuroimaging studies, this fMRI study revealed a consistent cerebellar activation at all stimulation rates.

Furthermore, several studies have explored the activation of the secondary somatosensory cortex upon stimulation of the hand area. This region is assumed to be responsible for higher order somatosensory processing and is of great interest since the involved pathways and its somatotopic organization are still debatable. Electrical stimulation on the fingers showed the anticipated activation of contralateral SI and bilateral SII [75]. Additionally, activation of the PPC, supplementary and cingulate motor area (SMA, CMA) as well as insula was observed. The PPC encompasses the superior and inferior parietal lobules and is regarded as a higher-order processing site of sensory information and sensorimotor integration and has also been reported in other EEG and MEG studies [77], [78]. The authors demonstrated that there exists a somatotopic arrangement within contra- and ipsilateral SII.

More recently, Avanzini *et al.* showed activation of various cortical regions following stimulation of the median nerve [4]. These regions included the contralateral SI, and SII, insular cortex as well as dorsal premotor cortex (PMd) and middle temporal gyrus. By taking advantage of the high temporal resolution of SEEG, temporal activation patterns from leads exploring the contralateral SII were assessed. The temporal activation patterns exhibited a dual time-course (i.e., phasic and tonic) where the phasic component (20-30ms) could be related to touch detection while the long-latency tonic component is still open to different interpretations. By comparing both ipsi/contralateral and phasic/tonic activation patterns one can also infer information about the communication of the distributed

neural networks related to somatosensory processing. Extending the work of Avanzini *et al.* the authors in [80] proposed that the long-lasting tonic activity may represent the neural substrate for maintaining somatosensory information in time while also enabling comparison and integration between different stimuli. In addition, the findings of the study supported the hypothesis that ipsilateral SII activity is mediated by direct callosal communication coming from contralateral SI. However, the serial or parallel activation of somatosensory processing in SI and SII remains an active debate among researchers [4], [78], [81].

Year	Identified active areas	No. subjects	Recording setup
1983 [82]	Prerolandic motor cortex, contralateral parietal scalp and contralateral prerolandic scalp	12	EEG (2)
1984 [66]	Ventral posterolateral thalamic nucleus	21	EEG & SEEG
1989 [62]	Brodmann areas 3b,1	52	Implanted electrodes & ECoG
1989 [63]	Brodmann areas 3b,1 and perisylvian area	54	Implanted electrodes & ECoG
1995 [77]	Bilateral SMI, SII and PPC	10	MEG (122)
2000 [83]	SI	5	EEG (1) & fMRI
2000 [56]	Parietal operculum and parietal ventral area	18	fMRI
2001 [75]	Contralateral SI, bilateral SII, PPC, SMA and CMA	8	fMRI

2003 [76]	Contralateral SI, contralateraal SII, contralateral and ipsilateral anterior insula and the medial wall	6	EEG (32) & fMRI
2003 [74]	Contralateral SI and bilateral SII	7	MEG (64)
2007 [71]	Contralateral SI, bilateral SII and bilateral insula	24	fMRI
2009 [79]	Contralateral SI, bilateral SII, bilateral insula, contralateral SMA and ipsilateral cerebellum	8	fMRI
2016 [4]	Contralateral SI, SII, insular, PMd and middle temporal gyrus	99	SEEG
2019 [78]	Brodmann areas 3b, 2 and SMA, PPC and SII	34 infants	EEG (18)

Table 2. Collection of studies on hand area stimulation.

The table above provides a summary of selected studies on hand area stimulation. The identified active areas are presented in the second column while the number of subjects involved in the study is given in the third column. It must be noted that the reported identified areas were not necessarily present in all subjects in the study and thus the results should be taken with caution. Moreover, the recording setup refers to the employed neurophysiological and/or neuroimaging method while the number of available channels (e.g., in EEG and MEG studies) is provided in parenthesis where applicable. From the table the following conclusion can be drawn:

1. The popularity of fMRI has significantly increased in studies where the functional properties of somatosensation are of interest. However, fMRI

studies might result in inconsistent findings depending on many factors including the magnet and stimulation rate. Another limitation of fMRI resides in the fact that the recorded signals are based on hemodynamic processes which are typically slower than neurochemical processes, thus, limiting the ability of fMRI to capture fast neural processes.

2. Most recent studies support the hypothesis that somatosensory processing of hand area stimulation is performed by distributed neural networks in cortical and subcortical areas where each area may be responsible for a specialized function including stimulus detection, integration and memory. There is a common appreciation of the key areas involved in somatosensation such as the primary somatosensory and secondary somatosensory area as well as insula, posterior parietal cortex and supplementary motor area.
3. To the best of our knowledge, no prior work has considered simultaneous intracranial SEEG and high-density extracranial HD-EEG recordings to study SEPs. We believe that the combination of these two modalities and the availability of high density sensors can provide new insights on the somatosensory processing enabling high temporal and spatial localization of neural activity.

4. Materials and Methods

This chapter provides information about the participants, the experimental protocol and an overview of the proposed methodology to process and analyze the simultaneous EEG and SEEG recordings. The proposed pre-processing workflow is then described in more detail followed by the source modelling analysis and intracranial activity prediction.

4.1. Overview of Proposed Methodology

Simultaneous recordings from HD-EEG and SEEG were obtained from 8 patients after median nerve stimulation. The data was processed using custom-built functions in Python using the MNE library [84], [85] to perform filtering, bad channel/trial and artifact removal through Independent Component Analysis (ICA) [86] and Autoreject [87] prior to analyzing the simultaneous recordings. The proposed pre-processing pipeline involved both automatic and manual processing blocks to ensure minimum bias while at the same time visual inspection ensured that the automatic processes did not corrupt or distort the data.

Following preprocessing, the EEG signals were used for source reconstruction to reveal the location, and intensities of the current sources that produced the recorded activity. Popular distributed source modelling approaches (i.e., where the number of sources exceeds the number of EEG sensors) were investigated such as Minimum norm estimate (MNE) [88], Low-resolution electromagnetic tomography (LORETA) [89] and its variants standardized LORETA (sLORETA) [90] and exact LORETA (eLORETA) [91], as well as dynamic statistical parametric mapping (dSPM) [92]. These methods were considered first due to their wide and successful use in the scientific literature but also due to the fact that the somatosensory processing is performed by distributed neural networks. The

optimal source modelling approach for the given data was selected using a grid search optimization of the explained variance and visual inspection of the time-course of the estimated sources. Time-frequency analysis using short-time Fourier Transform (STFT) of the activity of the estimated sources was performed to reveal the spectrotemporal dynamics of the estimated activity.

Given the potential similarities between intra- and extracranial EPs following median nerve stimulation, the possibility to find a mapping between intracranial and extracranial space was investigated. Since intracranial recordings are rarely available, obtaining a mapping from extracranial to intracranial space can enable better diagnosis and treatment of diseases related to somatosensation even in cases where intracranial invasive recordings are not possible. Therefore, the multivariate temporal response function (mTFR) was used to predict the intracranial activity which mapped the brain signals recorded at the surface of the scalp to the intracranial activity. This method has been recently used to reconstruct the speech signal that gave rise to EEG recordings [17]. In the context of this thesis, we implemented this method to perform prediction of the intracranial activity based on HD-EEG (i.e., backward modeling). The acquired mapping allowed us to predict the neural response at the SEEG level given the HD-EEG activity enabling the analysis of the underlying decoding and encoding mechanisms, respectively.

Subject	Age	Sex	Laterality of electrodes	Epileptic zone	Pharmacology
sub-01	31	F	left	n/a	brivaracetam, perampanel
sub-02	25	F	right	right operculum	levetiracetam, topiramate
sub-03	44	M	left	left	lacosamide,

				supramarginal, opercular	valproate, topiramate
sub-04	39	F	left	left mesial temporal	carbamazepine, clobazam, levetiracetam
sub-05	31	F	left	left parietal cingulum	carbamazepine , lamotrigine
sub-06	35	M	left	left mesial temporal	levetiracetam, carbamazepine, lacosamide
sub-07	23	F	right	right operculum	valproate, lacosamide
sub-08	37	M	right	right operculum, insula	lacosamide, oxcarbazepine

Table 3.Demographic and clinical information of the patients.

4.2. Participants

Simultaneous recordings from EEG and SEEG were obtained from 8 patients in the Niguarda Hospital, Milan, Italy. All subjects were patients undergoing intracranial monitoring for pre-surgical evaluation of drug-resistant epilepsy and provided their Informed Consent before participating (Table 3). The study was approved by the local Ethical Committee (protocol number: 463-092018, Niguarda Hospital, Milan, Italy) and it was carried out in accordance with the Declaration of Helsinki.

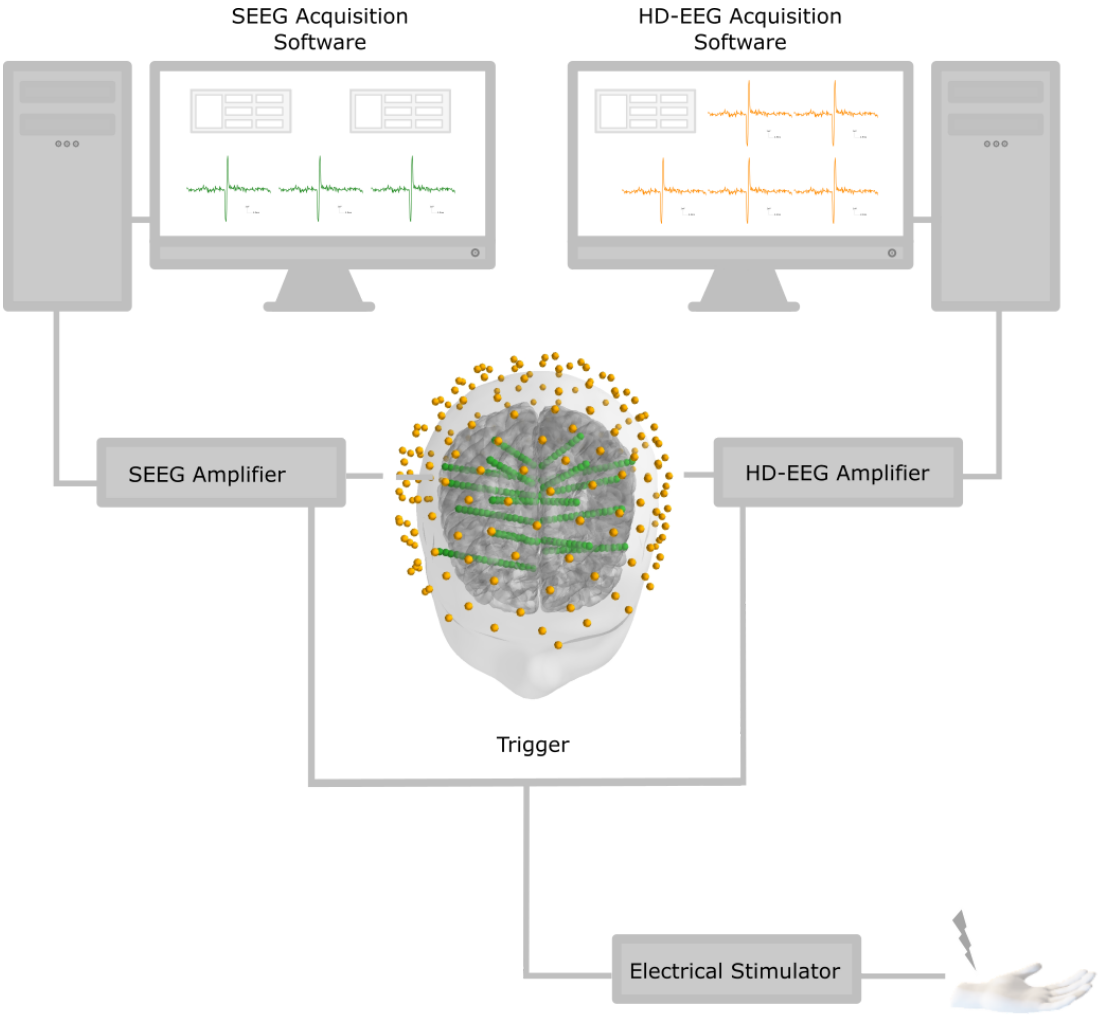

Figure 4.1. The simultaneous HD-EEG and SEEG acquisition system (*image adjusted from* [42]).

4.3. Median Nerve Stimulation

The median nerve was stimulated opposite to the hemisphere with the implanted electrodes at the wrist, using constant-current pulses of 0.2 ms duration at a rate of 1 Hz. The intensity and the exact location of the stimulation was determined when an observable thumb twitch was obtained. The motor threshold ranged from 3.2 to 5.8 mA while the stimulation intensity was set to 10% above the motor threshold [4]. More information about the number of trials and the intensity of the stimulation for each session is given in Table 4. Figure 4.1 illustrates the

experimental setup with the co-registered HD-EEG and SEEG acquisition system as well as the trigger signal used to synchronize the recording systems. The localization of the intracranial and extracranial electrodes was also performed to enable spatial co-registration.

4.4. Electrode Localization

The location of implanted SEEG electrodes was solely determined by the clinical necessity for identifying the epileptogenic zone. The SEEG planning was supported by individual brain MRI (Achieva 1.5 T, Philips Healthcare) and CT (O-arm 1000 system, Medtronic) recordings. The investigated hemisphere/s as well as the location and number of explored sites were determined based on non-invasive clinical assessment while the duration of the SEEG investigation was determined only by the clinical needs. Placement of the SEEG electrodes was carried out under general anaesthesia using a robotized passive tool-holder (Neuromate, Renishaw Mayfield SA). The implanted electrode location was assessed using pre-implant MRI and post-implant CT (O-arm 1000 system, Medtronic). The single lead position was further assessed with respect to the MRI using Freesurfer [93], 3D Slicer [94] and SEEG assistant [95] software. In cases of mismatch between the pre-implant MRI and the EEG digitization MRI, the contacts position were transformed from the SEEG to the EEG space using affine transformation in the ANTs software [96]. The normalized coordinates of the contacts were estimated through non-linear registration between the individual skull-stripped MRI and skull-stripped MNI152 template 21 (ICBM 2009a Nonlinear Symmetric) using ANTs' SyN algorithm. Lastly, visual inspection was performed to verify the accuracy of the normalization process.

4.5. Simultaneous Recordings

The simultaneous recordings were performed using a 256-channel EEG cap (Geodesic Sensor Net; HydroCel CleanLeads). The whole procedure was carried out using the sterile technique to minimize and prevent infections. The EEG signals were sampled at 1000 Hz with an EGI NA-400 amplifier (Electrical Geodesics, Inc; Oregon, USA). A SofTaxicOptic system (EMS s.r.l., Bologna, Italy) was used to digitize the spatial locations of the EEG electrodes and anatomical fiducials, coregistered with a pre-implant MRI (Achieva 1.5T, Philips Healthcare). The recorded signals were referenced to the Cz electrode and were downsampled to 500 Hz to improve computational efficiency while still retaining enough samples to capture the signal dynamics.

At the same time, the SEEG recordings were performed using a variable number of platinum–iridium semi flexible multi-contact intracranial electrodes (Microdeep intracerebral electrodes, D08, Dixi Medical, or Depth Electrodes Range 2069, Alcis). The SEEG signals were acquired with a Neurofax EEG-1100 (Nihon Kohden System), sampled at 1000 Hz sampling frequency. The SEEG recordings were then downsampled to 500 Hz to reduce the computational cost. The intracranial reference was selected by clinicians using both patient-specific anatomical and functional criteria and was computed as the average of two adjacent white matter leads. The implanted electrodes had the following characteristics:

- Diameter: 0.8 mm
- Contact length: 2 mm
- Intercontact distance: 1.5 mm
- Number of contacts: 8-18 contacts per electrode

The implantations for all 8 subjects were unilateral since clinical evidence generally indicates which hemisphere is responsible for generating the seizures.

More information about the number of EEG and SEEG channels, trials and laterality of the stimulation of the simultaneous recordings can be found in Table 4.

Session	Subject	Stimulation side	Stimulation intensity (mA)	No. SEEG/ HD-EEG channels	No. of trials
ses-01	sub-01	right	7	195/256	1000
ses-02		left	4		500
ses-03	sub-02	left	8	239/256	974
ses-04	sub-03	right	7	214/256	960
ses-05	sub-04	right	9	201/256	1000
ses-06		left	9		500
ses-07	sub-05	right	8	214/256	998
ses-08	sub-06	right	5	157/256	1140
ses-09	sub-07	right	8	182/256	214
ses-10		left	8		363
ses-11	sub-08	left	7	178/256	1000

Table 4. Information about the individual sessions.

4.6. Preprocessing Workflow

The EEG and SEEG signals were pre-processed differently as they have different characteristics arising from the nature of the recordings. SEEG signals do not suffer from eye blink and muscle artifacts, thus a different pre-processing pipeline was developed. At the same time, the signal amplitudes across neighbouring electrodes in implanted shafts can vary significantly if they sample a different subcortical or cortical region. Therefore, channel and trial rejection on SEEG signals is not based on amplitude thresholding and requires a much more detailed

review given the sparsity of such recordings. Despite the differences in the recording nature of EEG and SEEG, several preprocessing steps were common as seen in Fig. 4.2.

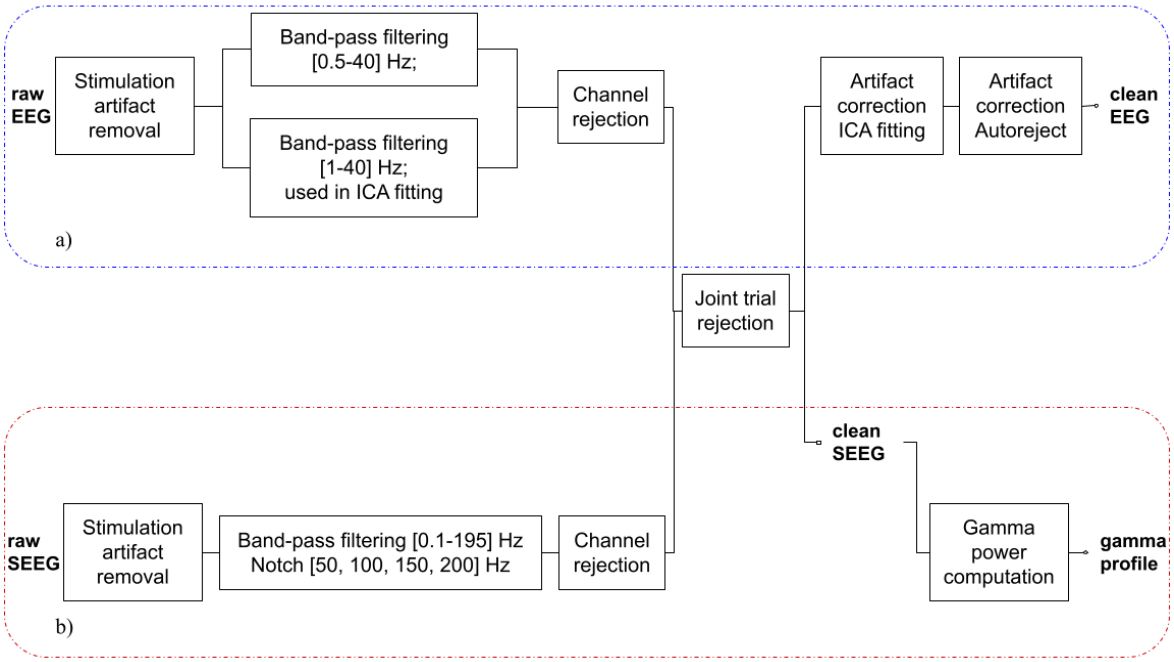

Figure 4.2. Proposed preprocessing pipeline for a) EEG and b) SEEG signals. The trial rejection step was performed through a joint analysis of the synchronized EEG and SEEG trials.

The synchronization of the simultaneous recordings was achieved using information from the stimulation trigger signal. This trigger signal allows epoching and averaging to obtain evoked responses from the synchronized EEG and SEEG recordings. One-minute long epochs were generated and split into -300 ms pre-stimulus and 700 ms post-stimulus intervals. The epochs were then baseline corrected using the mean of the pre-stimulus activity to remove DC offsets. Next, the montage was set up as it allows the visualization of topological order of scalp and intracranial electrodes in a 3-dimensional coordinate system. This step required the position of 3 fiducial landmarks, namely, the nasion, left

and right auricular to establish the topographic relationship of the digitized electrode positions.

4.6.1. Stimulation Artifact Removal

The electrical stimulation presented at the median nerve has been shown to contaminate the EEG and SEEG recordings since the stimulation signal can be picked up by both intra and extracranial recordings. To remove the volume conduction artefacts, a Tukey/windowed median filter was employed within 38ms of each stimulus [97]. The raw data was firstly filtered with a median filter of order 19, channel by channel. Next, the raw data centered within the 38ms window around the stimulus was replaced with a weighted average of the raw data and the median filtered data. The weights for the median filtered data were determined by a Tukey window [98] while they are zero for ±19ms away from the stimulus as shown in Fig. 4.3. The weighting applied to the raw data was 1 minus those applied to the median filtered data. The median filter and Tukey window length were varied to find an optimal value for reducing the stimulation artifact while minimally affecting the evoked responses. A median with more samples than 19 was found to distort the signal possibly because it took into account samples that were closer to actual neural responses with high activity, thus contaminating the smoothing process. On the other hand, if very few samples than 19 were considered, the stimulation artifact could not be reduced sufficiently. Although the stimulation artifact was greatly reduced as seen in Fig. 4.4, it was not completely removed.

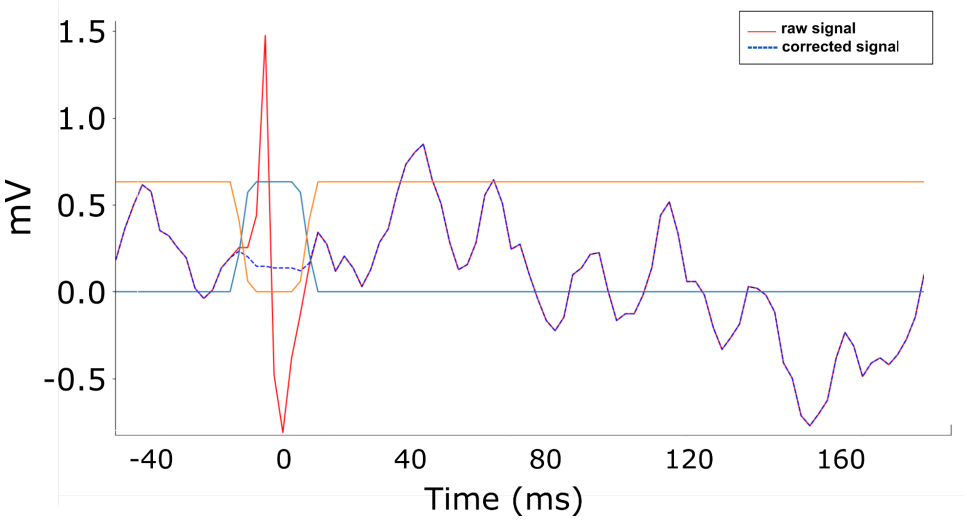

Figure 4.3. Tukey-windowed median filtering for eliminating volume conduction artifacts in SEEG recordings. The weights of the original and the median-filtered signal were determined by the orange and cyan Tukey window, respectively.

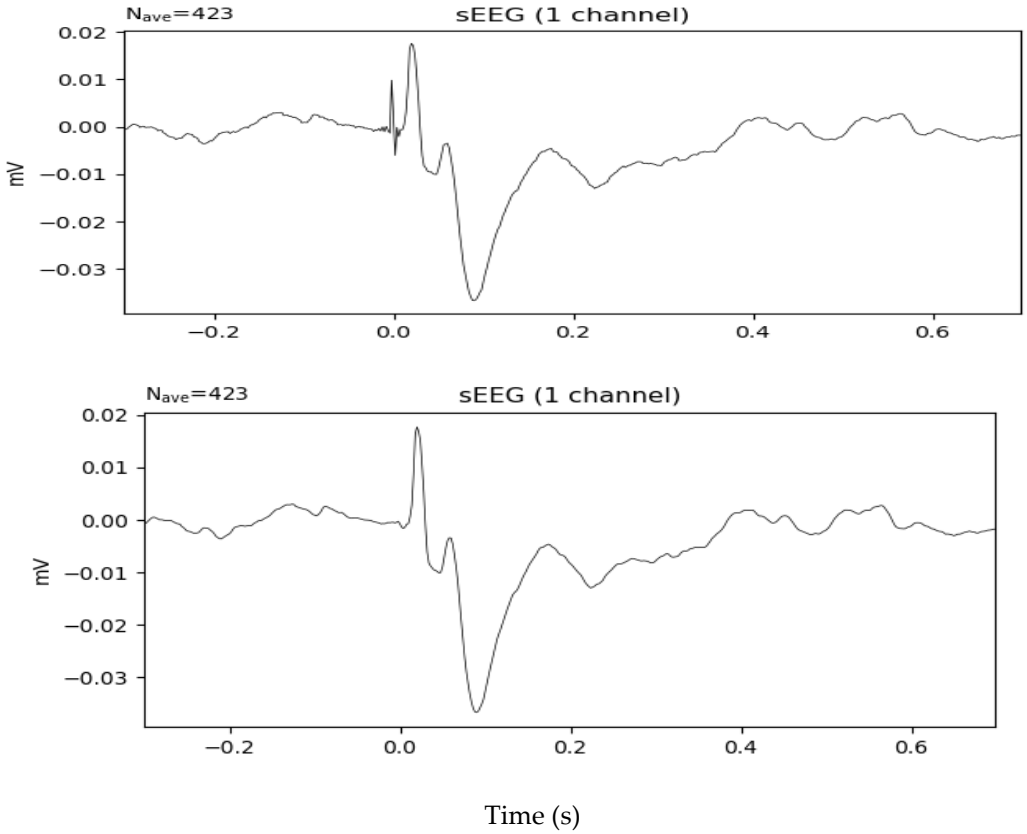

Figure 4.4. Stimulation artifact removal effect on evoked response with 423 available trials: (top) raw SEEG signal from one channel, (bottom) median filtered SEEG signal.

4.6.2. Raw Signal Filtering

Filtering is a well-established preprocessing step in electrophysiological studies as it is a necessary tool to improve the signal-to-noise ratio (SNR). However, filtering can have a negative effect on the quality of the data if not used with caution since it can severely affect the signal by either distorting the signal content or filtering out useful information of the signal [99]. An active debate in the scientific community has been ongoing around the potential positive and negative effects filtering can have on the electrophysiological recordings [100]–[104]. It must be noted that any filtering operations smear and change the signals in the time domain and must be carefully performed to ensure that the SNR is improved without altering the signal content of interest. Depending on the type of available data, different filtering techniques are recommended [105]. Additionally, the filtering choice is also highly dependent on the information of interest and experimental protocol (i.e., different neural oscillation bands may be of interest to study a specific mental state) [29]. Traditionally, two classes of filters have been devised, namely Finite impulse response (FIR) and Infinite impulse response (IIR) filters. Although IIR filters can achieve a more selective filtering, they can be unstable and exhibit non-linear phase response. On the contrary, FIR filters are inherently stable and do not suffer from non-linear phase response. In the scope of this project, zero-phase FIR filters with a hamming window and automatic selection of the transition bandwidth were used [105].

In more detail, the filtering design choices for the EEG recordings were determined by ensuring that the content of the somatosensory EPs was not distorted [29]. High-pass filtering has also been shown to affect the quality of ICA and source modelling with a recommended cutoff frequency of 1-2 Hz to remove the baseline drifts and low frequency components [106]. However, since the late components of the somatosensory ERPs were of interest, a high-pass filter of 0.5

Hz was used to reduce distortion of the more prolonged components of the raw EEG signals. The EEG signals were also high-pass filtered at 1 Hz in parallel as seen in Fig. 4.2 for computing the ICA sources as described in Section 4.6.4.1. A notch filter was used to attenuate the power-line component at 50 Hz. The raw EEG signals were then low pass filtered at 40 Hz to suppress muscle-related activity [107], [108]. On the other hand, the SEEG recordings were filtered differently, since intracranial recordings do not suffer from muscle activity contamination and therefore higher frequency components can be retained in the filtered signal. The raw SEEG signals were band-pass filtered at 0.1-195 Hz whereas a notch filter was used at [50, 100, 150, 200] Hz to suppress the power-line component and its harmonics. Once the signals were filtered, the raw signals were epoched to allow for the formation of the somatosensory evoked responses (SEPs). Figures 4.5 and 4.6 show the effect of filtering on the raw signals in the frequency domain and time domain, respectively. It can be seen that both the high frequency noise and the power line interference that was contaminating the raw EEG and SEEG signals was reduced after filtering.

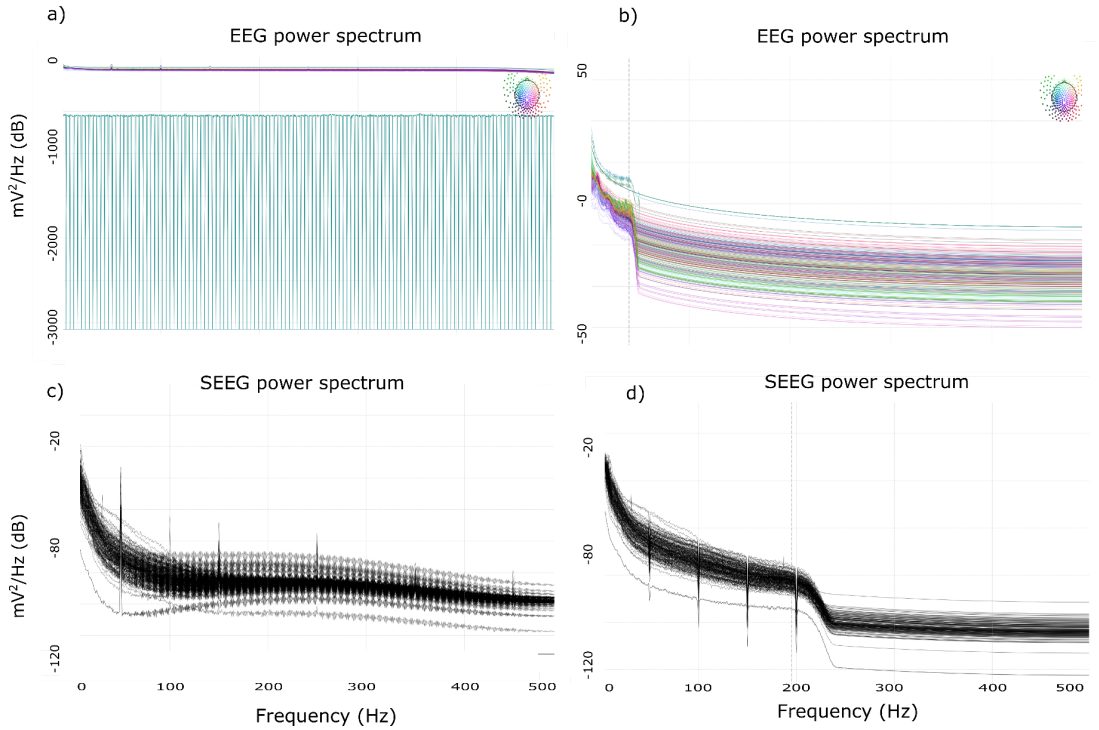

Figure 4.5. Effect of filtering: Power spectrum of a) raw EEG signals, b) filtered EEG signals, c) raw SEEG signals, d) filtered SEEG signals. The power-line interference in a) and c) significantly affects the power spectrum of the signals. After filtering b) and d), the power-line interference has been effectively reduced.

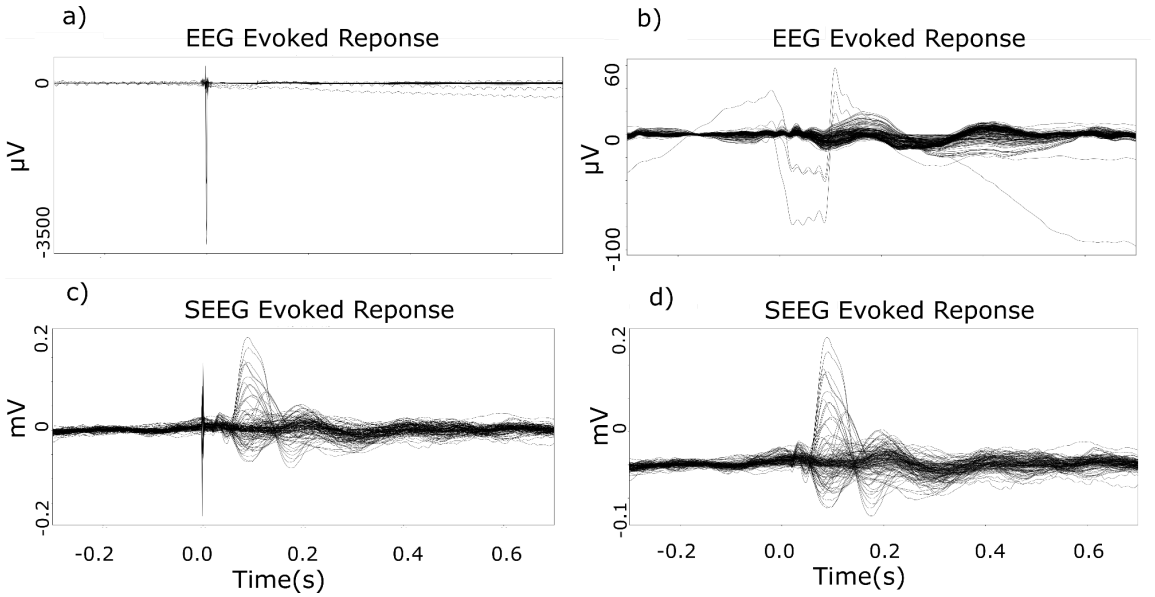

Figure 4.6. Effect of filtering: Time-course of evoked response of a) raw EEG signals, b) filtered EEG signals, c) raw SEEG signals, d) filtered SEEG signals.

4.6.3. Visual Inspection and Manual Rejection

Visual inspection of the recorded signals is arguably the most important step of any preprocessing pipeline for electrophysiological recordings. Due to the intra-subject variability and the artifact-sensitive nature of these recordings, a non-automatic visual inspection is recommended. This inspection can provide a rich overview of the recorded signals and the presence of potential artifacts including muscle activity, electrode disconnections, and saccades during the experimental procedure. Manual rejection of noisy or bad EEG channels and epochs was firstly performed. A segment of the epoched EEG signals is shown in Fig. 4.7, where high frequency noise and blink artifacts are present in several epochs and channels. Rejected channels suffered mainly from epileptic events or other artifacts that would distort the EP, or were disconnected. This step was very decisive as poor quality channels could affect artifact removal through inaccurate ICA decomposition but also distort average re-referencing.

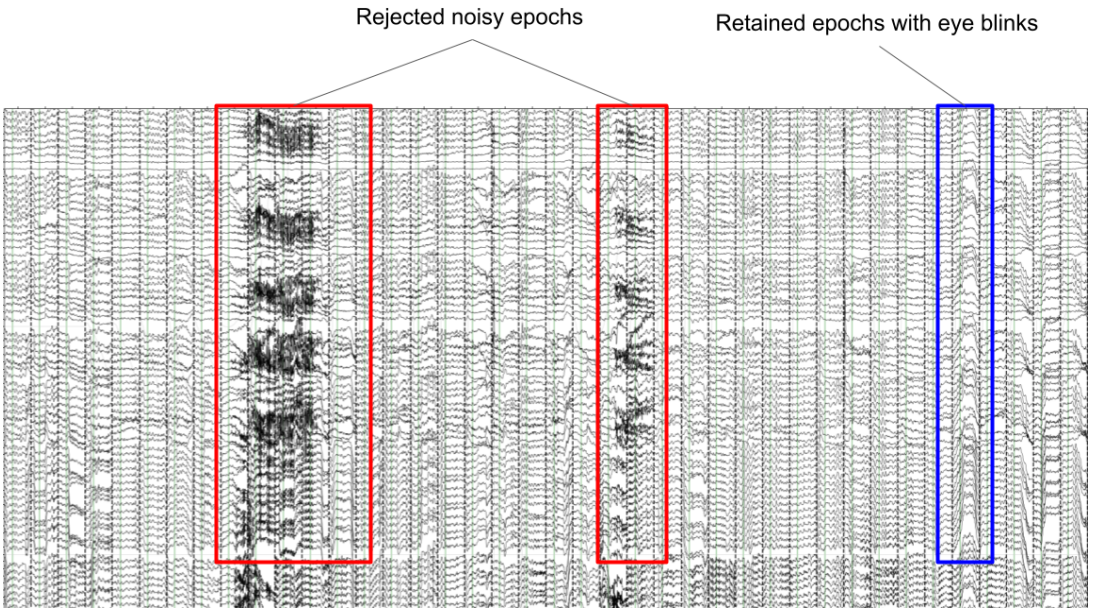

Figure 4.7. Segment of several epochs of the EEG signal.

As it can be seen in Fig. 4.8, the original signals were heavily distorted before manual rejection due to extreme amplitudes of channels caused by improper

electrode connection or epiletic events. However, after visual inspection and manual rejection of the bad channels, the typical SEP response was obtained. The further pre-processing steps such as artifact removal (ICA [86]) and artifact correction (Autoreject [87]) ensured that the residual noise due to eye blinks or other artifacts will be reduced.

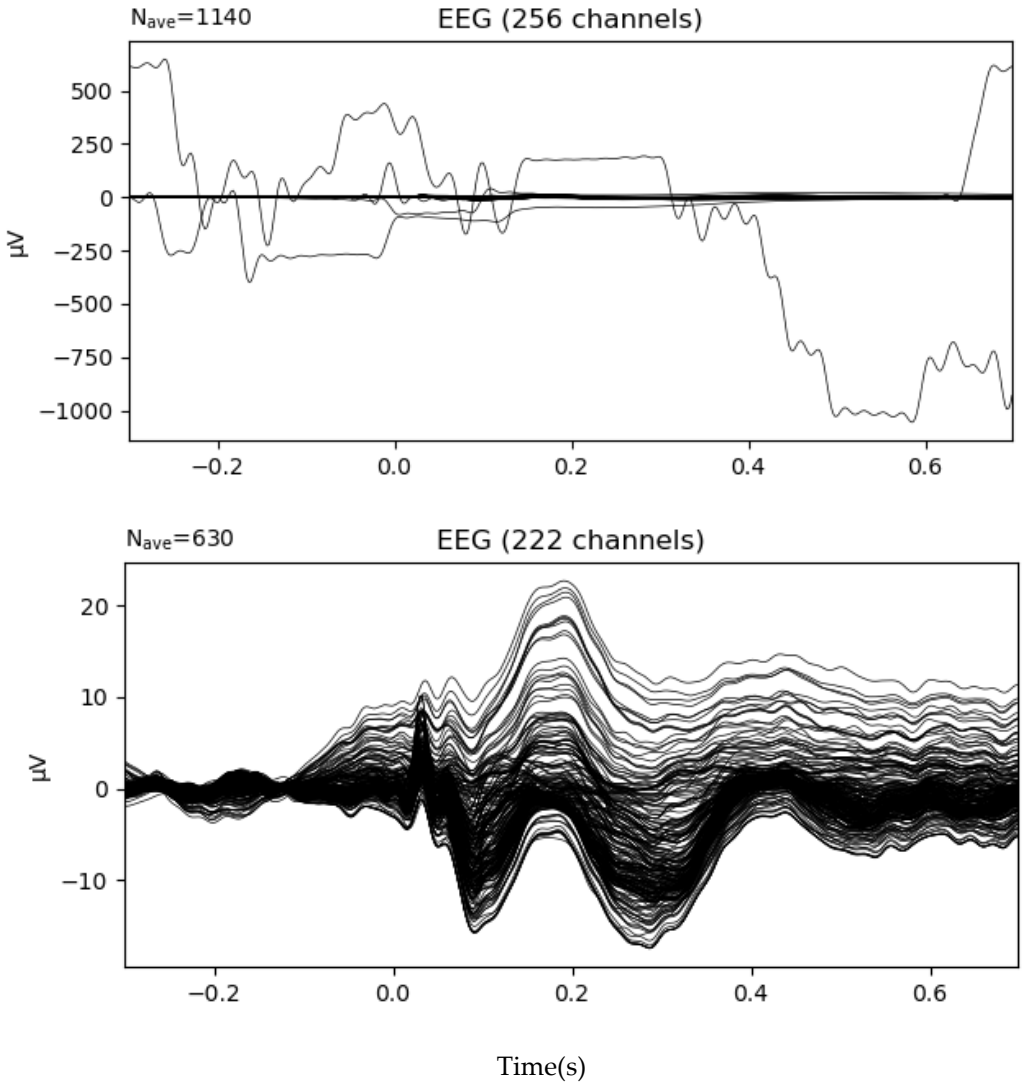

Figure 4.8. Manual rejection, filtering and stimulation artifact removal effect: (top) before and (bottom) after manual rejection EEG evoked responses. The number of trials for each of the evoked responses is shown at the top left corner of each graph. The number of retained channels before and after manual rejection is shown at the title of each subplot i.e.256 and 222, respectively.

4.6.4. Artifact Correction and Rejection

4.6.4.1. Independent Component Analysis

Independent Component Analysis has been successfully applied in the field of blind source separation in applications ranging from financial analysis to MEG data processing [86]. In the field of EEG processing it can be used to decompose the EEG recordings from each channel into a series of independent components [109]. Given the *-M-* EEG channels of extracranial recordings, ICA finds *-P-* unobserved statistically independent and non-gaussian generators (typically less than or equal to *-M-*) that can explain the observed data variance. An overview of the ICA-based artifact rejection module is shown in Fig. 4.9. The data in the sensor space was whitened using the noise covariance matrix. Then Principal Component Analysis projected the data from the sensor space onto a subspace with lower dimensionality whose dimensionality was dictated by the desired explained variance. It is worth mentioning that the assumptions governing ICA, namely, statistical independence and non-gaussianity do not hold from a physiological standpoint as it is known that there is a strong intercommunication in neuronal populations that renders the statistical independence hypothesis not true [109]. Despite the modelling imperfections, ICA has been shown to work well in isolating certain inherent and artifactual generators of the EEG signals such as cardiac rhythm contributions [110], muscle artifacts, and epileptic events [111], [112]. Most notably, ICA has been successful in capturing eye-related artifacts such as eye blinks and saccades, and has been used in most EEG analysis pipelines [113], [114]. Eye blinks are related to vertical eye movements and have typically a frontal distribution as seen in Fig. 4.10(a), with much larger amplitude than the background EEG activity. On the other hand, saccades are horizontal movements that project bilaterally on the frontal leads, shown in Fig. 4.10 (b) and have a stereotypical step-like time course. The time course of the first 6 independent

components arranged by the amount of the explained variance are shown in Fig. 4.11 where the eye blink and saccade artifact can be distinguished as the first and fourth ICA sources.

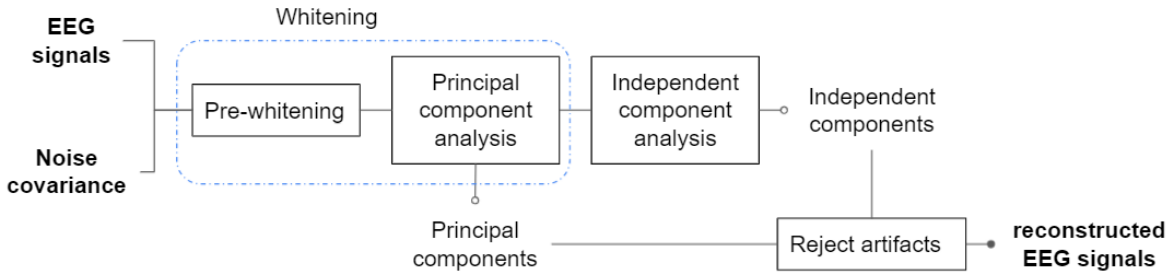

Figure 4.9. Artifact correction ICA module. The whitening step that removes spatial correlation between channels is illustrated inside the blue dotted frame. Once the independent components and principal components have been estimated using the FastICA algorithm, certain components associated with artifacts (e.g., blink) can be removed to produce the reconstructed artifact-free EEG signals.

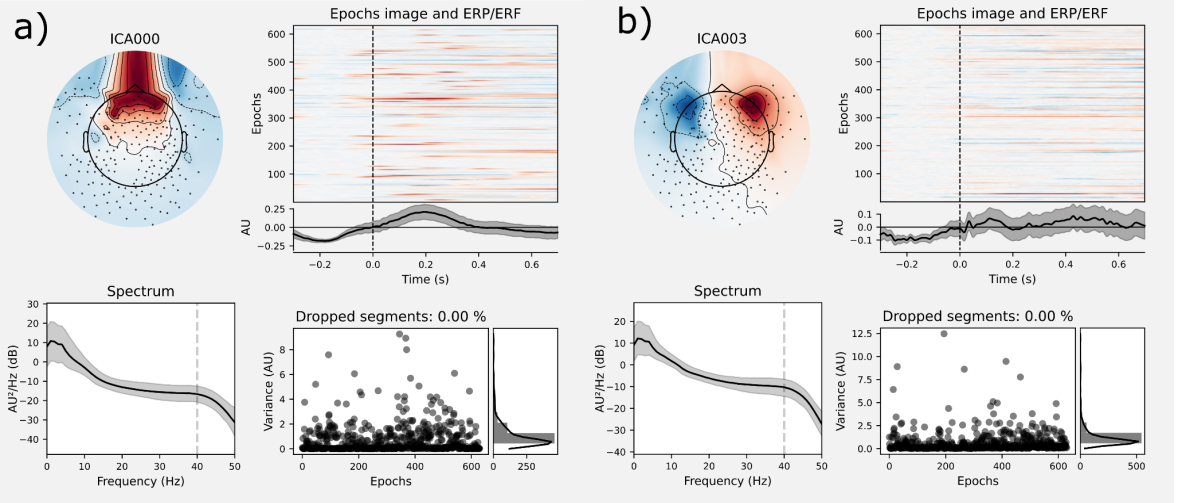

Figure 4.10. Rejected ICA components: (a) eye blink component scalp distribution and (b) saccades component scalp distribution

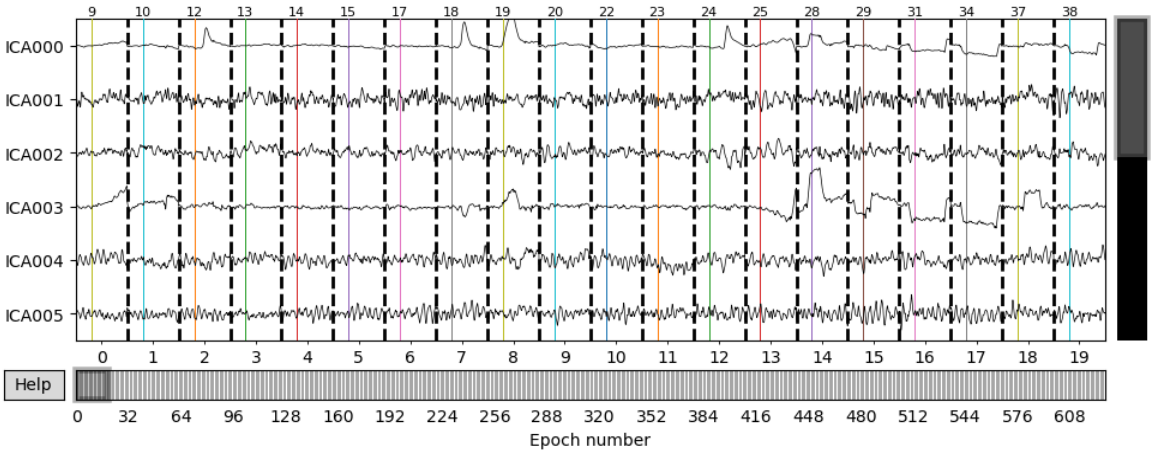

Figure 4.11.Time course of first 6 independent components where the eye blink and the saccade artifact is explained by the first component ICA000 and fourth component ICA003, respectively.

Given that any ICA source cannot ideally isolate only the artifactual components but instead captures also some physiological activity, in this project, ICA was used to remove eye blink artifacts and persistent saccadic movements. The selection of the rejected ICA components was done by inspecting the time course of the ICA sources and scalp field distribution of the ICA components. The results of the ICA-based eye blink artifact removal is shown in Fig. 4.12, where it can be seen that eye blinks heavily contaminate the evoked response. The strong contribution of eye blinks may be attributed to the fact that during electrical median nerve stimulation the subjects tend to naturally react by blinking.

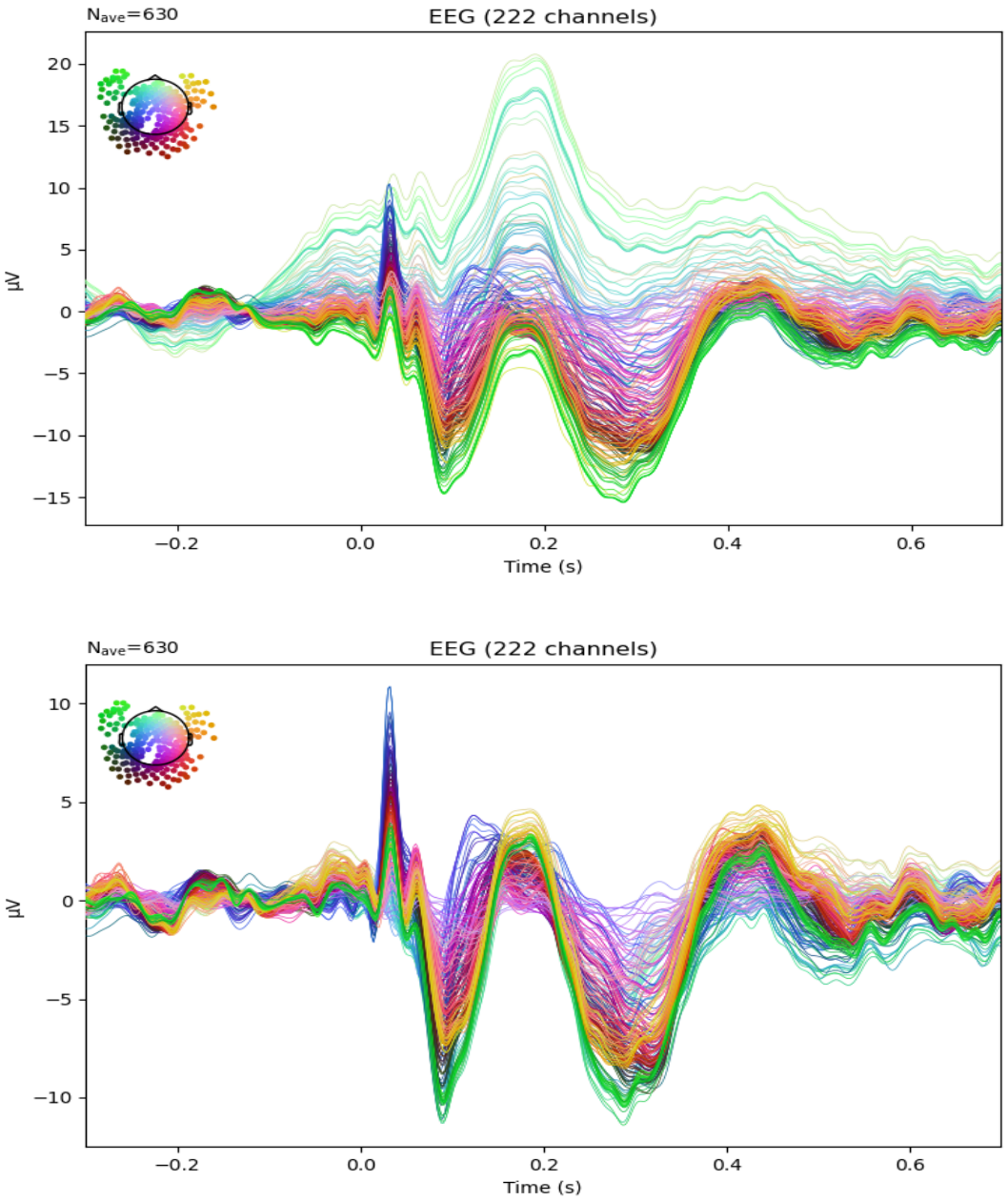

Figure 4.12. Effect of ICA-based artifact correction on the EEG signals: (top) before and (bottom) after artifact correction.

4.6.4.2. Automatic Trial Correction and Rejection

After ICA-based artifact rejection of eye blinks and strong saccades has been performed, the automatic artifact correction algorithm Autoreject was employed to correct or reject trials based on the statistical properties of the available channels [87]. More specifically, cross-validation was used to estimate the channel-wise optimal peak-to-peak thresholds, thus, enabling the designation of bad trails at the level of individual channels. By using two learned parameters, namely, -κ- the maximum number of bad channels in non-rejected trials and, -ρ- the maximum number of sensors that can be interpolated, the algorithm can select to repair bad trials by interpolation or by exclusion [87]. In practise, sensor-level thresholds were firstly determined followed by marking of bad segments for each sensor. Then, trials were rejected only if the number of bad sensors was higher than κ while the worst ϱ sensors were interpolated using spherical splines [115]. The effect of Autoreject on the epoched EEG data is shown in Fig. 4.14. Although ICA has effectively reduced the strong eye blink and saccade artifacts, Autoreject rejects those trials that are statistically different between adjacent channels, thus resulting in more consistent statistical properties between channels. Figure 4.13 shows a screenshot from several EEG epochs, where the rejected, retained channels and trials are highlighted in different colours. It can be seen that some trials have been rejected (red colour) which are significantly different from the remaining trials. Additionally, certain trials were corrected (gray) which allows to retain epochs that would otherwise need to be rejected.

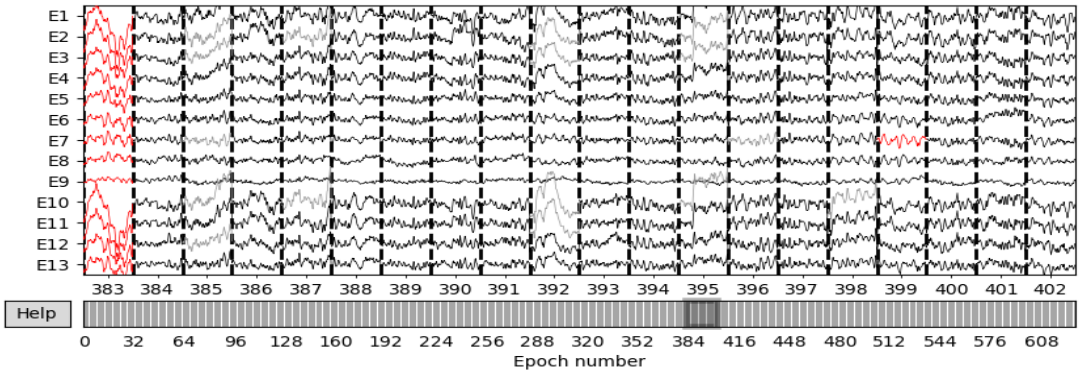

Figure 4.13. Autoreject-based artifact correction: retained (black) and rejected (red) and corrected (gray) trials.

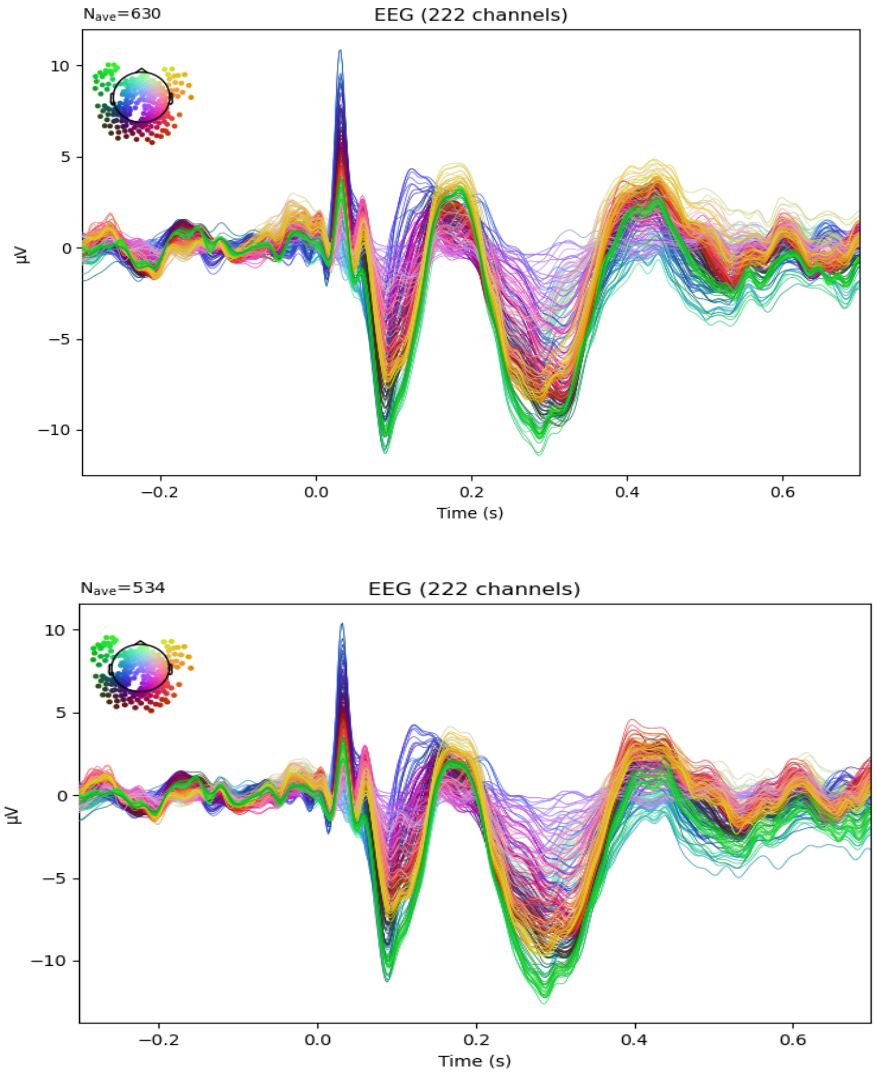

Figure 4.14. Effect of Autoreject-based artifact correction on the EEG signals: (top) before and (bottom) after artifact correction.

4.7. Averaging and Re-reference

Once the raw signals have been visually inspected, filtered, epoched and the EEG artifacts have been corrected, the somatosensory evoked responses (SEPs) and intracranial SEPs (iSEPs) can be formed. Obtaining the SEPs/iSEPs requires averaging across all available trials to remove background noise as seen in Fig. 4.15. It is expected that during the averaging process, noise which is stochastic across different trials will be reduced while the response which is time-locked to the median nerve stimulation will be strengthened. Although the aforementioned preprocessing workflow has been designed in a way to reduce artifacts and enhance the information of interest i.e., SNR of SEPs, some residual undesirable background activity may still be present in the clean signals. Consequently, if the unipolar reference channel (e.g., Cz) is contaminated with residual artifacts, it can influence the quality of all other channels. To remove such dependency, average re-reference of the clean signals was performed as the last step of the pre-processing workflow. This step ensured that the reference signal was composed by averaging signals from all available channels, thus, reducing channel-specific artifacts.

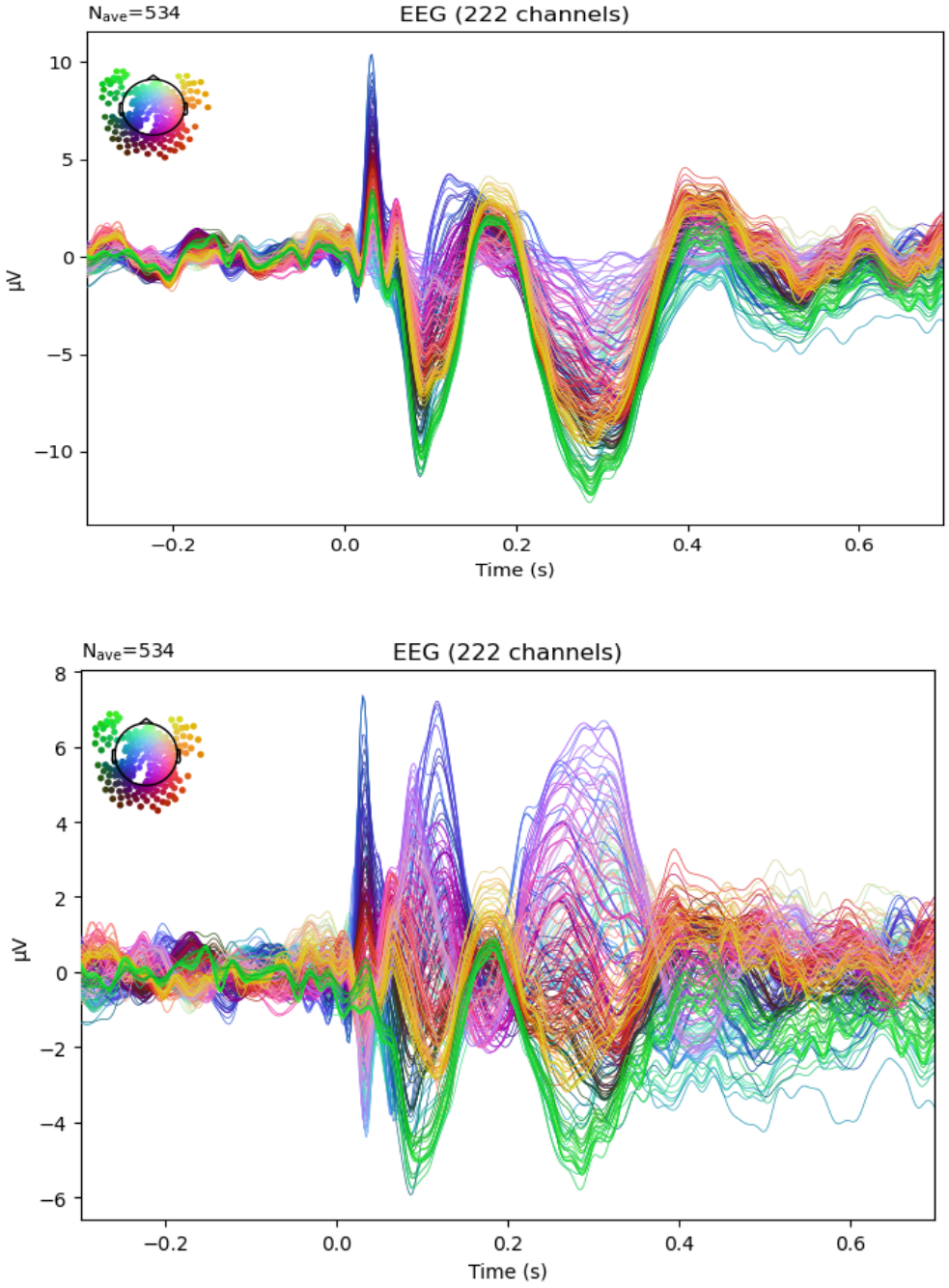

Figure 4.15. Effect of average re-referencing on the EEG signals: (top) before and (bottom) after re-referencing.

4.8. Gamma Profile of Intracranial Signal

The SEEG electrodes were categorized in 2 classes based on the gamma profile clustering algorithm developed by Avanzini *et al.* [4]. High-frequency broadband gamma activity (50-150 Hz) was used as an index of cortical activity since it is spatially and functionally more specific compared to other frequency bands and reflects activation of neural population, enabling the study of neural networks at millisecond-scale. The authors have shown that certain brain structures associated with somatosensory processing such as area 3b and operculum respond differently to the median nerve stimulation. More specifically, two distinct responses were identified, namely, phasic and tonic corresponding to an early, short lasting or a late, prolonged response, respectively. The results of this study were reproduced for the purpose of this thesis by implementing the following steps:

1. The raw SEEG signals from all leads in the gray matter were filtered (band-pass: 0.1-195 Hz, notch: 50, 100, 150, 200 Hz)
2. Individual channels and trials were rejected upon visual inspection.
3. Morlet wavelet transform was applied on each trial for each SEEG channel. The computed coefficients were used to compute the power in the gamma frequency band [50-150] Hz in the window [-100, 500] ms, divided into 60 non-overlapping 10 ms bins.
4. Normalization (z-score) relative to the prestimulus interval [-100, 0] ms was used to allow for comparison between patients and leads.

The obtained results shown in Fig. 4.16, match closely the ones presented in the literature as shown in Fig. 4.17, where an early (~30 ms) increase in gamma activity is associated with the primary somatosensory area such as Brodmann area 3b while a later (>50ms) increase in gamma activity is linked to secondary somatosensory areas such as the insula and operculum.

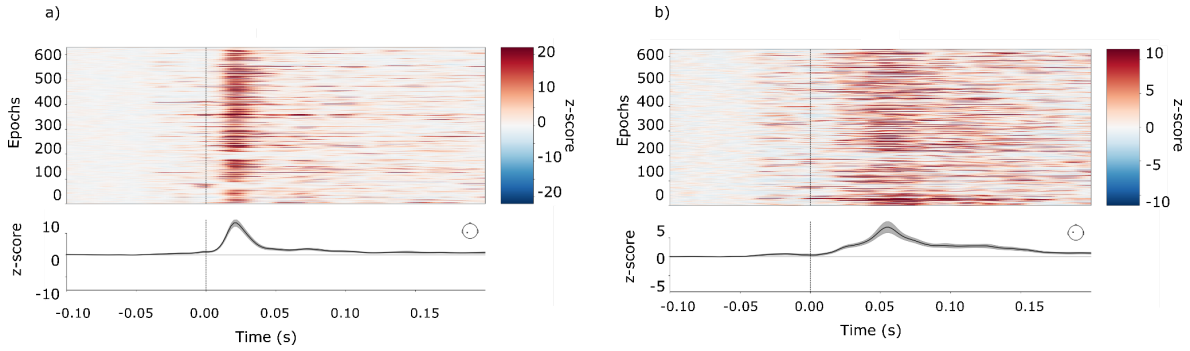

Figure 4.16. Clustering of iSEPs based on the position of the SEEG electrode using a custom-built function: (a) phasic, and (b) tonic area.

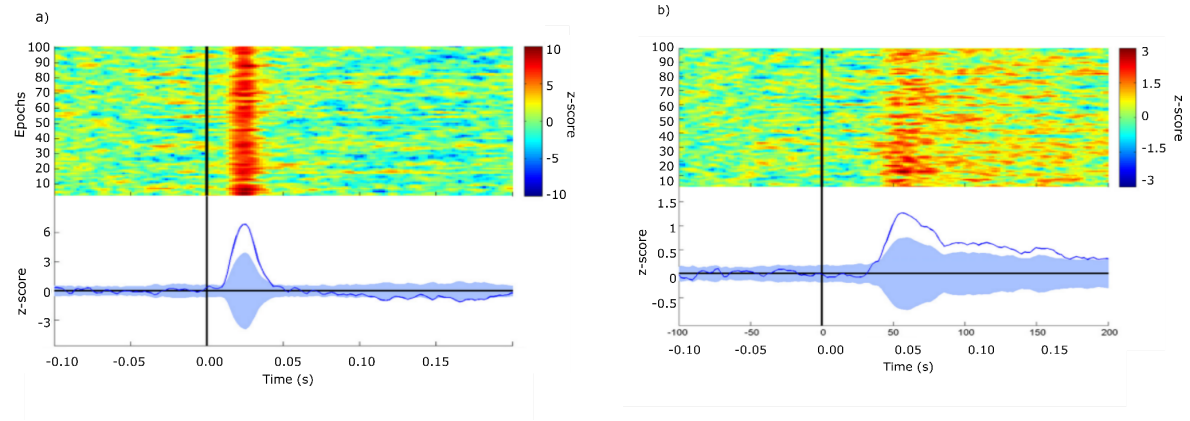

Figure 4.17. Clustering of iSEPs based on the position of the SEEG electrode: (a) Brodmann 3b area, (b) parietal opercular OP1 area (*image adjusted from* [4]).

4.9. Source modelling

Recordings from the scalp such as EEG or MEG can provide information about the activation distribution of cortical areas in the millisecond scale. However, it may often be of interest to pinpoint the location of the neural generators that gave rise to the signals recorded at the scalp level. To this end, source localization or source modelling can be employed to reveal the underlying brain areas responsible for the generated EEG signals [14]. Typically, source modelling involves modelling how neural signals propagate through the brain volume to the surface electrodes, termed as forward solution as well as estimating the locations/ orientations/

intensities of signal generators, termed as inverse solution. Estimating the location/orientation/intensity of the signal generators (i.e. sources) that gave rise to the surface recordings, one can associate active neural structures with the SEPs. It has been postulated through SEEG studies that the somatosensory processing involves a wide network of neural structures with specific structures being active short (e.g., 20-30 ms) (i.e., phasic components) while others become active later and remain active for longer time (i.e. tonic components) after median nerve stimulation [4], [53], [80]. In this thesis, source modelling is performed using EEG whereas the reconstructed sources are then compared and analysed with the simultaneous SEEG recordings.

4.9.1. Forward Solution

The first step in source modelling is obtaining the forward solution which aims at finding a mapping between a set of predefined brain sources and the available EEG recordings [15]. The forward solution requires:

1. Establishing the conductivity parameters in the brain volume
2. The type of sources (e.g., dipoles) and their location.
3. The EEG electrode position.

The determination of the conductivity parameters in the brain volume depends on the assumed head model. In the literature, several models have been proposed ranging from simulated or MRI-derived head shapes where the most popular are summarized below:

- Simulated head models offer the simplest head models. Although a forward solution can be efficiently obtained by analytical solvers, these models do not exhibit neurophysiological plausibility:
    - The single layer spherical model assumes that the whole brain volume has constant and identical conductance.

    - The 3-layer spherical model assumes that the brain consists of 3 layers whereas each layer has different conductance.
- Realistic head models are more accurate from a neurophysiological point of view since they are MRI-derived but require numerical solves which are more computationally expensive:
    - The finite element method (FEM) digitizes the entire brain volume in small elements whereas the vertices of the elements are used as computational points. Several considerations exist when FEM is implemented such as the way the dipoles are represented in the model. A thorough investigation of FEM is outside the scope of this thesis and the reader is referred to [15] for a thorough review of forward solutions.
    - The finite difference method (FDM) breaks down the brain volume in a structured grid which agrees with the segmented volume conductor constructed using cubic voxels. A thorough investigation of FDM is beyond the scope of this thesis and the reader is referred to [15] for a thorough review of forward solutions.
    - The boundary element method separates the brain volume into different compartments such as brain, skull and scalp. The different brain compartments are separated by interfaces (i.e., triangulated surfaces) and are assigned different conductivity values. The accuracy of the forward model depends on the number of mesh nodes of the triangulated surfaces. Increasing the available nodes where the potential can be calculated increases the accuracy of the model while the computational complexity is also increased.

Both FEM and FDM lead to a significantly larger number of computational points than the boundary element method (BEM) which was chosen for this thesis.

Furthermore, the type of sources as well their location/orientation/intensity may be varied and depend on the tradeoff between desired accuracy and computational efficiency. Once the sources and the volume conduction properties have been determined, the Poisson's equations can then give the relationship between the current sources and the potentials at any point in the considered volume conductor. Lastly, the EEG digitized electrode positions are used to compute the obtained signals at scalp level given a specific source-conductivity configuration. Figure 4.18 shows an overview of the forward problem and the different factors that influence the forward solution. The output of the forward model is the gain matrix which provides a mapping from the assumed sources to the scalp electrode position. Therefore, the potential at all EEG channels can be estimated using the gain matrix.

Source modelling was implemented using the MNE-Python package where the surface reconstructions were obtained using FreeSurfer. The BEM model was generated, having 3 layers, namely brain, skull and scalp compartments of 0.3, 0.006, 0.3 S/m conductivity, respectively. In total 5120 triangles were used while the source spaces were created with 4098 sources (i.e., vertices) in each hemisphere. The obtained forward solution was then used to solve the inverse problem and estimate the brain areas responsible for the recorded EEG signals.

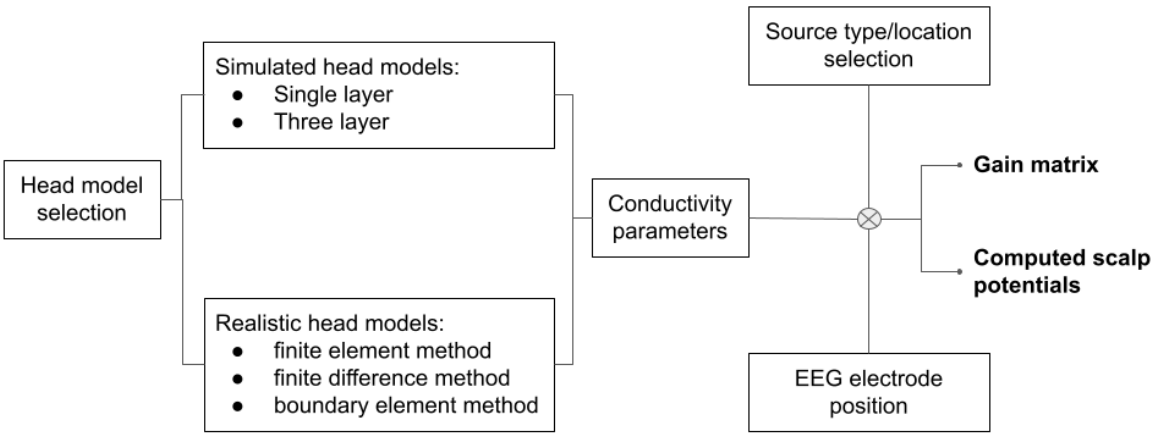

Figure 4.18. Overview of the forward solution in source modelling. The main three parameters that define the forward solution are the head model selection and therefore the conductivity parameters, the source type and location as well as the EEG electrode position. These three factors determine the gain matrix and the computed scalp potentials.

4.9.2. Inverse Problem

The second stage of the source modelling comprises the inverse problem, where the position, orientation and strength of the neural sources that gave rise to the recorded EEG signals are estimated. Given that many signal sources are assumed to be present in the brain volume, different combinations of the generated signals can lead to the same measured electrodes. To tackle the ill-posedness of the inverse problem, electrophysiological neuroanatomical constraints have to be applied to reduce the possible configurations of the neural sources. Typically, EEG inverse modelling involves estimating the six parameters that uniquely specify a dipolar signal source, namely, three spatial coordinates and three dipole moment components (two orientation angles and the moment strength). However, the

unknown parameters can be reduced, thus reducing the computational complexity if some physiological constraints are imposed. For example, one may consider that the orientation of the dipoles is perpendicular to the cortex since this is how pyramidal neurons are arranged near the brain surface [1]. One should note that the correctness of these constraints determines the correctness of the inverse modelling. Other factors that can affect the accuracy of inverse modelling include the forward model accuracy, the considered head model, and EEG noise [14]. An overview of the inverse solution in source modelling is shown in Fig. 4.19.

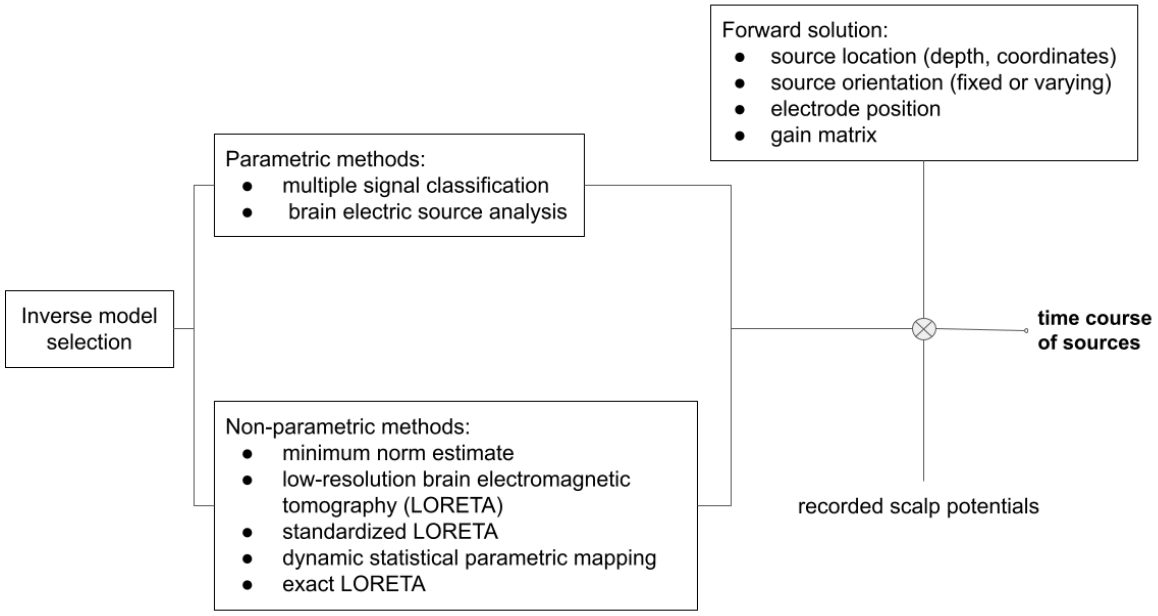

Figure 4.19. Overview of inverse solution in source modelling. The inverse solution results in estimating the time course of the reconstructed neural sources. This estimation depends on the forward solution, the EEG recordings and the neurophysiological constraints imposed during inverse modelling.

Significant advances have been achieved in EEG source localization in recent years, evolving from single dipole searching methods to distributed source estimation approaches [1]. Additionally, depending on whether a fixed number of

dipoles is assumed *a priori* or not, non-parametric and parametric approaches have been proposed in the literature [14]. To reduce computational complexity and constraint the optimization problem, a typical approach is to assume that the orientation of the dipoles is perpendicular to the cortex (the amplitudes and directions are then estimated leaving only unknown the position). In this section, parametric methods are briefly presented while the main focus is on non-parametric inverse modelling approaches. Various non-parametric methods were investigated in this thesis in an effort to find an optimal approach for the given data. The results of the selected method are presented in Section 5.4.

4.9.2.1. Parametric methods

Parametric or source scanning methods can be used to solve the inverse problem by scanning the brain volume and assigning a certain probability that any given point in the volume is active. As a result, the best dipole position(s) and orientation(s) are returned while the models range from a single dipole in a simulated head model to multiple dipoles in a realistic head model [14]. Popular parametric methods include beamformers (i.e., spatial filters), the multiple signal classification (MUSIC) and the brain electric source analysis (BESA). MUSIC has been used to identify signal sources inside the brain volume (i.e., solution space) that produce patterns that reside in the signal subspace of the EEG measurement [116]. BESA considers consecutive time points in which the dipoles position is fixed while the orientation can be also fixed or varying. Although this method minimizes a cost function that takes into account several statistical factors such as the residual variance, the accuracy depends on the initial guess of the number of dipoles [117].

4.9.2.2. Non-parametric

The class of non-parametric inverse modelling methods considers that reconstructed brain activity may span more than a few focal dipolar sources. Distributed source models assume that several dipoles with fixed location and fixed/ varying orientation are distributed within the brain [14]. Typically the whole cortex is modelled by dipoles and then probability values are assigned to each dipole given the potential distribution at scalp EEG. Moreover, regularization can be used to impose neurophysiological constraints and penalize a solution that deviates from the prior assumptions or the predetermined smoothness of the current distribution [90]. Several non-parametric methods are presented:

- Minimum Norm Estimate (MNE) can be used when the dipole activity is expected to extend over several areas near the cortical surface. Although MNE is a well-established method that searches for the solution with minimum power, poor estimation of the true locations of the signal sources has been reported [118]. The poor performance may also be attributed to the fact that MNE privileges superficial dipoles due to smaller magnitude.
- Low-resolution brain electromagnetic tomography (LORETA), introduced by Pascual-Marqui, achieved a superior performance than MNE [89], [118]. By assuming that sources are distributed smoothly in the brain volume, LORETA maximizes the smoothness of the solution. A significant advantage over MNE is that LORETA allows for depth compensation by giving shallow and deeper dipoles the same opportunity to be reconstructed [89]. However, LORETA may not perform optimally when focal sources need to be estimated.
- Standardized LORETA (sLORETA) uses the current density estimation provided by MNE and standardizes the solution using its variance. The variance is assumed to be due to actual source variance and variations due to noise in measurements [90].

- Dynamic statistical parametric mapping (dSPM) is another popular method that standardized the estimated density. In contrast with sLORETA, the standard deviation for the current density in dSPM is assumed to be due to exclusively measurement noise [92].
- Exact LORETA (eLORETA) was most recently developed to achieve a zero localization error for point sources positioned anywhere in the brain volume under ideal conditions [91].

The computation of forward solution as well as the inverse solution through distributed source models assume zero mean Gaussian noise with equal variances across channels. The recorded data may be contaminated with i) biological noise including the heart beat, eye blinks, and muscle activity, ii) environmental noise such as power line interference and iii) channel-related noise. In addition, purely channel-related noise is expected to be independent across channels. Therefore, the between-channel correlations related to channel-related noise need to be suppressed. This process is also termed spatial whitening and involves estimating the additive noise from the recorded data and transforming the data into independent white noise vectors with identical variance across the different channels. Several approaches have been proposed to estimate the spatial covariance based among others on the computation of empirical covariance, shrinkage models [119] and factor analysis [120]. For the source modelling of this project, an automatic algorithm was used for selecting the best estimator of the spatial covariance based on log-likelihood and cross-validation on unseen data [40].

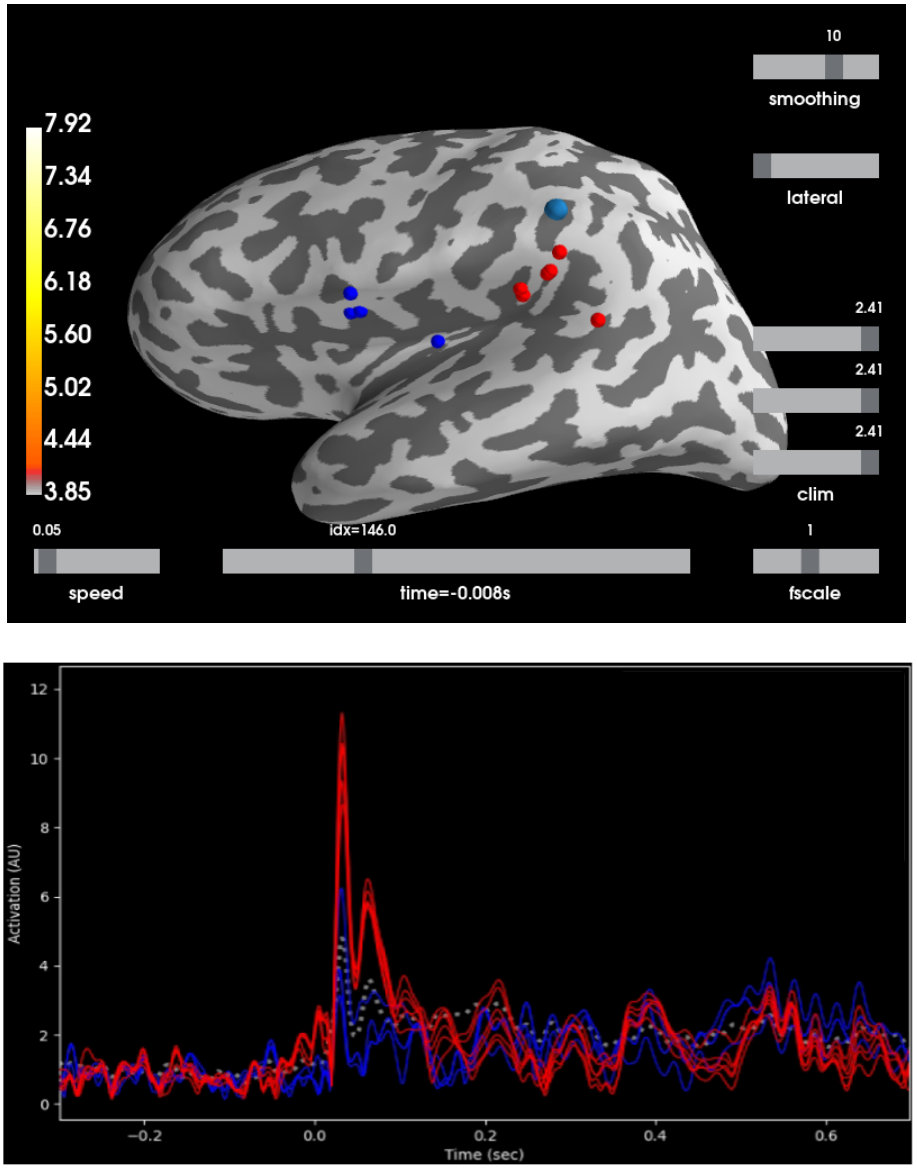

Figure 4.20. Graphical user interface showing the setup for the analysis of source modelling: The location (top) /time course (bottom) of phasic and tonic electrodes is shown in red and blue, respectively.

In the context of this thesis, the epochs were re-referenced to the average of all retained channels (*see* Section 4.7) following bad channel and trial correction and rejection. After computing the forward solution, inverse solutions were calculated using MNE, dSPM, eLORETA and sLORETA. The results of the source modelling

are presented and discussed in Chapter 5. Once the source modelling was completed, the activity of all 8196 considered signal sources in both hemispheres was reconstructed. Certain reconstructed sources were selected from the available sources to be further investigated based on their proximity to the tonic/phasic SEEG contacts clustered as described in Section 4.8. More specifically, the activity of sources located at brain areas known to be assigned to a phasic and tonic cluster was plotted along with the exact positioning of the intracranial sources on an inflated brain using an adjusted graphical user interface (GUI) from MNE software. This GUI allowed for comparison of the temporal dynamics between the reconstructed sources and the ones obtained from the intracranial study by Avanzinin *et al.* [4]. More details on the GUI are provided in Fig. 4.20 and Chapter 5. The source modelling for the presented subject involved 4 phasic (red) and 4 tonic (blue) sources. Figure 4.20 shows the location of the sources on an inflated brain as well as the point with maximum activation (dark cyan) during median nerve stimulation.

4.10. Estimated Sources Time-Frequency Analysis

If the spectrotemporal variations of the reconstructed sources is of interest, time-frequency analysis methods such as short-time Fourier transform (STFT) can be used. The STFT method was used to transform the 1-D time signal into a 2-D time-frequency plane, where the variations of the spectral content could be revealed over time. Since previous work on iSEPs exploited the gamma band for clustering the iSEP components into phasic or tonic, it was of interest to investigate if the reconstructed sources also exhibited distinct spectral properties that depended on the location of the sources. The 2-D time-frequency plane was calculated by sliding a moving Hann window of 20 ms along the reconstructed source time course and computing the fast Fourier transform (FFT) with 1024 points at each window (zero padded at both ends). An overlapping of 50% was

employed to avoid losing points near the edges of the tapering window. For each time window, the spectral content was computed in the range [0.5, 40] Hz since that was the original frequency range of the filtered EEG signals used in the source modelling. The magnitude of the complex exponentials taken as output from the FFT algorithm was used to quantify the activation of specific frequencies along time as shown in Fig. 4.21. The time-frequency plane consists of the frequency range in the y-axis and the time in the x-axis. Thus, it can provide information about the activity of a source in a specific time point and frequency value.

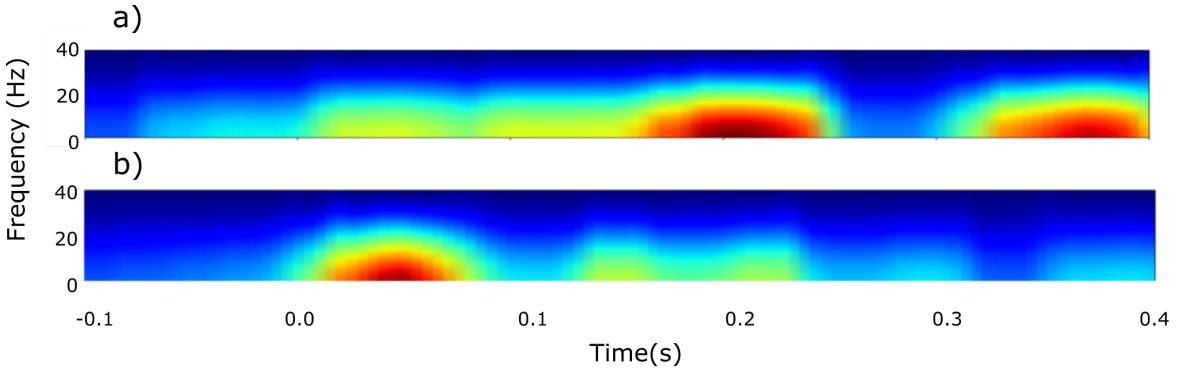

Figure 4.21. Time-frequency analysis of a) tonic and b) phasic reconstructed sources.

4.11. Intracranial activity prediction

Predicting the intracranial activity based on extracranial recordings such as M/EEG can be of great importance when activity from certain brain structures such as insula or amygdala cannot be measured noninvasively. There is an increasing interest to enable the disentanglement between activity originating from deeper structures and neocortical networks. Recently, independent component analysis (ICA) has been exploited to correlate activity recorded by MEG and SEEG from mesial sources [121]. Although ICA topographies have been extensively used to localize brain activity, there has been a debate on whether such methods can provide neurophysiological interpretability. More specifically, one

may consider multivariate linear models used in neuroimaging (e.g., ICA) as both forward and backward models. Forward models of the data express how the recorded neurophysiological data was generated from the neural sources, thus expressing the recorded data as a function of latent variables (i.e. encoding). On the other hand, backward models of the data aim to reverse the data generating process, thus, expressing the neural latent variables as a function of the recorded data (i.e. decoding). It has been shown that the parameters of forward models exhibit neurophysiological interpretability as opposed to parameters of backward models [122]. To this end, temporal response functions (TFRs) have been introduced in [17] as encoding forward models. The multivariate TFR (mTFR) is derived from a regularized linear regression function that maps the brain signals recorded at the surface of the scalp to the stimulus (e.g. audio signal) or the intracranial activity. Alternatively, mTFRs can be considered as filters that transform the ongoing stimulus to the ongoing neural response. This method has been recently used to reconstruct the speech signal that gave rise to EEG recordings [17].

In the context of this thesis, we implemented this method to perform intracranial activity prediction based on the EEG recordings. The acquired mapping allowed us to predict the neural response at the SEEG level given the EEG activity enabling the analysis of the underlying decoding and encoding mechanisms, respectively. It was shown that the tonic activity, i.e., activity present in the opercular and insular areas, could be estimated by exploiting extracranial recordings. The predicted tonic activity was compared with the ground truth SEEG tonic activity to evaluate the performance of the prediction.

5. Results and Discussion

In this chapter, the statistical characteristics of the available data are presented along with the coregistration of EEG and SEEG. The results of the proposed preprocessing workflow are analyzed and discussed. The source modelling of the EEG signals as well as the time frequency analysis of the source activities are presented followed by the introduction of preliminary results on the prediction of intracranial activity based on extracranial recordings. To the best of our knowledge, somatosensory evoked potentials of median nerve stimulation have not been explored with simultaneous HD-EEG and SEEG modalities.

In summary, the following hypotheses were tested as part of this thesis:

1. Reconstructed signals from source modelling on the EEG recordings exhibit phasic and tonic behaviour depending on the location of the source (e.g., SI vs SII).
2. Intracranial tonic activity can be predicted by extracranial recordings. The predicted intracranial activity is compared against the groundtruth activity provided by the SEEG recordings.

An overview of the project is shown in Fig. 5.1, where the different stages of processing and analysis are schematically displayed. The median nerve stimulation protocol was performed at stimulation intensities ranging from 4-9 mA in a total of 11 sessions as illustrated in Fig. 5.2. Coregistration of HD-EEG and SEEG signals was performed during median nerve electrical stimulation in 8 subjects. Section 5.2 discusses some unique features of simultaneous HD-EEG and SEEG recordings. The EEG signals were preprocessed (top trace) to improve the SNR and correct artifacts such as eye blinks and strong saccades. It was shown that after implementing the proposed preprocessing workflow, the activity of somatosensory processing areas were revealed (*see* Section 5.3). The artifact-free

EEG signals were then averaged to obtain the somatosensory evoked responses (SEPs). Moreover, the clean SEPs were used to obtain the forward solution based on realistic MRI-derived head models with 8196 sources. Following forward modelling, non-parametric distributed inverse solutions were investigated to reconstruct the neural sources involved in somatosensation. It must be noted that the distributed nature of somatosensory processing was shown to require distributed inverse modelling to enable testing of the hypotheses presented at the start of this chapter. Time-frequency analysis of the time course of signals showed that electrodes near SI and SII exhibit different activation patterns, supporting the finding of the intracranial study in [4]. The SEEG signals were preprocessed (bottom trace) to remove epileptic and stimulation artifacts. Clustering of the intracranial contacts was performed based on their gamma profile to assign certain electrodes as phasic or tonic [4]. Given the ground truth of intracranial activity of phasic and tonic SEEG electrodes, it was shown that the intracranial activity can be predicted using EEG signals.

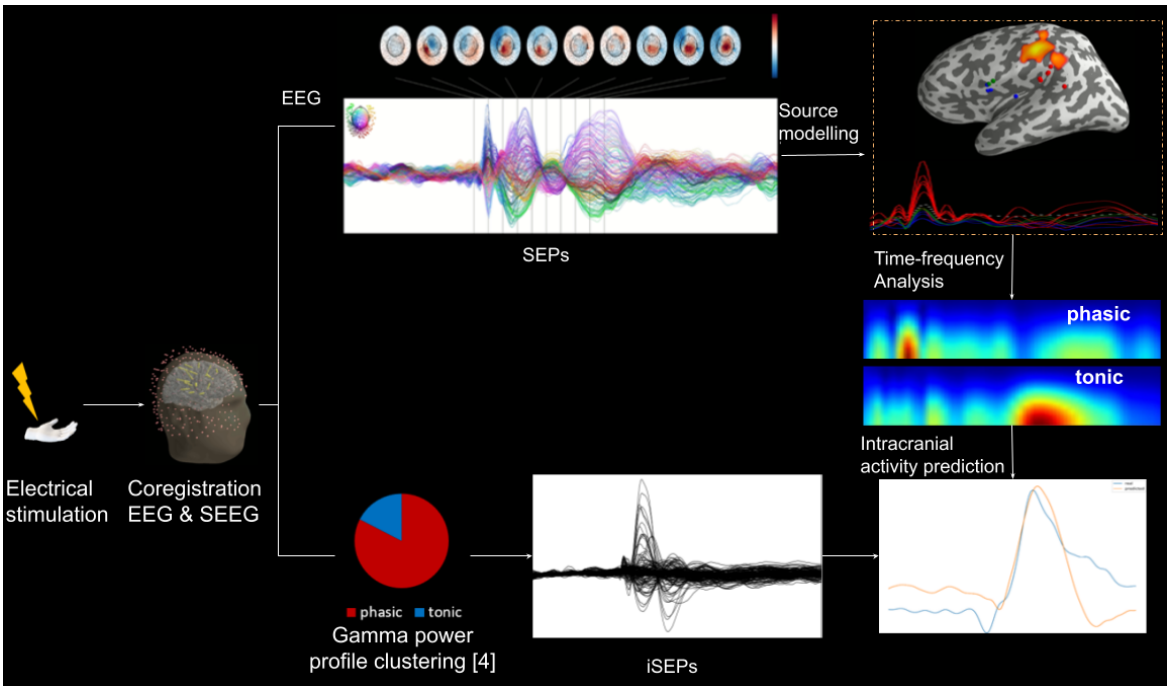

Figure 5.1. Overview of the thesis methodology and results.

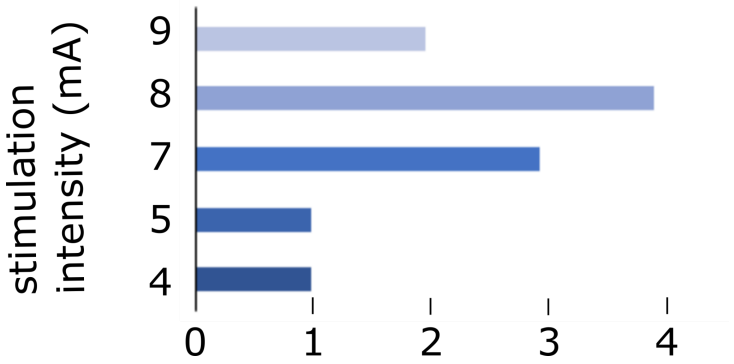

Figure 5.2. Number of sessions by stimulation activity.

5.1. Challenges of simultaneous HD-EEG and SEEG analysis

The recording setup used to acquire the simultaneous EEG and SEEG signals as well as the proposed preprocessing workflow exhibit distinct characteristics compared to other state-of-the art studies employing solely EEG, or SEEG. The distinctive features are listed below:

1. Synchronizing the EEG and SEEG recordings is very important as the activity recorded intra- and extracranially must reflect the same exact instance to enable the simultaneous analysis. An example to appreciate the importance of synchronizing EEG and SEEG signals is the case where an epileptic spike is present in a SEEG trial. One may consider removing only the SEEG trial since the EEG signal does not necessarily appear contaminated with the epileptic activity. However, such an action would distort the timing of the intra- and extracranial activity. Therefore, it is important to perform trial correction and rejection in a unified EEG and SEEG framework by ensuring synchronization and the same number of trials intra- and extracranially.
2. The coregistration of EEG and SEEG implies that an EEG cap is placed on top of the implantable electrodes, thus, leading to potentially unstable EEG contacts. In addition, the laterality of SEEG implantation typically

introduces an asymmetry of the EEG electrode arrangement. An example of coregistration in 3D from two different patients is shown in Fig. 5.3. The SEEG electrodes located on the left hemisphere caused some EEG electrodes to have a less close connection with the scalp compared to the right hemisphere. This effect can also be viewed in Fig. 5.4 where the EEG electrodes are placed on a two-dimensional grid.

3. A different effect of the coregistation is that the activity and artifacts picked up by the SEEG electrodes may contaminate the EEG signals. Due to the fixed position of the implanted electrode, EEG placement becomes significantly more challenging while high density EEG (HD-EEG) involves 256 electrodes which inevitably may be close toSEEG electrodes. An example of an artifact which typically is not present in studies employing solely EEG, is the stimulation artifact. Although it has been shown that intracranial electrodes pick up the electrical stimulation signal due to volume conduction [97], EEG recordings are normally free of stimulation artifacts possibly due to the skull, cutaneous tissue and skin layer which acts as an additional filter on the picked up electric field. Figure 5.5 shows the effect of volume conduction on both EEG and SEEG recordings. Moreover, the presence of stimulation artifact in the EEG signals was shown to affect the source modelling since the stimulation artifact can be topographically different from the background activity and thus cannot be removed during spatial whitening. Consequently, if the stimulation artifact is not removed from the EEG signals, the reconstructed sources derived from the inverse solution exhibit a peak at 0 ms which can affect the interpretation of the estimated activity. Therefore, the stimulation artifact procedure is recommended to be performed on both the EEG and SEEG signals as a first step of preprocessing.

4. When processing and analyzing simultaneous EEG and SEEG recordings, one should take into account that there may be certain timing discrepancies between the acquired EEG and SEEG data which may be due to the inherent difficulty to synchronize the EEG and SEEG amplifiers with the trigger signal. Additionally, from a neurophysiological perspective, the SEEG electrodes sample directly activity from brain regions while EEG electrodes record electrical field changes that initiate from potentially distant subcortical sources. Consequently, inferring intracranial activity based on extracranial recordings and vice versa should be cautiously performed and account for timing discrepancies between EEG and SEEG due to electric field propagation delays, volume conduction and other limitations presented in this section.

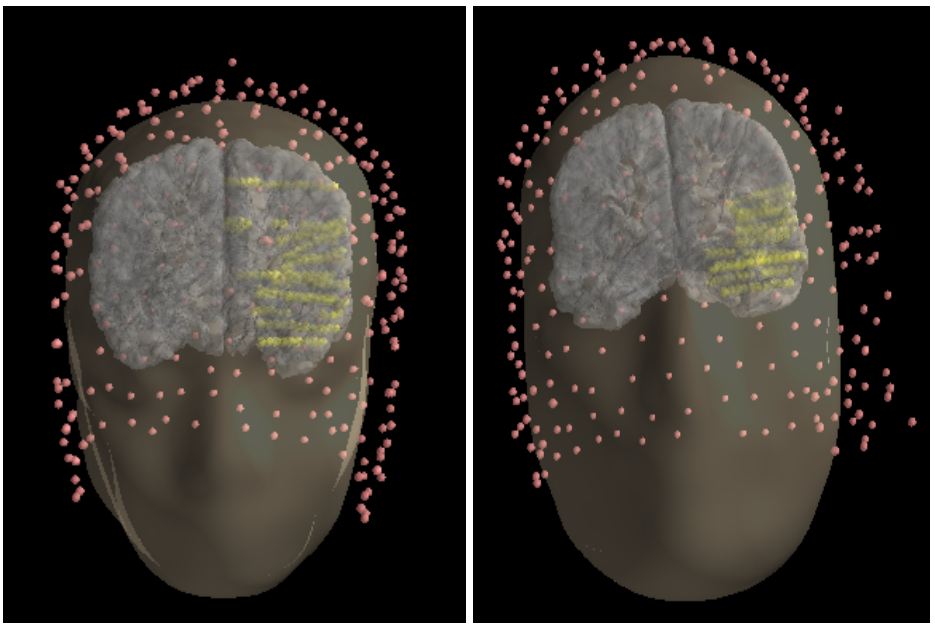

Figure 5.3. Co-registration of HD-EEG and SEEG electrodes arrangement in drug-resistant epilptic patients undergoing preoperative evaluation: a) normal and b) non-symmetrical placement of HD-EEG cap.

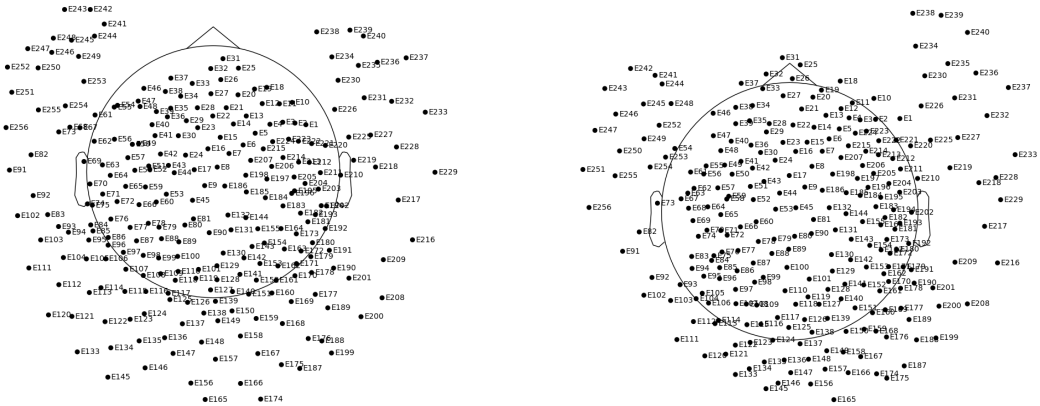

Figure 5.4. The EEG montage is plotted on a two-dimensional projection of a standardized head model: (left) normal and (right) non-symmetrical placement of HD-EEG cap.

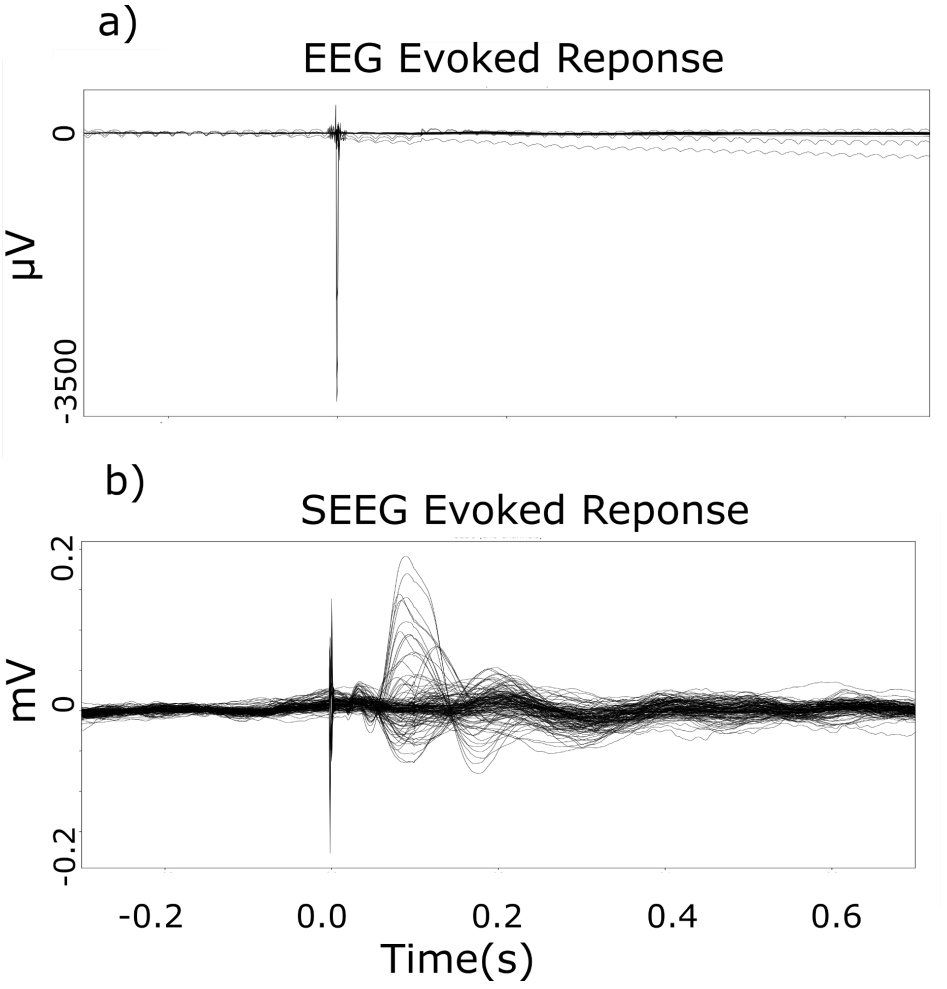

Figure 5.5. Stimulation artifact contamination of the (a) EEG and (b) SEEG recordings.

5.2. Preprocessing pipeline for simultaneous EEG and SEEG signals

The proposed preprocessing steps described in Section 4.6 can effectively remove and correct bad channels/trials and artifacts. The preprocessing workflow improves the SNR of the SEPs and iSEPs as it can be shown in Fig. 5.6 and Fig. 5.7, where the output of the major processing stages are presented for two patients. Regarding the EEG signals, the first stage, i.e., manual removal of bad channels and filtering successfully revealed the typical SEP waveform that was before hindered due to broken or noisy channels. However, the SEPs still contain artifacts that could be reduced, such as the high voltage eye blink contributions. In the next stage, ICA captures the eye blink and strong saccades artifacts and enables correcting these artifacts without having to reject multiple trials that were contaminated by superimposed eye blink contributions. Autoreject method allows then to retain as many trials/channels as possible since it automatically checks if certain trials/channels can be corrected before rejecting them. As far as the SEEG signal preprocessing is concerned, only stimulation artifact rejection, manual rejection and filtering were performed, as shown in Fig. 5.8 and Fig. 5.9 for two patients. It is worth mentioning that SEEG signal levels can exhibit significant differences even between neighbouring electrodes. Additionally, SEEG electrodes record directly the activity from neural structures and are available only when epileptic patients undergo presurgical evaluation. For this reason, these recordings should be treated with care to avoid rejecting information that is typically not available when only extracranial recordings are used. Figure 5.10 shows a topographic map of the activation arising from the median nerve stimulation as recorded from the EEG channels for 3 patients in the first 300 ms after the stimulation. More specifically, the arrival of the somatosensory signal to the contralateral SI area is clearly visible at around 30 ms [62], while the bilateral

activation of posterior parietal cortex (PPC) and the primary somatosensory cortex (SMI) was observed after 50 ms [76]–[78].

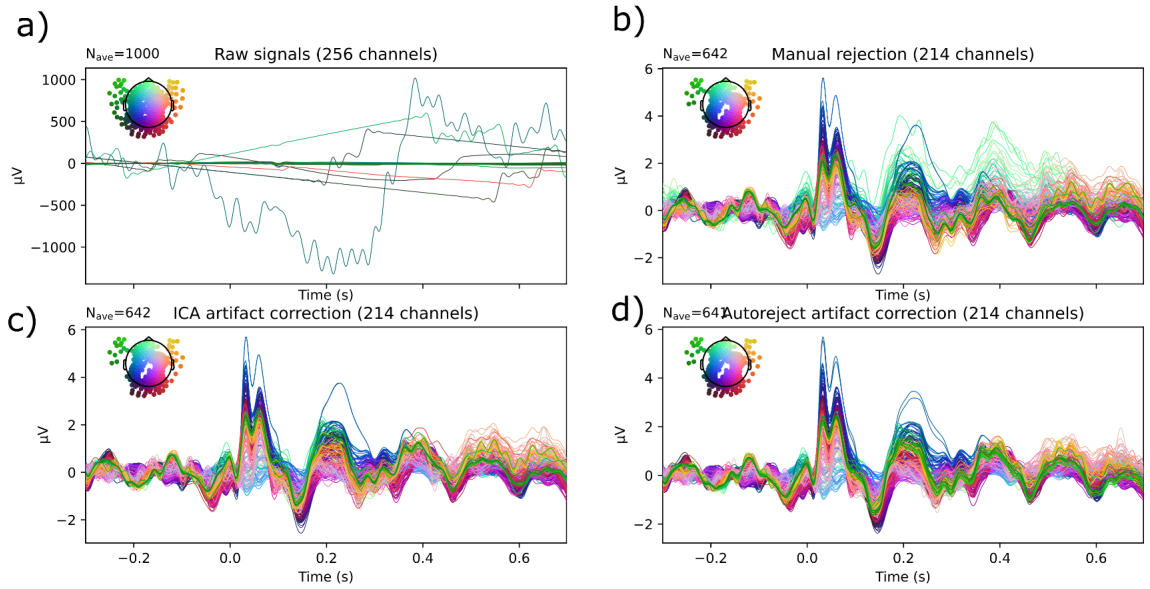

Figure 5.6. Output of each preprocessing stage for EEG signals of sub-01; (a) raw EEG signals, (b) after filtering and manual rejection, (c) after ICA-based artifact correction, and (d) after Autoreject-based trial correction.

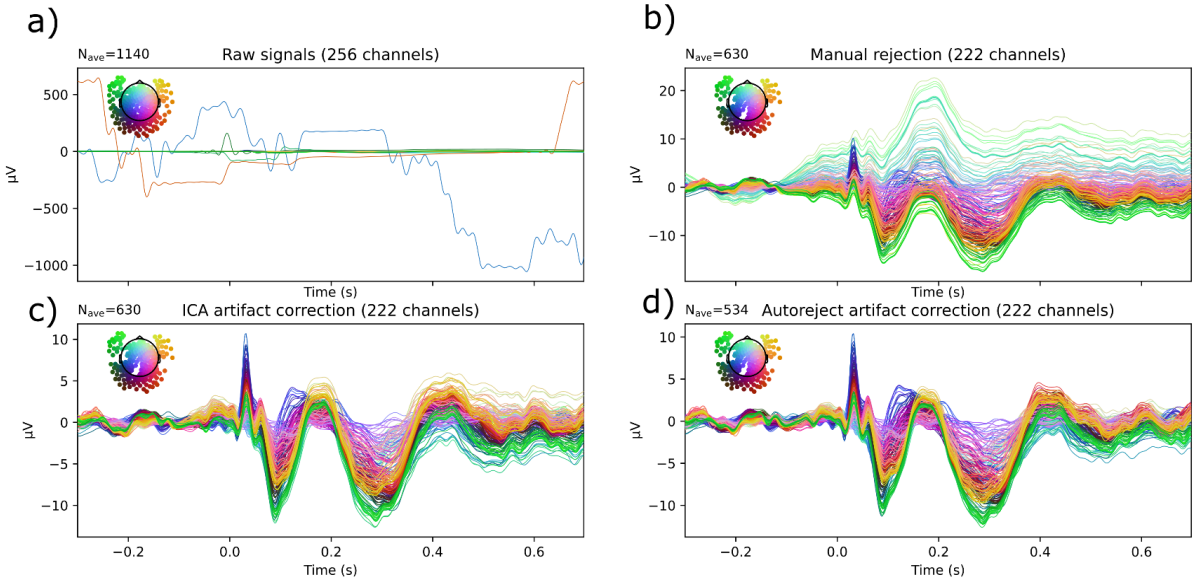

Figure 5.7. Output of each preprocessing stage for EEG signals of sub-06; (a) raw EEG signals, (b) after filtering and manual rejection, (c) after ICA-based artifact correction, and (d) after Autoreject-based trial correction.

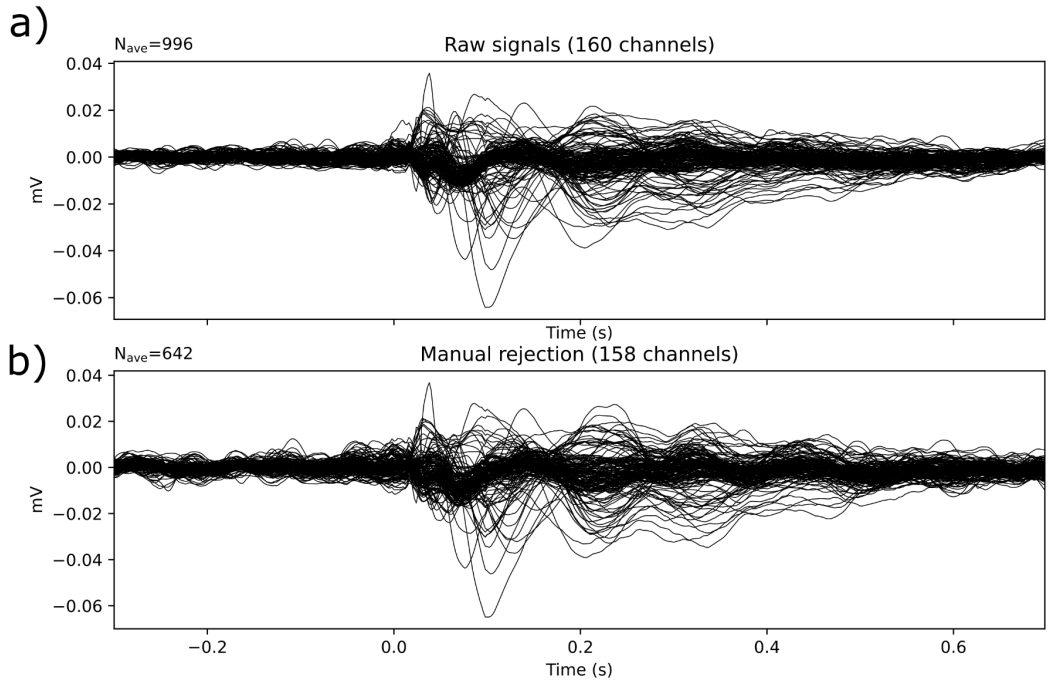

Figure 5.8. Effect of SEEG pre-processing stages for sub-01: a) raw SEEG signals, and b) after stimulation artifact rejection and manual rejection of bad channels and trials.

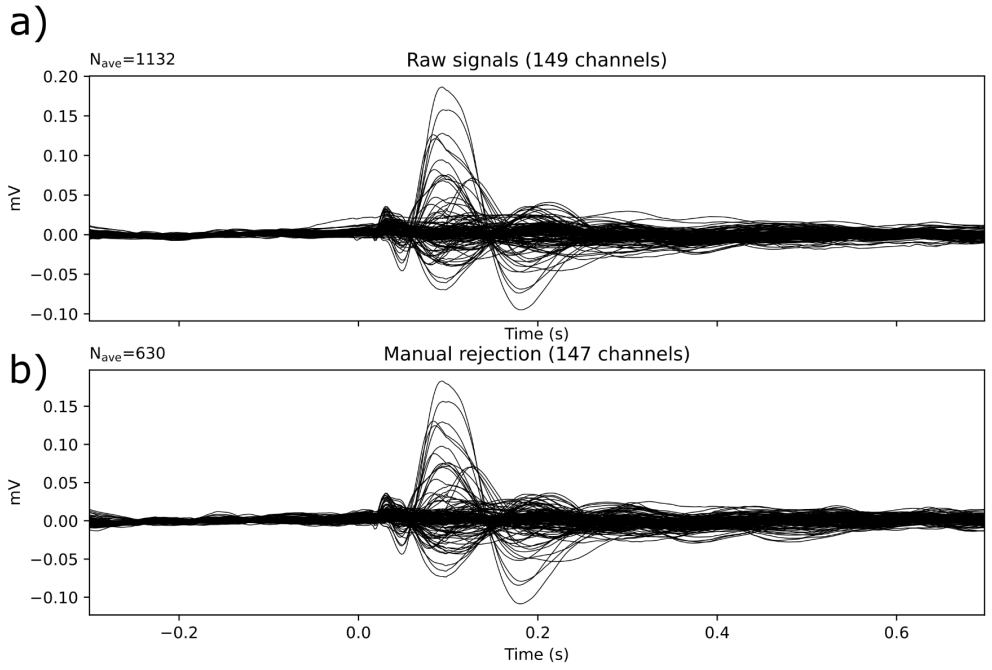

Figure 5.9. Effect of SEEG pre-processing stages for sub-06: a) raw SEEG signals, and b) after stimulation artifact rejection and manual rejection of bad channels and trials.

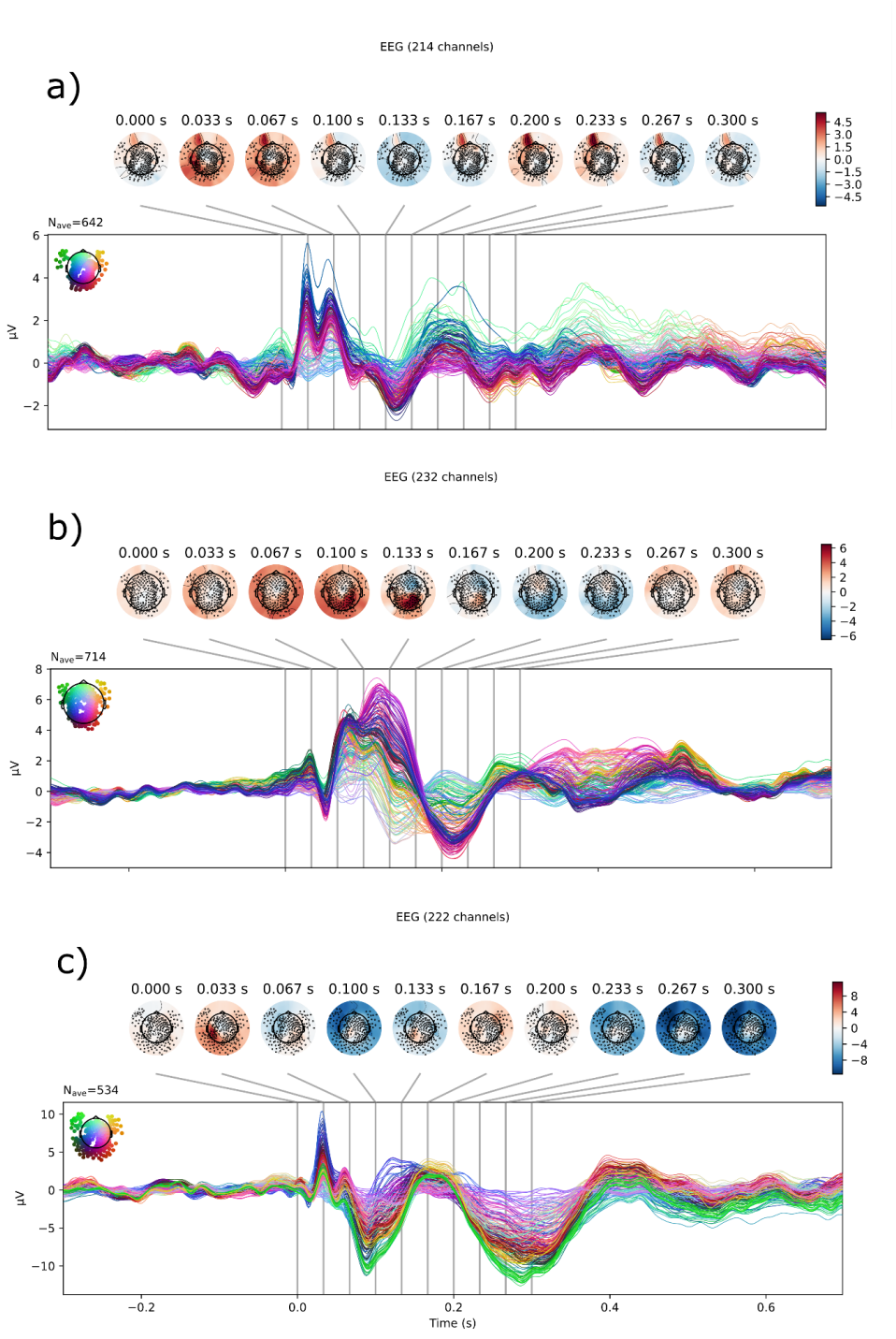

Figure 5.10. Topographic map of the somatosensory evoked potentials after preprocessing from 3 patients: a) sub-01, b) sub-02, and c) sub-06.

5.3. Intracranial gamma profile clustering

Cortical activity at population level can be assessed using high-frequency broadband gamma activity since it is spatially and functionally more specific than other frequency bands [123]. The clean SEEG signals were used to compute the time-course of the average gamma power (50-150 Hz) for each channel. The computed gamma power profile was clustered as described in the intracranial study by Avanzini et. al [4]. This study showed that the gamma power profile of intracranial evoked potentials after median nerve stimulation can be grouped in 5 categories depending on the type of response of the intracranial contact. An important finding is that some cortical areas have an early and short response (i.e., phasic components) while others have a late and long response (i.e., tonic components). After applying the same algorithm in the data used in this thesis, it was validated that certain SEEG electrodes exhibit a phasic, tonic or mixed response as seen in Fig. 5.11, 5.12 and 5.13.

Figures 5.11 and 5.12 show the clustering result of a phasic and tonic SEEG electrodes, respectively. It can be seen that both the time-frequency (TF) distribution and the gamma profile exhibit distinctive behaviours between phasic and tonic clustered electrodes as in [4]. Although examining the intracranial SEP can be challenging to differentiate between electrode response, the gamma profile shown in bottom section of Fig. 5.11 and 5.12 presents a clear distinction between phasic (i.e., early and short) and tonic (i.e., late and longer) activations. Interestingly, certain SEEG electrodes presented a mixed gamma profile, where activation was observed both early and later in time as shown in Fig. 5.13. These results may be explained by the intercommunication and simultaneous activation of some higher order processing areas with SI. Additionally, depending on the entry angle of SEEG shafts and the areas they sample, SEEG electrodes may pick up activity from structures in the proximity if monopolar reference is used.

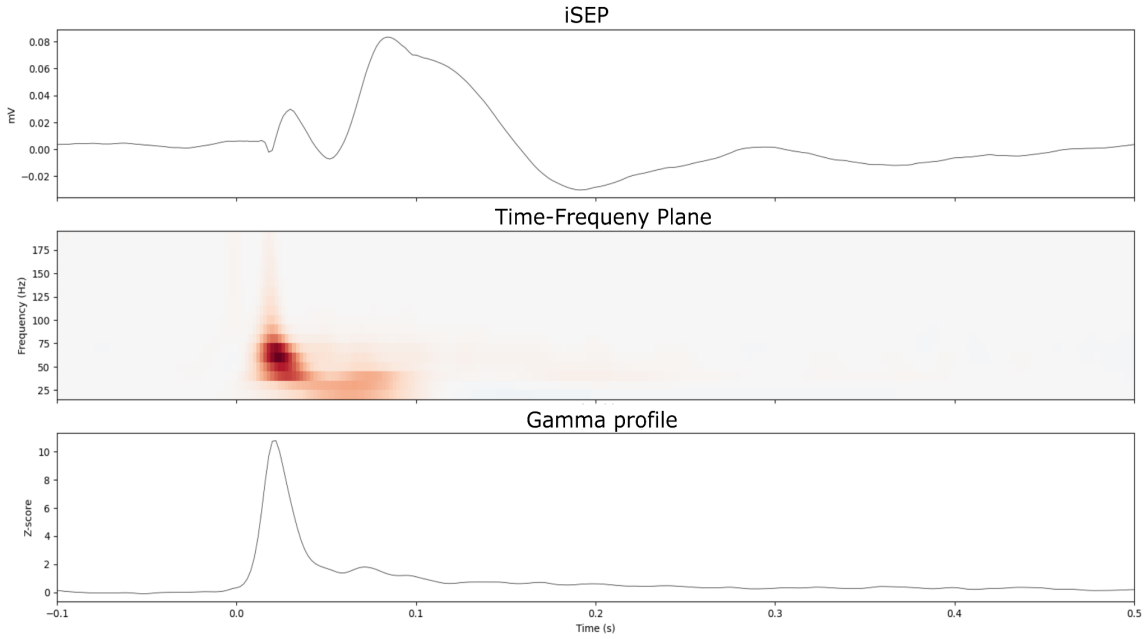

Figure 5.11. Time-course of average gamma power in a phasic electrode located in the left supramarginal area: (top) intracranial SEP, (middle) TF distribution computed using wavelet transform, and (bottom) the gamma power profile.

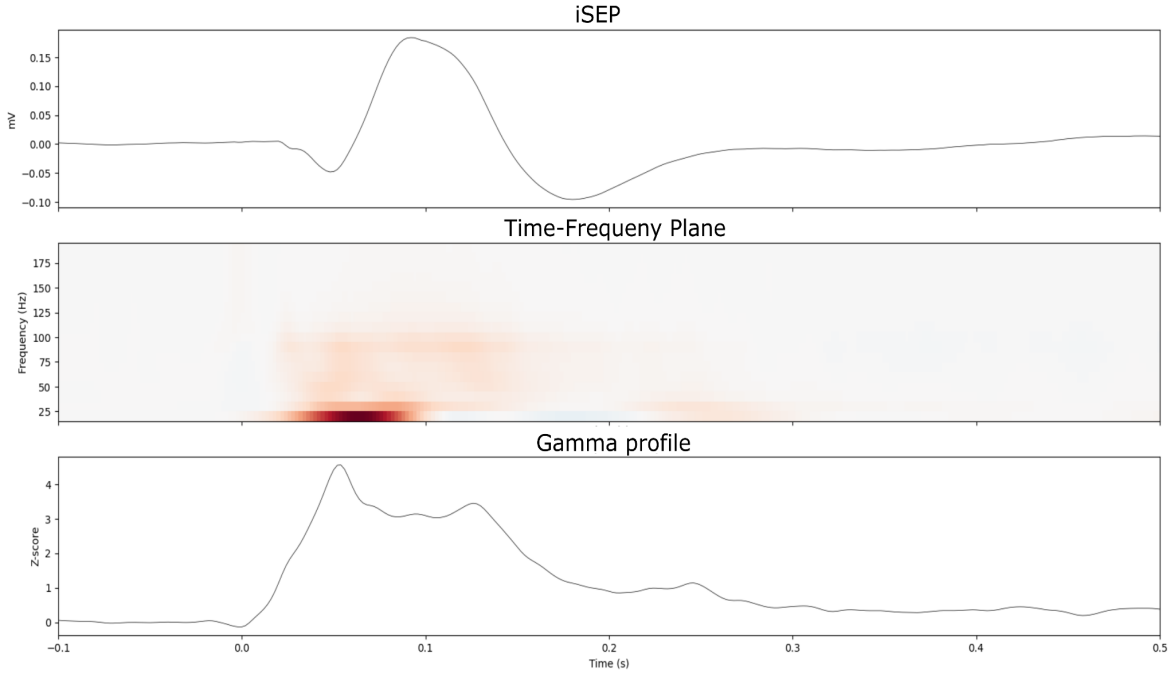

Figure 5.12. Time-course of average gamma power in a tonic electrode located in left insular, precentral area: (top) intracranial SEP, (middle) TF distribution computed using wavelet transform, and (bottom) the gamma power profile.

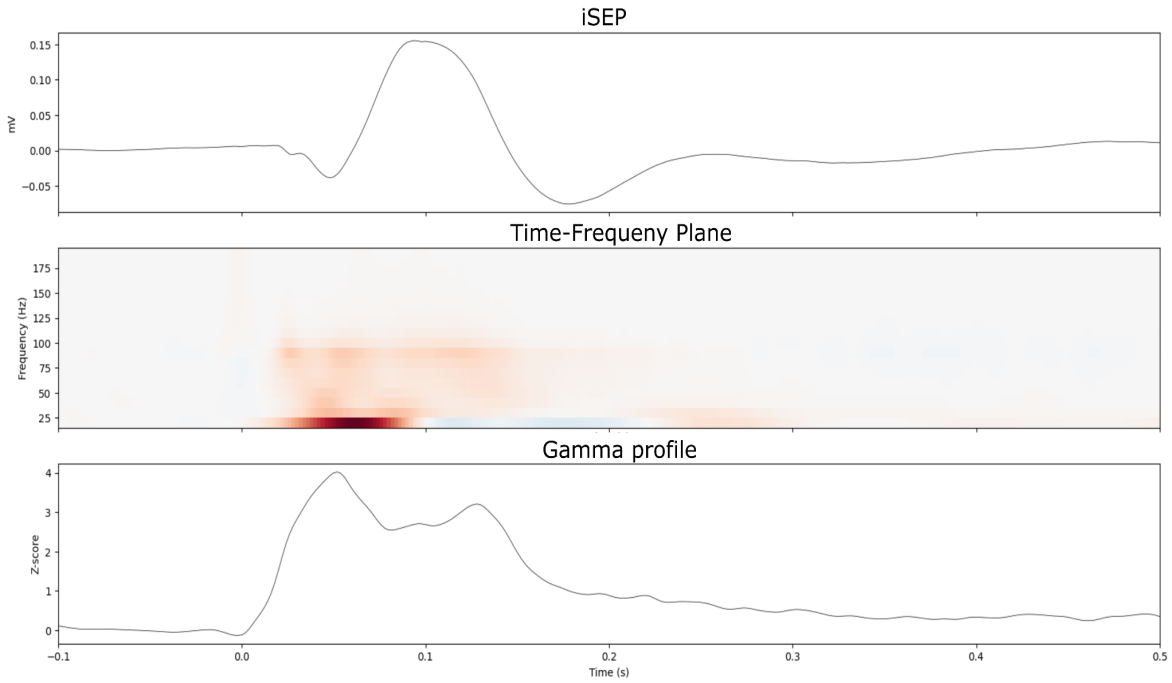

Figure 5.13. Time-course of average gamma power in a mixed-response electrode located in left precentral area: (top) intracranial SEP, (middle) TF distribution computed using wavelet transform, and (bottom) the gamma power profile.

Lastly, it is important to note that both phasic and tonic responses were found to be consistent among epochs, showcasing the regular activation of the involved somatosensory areas. Visualizing many epochs simultaneously was achieved by plotting them as an image map, where each row of pixels in the image corresponded to a single epoch while the horizontal axis represented time. The pixel colour quantified the signal value at a specific time sample and epoch. Figure 5.14 and 5.15 show the gamma power profile of a phasic (near the supramarginal area) and tonic (near the insula, precentral area) electrode, respectively, across all epochs and normalized using the baseline activity. It can be seen that there is a consistent increase of average gamma power both in phasic and tonic electrodes

compared to the prestimulus interval. However, the tonic response presented in Fig. 5.15 shows a more dispersed and varying activation across the different epochs, suggesting that neural populations are activated in less well defined time intervals in tonic areas compared to phasic areas. On the contrary, early phasic responses are very well defined in time with highly selective activation in around 30-40 ms. Future research could focus in the direction to understand why somatosensory areas involved later in somatosensory processing such as parietal operculum and insula exhibit a tonic response.

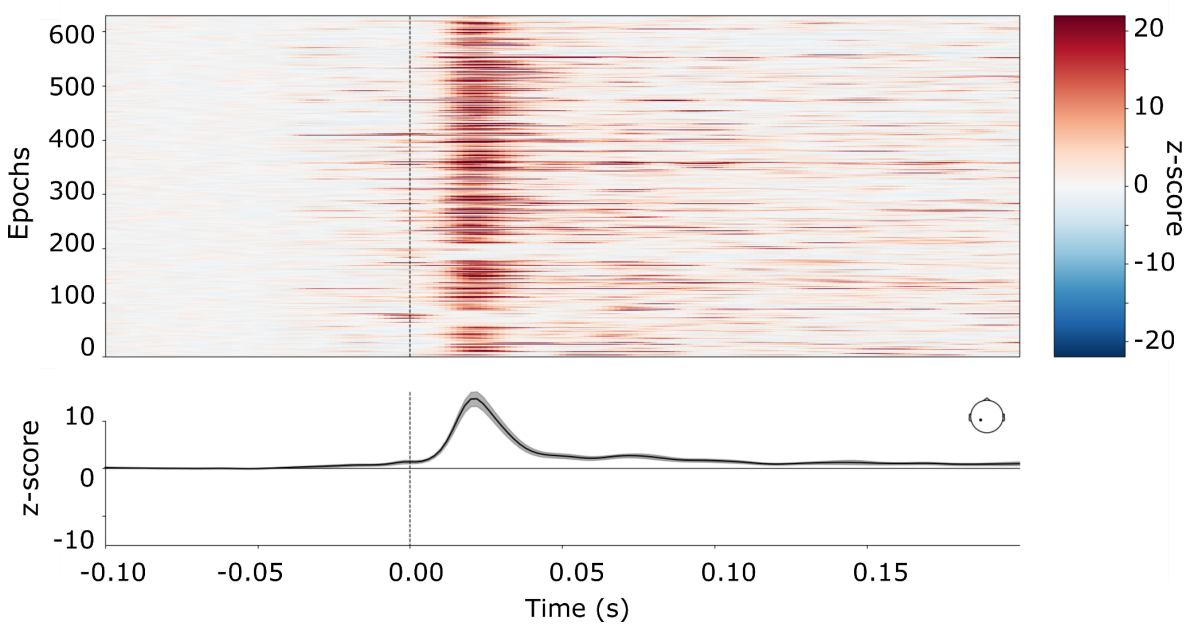

Figure 5.14. Image map (top) and normalized average gamma power profile (bottom) for a phasic electrode near the supramarginal area. The normalization was performed using the prestimulus interval.

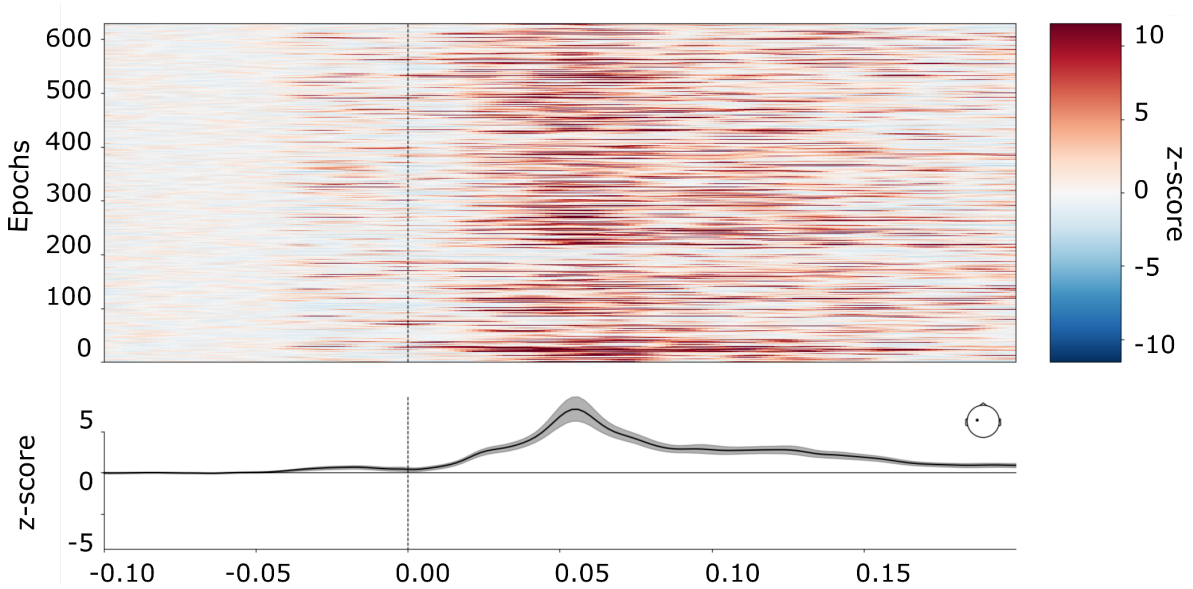

Figure 5.15. Image map (top) and normalized average gamma power profile (bottom) for a tonic electrode near the insular area. The normalization was performed using the prestimulus interval.

5.4. Localizing somatosensory processing using distributed source modelling

Following preprocessing which produced artifact-free EEG signals with clear topographic distribution of the potentials, source modelling was performed to identify the signal generators that gave rise to the recorded signals. For this purpose, various inverse methods were considered such as equivalent current dipole (ECD) [124] and distributed models such as MNE [118], sLORETA [89], [90], eLORETA [91], dSPM [92]. Since in this thesis we are interested in capturing the activity of certain locations within the brain clustered as phasic or tonic as described in Section 4.8 and 5.3 [4], the ECD approach did not provide the desired results to enable an activity characterization of various neural structures. In principle, ECD can provide the best dipole signal generator(s) that explains the recorded data and thus may be used to selectively localize activity for a time point or period. When ECD was used with the recorded EEG signals, a single dipole was

returned in the contralateral postcentral gyrus. Although this signal generator is known to exist and give rise to the first peak of the SEP, we expect the somatosensory processing to be accommodated by simultaneous activation of many cortical and subcortical areas, thus ECD was not selected for this thesis. Additionally, time-frequency mixed-norm estimates (TF-MxNE) method which uses time-frequency analysis to tackle the ill-posed inverse problem, was implemented to reveal the signal generators. This method employs sparse priors defined in the TF domain which allows capturing the nonstationary source activations. Although neural signals are in nature nonstationary and transient, the sparsity constraint imposed by TF-MxNE hinders the activity estimation of multiple distributed sources. Similarly to ECD, TF-MxNE was deemed sub-optimal for the scope of this thesis.

On the contrary, distributed models such as MNE, sLORETA, eLORETA, and dSPM enabled the reconstruction of activity of 8196 assumed sources in the brain. Although sLORETA, eLORETA and dSPM exploit neurophysiological principles to ensure spatial smoothness between adjacent sources, MNE does not take into account such constraints. It is worth mentioning that the spatial smoothness of the reconstructed sources reflects a macroscopic implementation of what actually occurs at the level of cells i.e., EEG signals are generated only if neighbouring pyramidal neurons are highly synchronized. The best method among these distributed models was chosen after investigating the location of the maximum activation and the source time-course. In addition, the optimal method was determined based on the explained variance provided by each method in a grid search approach. The explained variance reflects how accurately the sources have been reconstructed, whereas an accurate reconstruction implies that the sources explain most of the original data variance. At the same time, visual inspection of the reconstructed time course of the signal sources can be used to verify that the modelling has correctly captured the contralateral activation of SI following

median nerve stimulation. The MNE method was excluded from the grid search of the optimal inverse method as it has been shown to be significantly affected by the depth of the reconstructed source [42], [118]. On the contrary, dSPM and eLORETA have been shown to be more robust when the source distance is varying [42]. To enable the selection of the most suitable method for the given data, the graphical user interface (GUI) by MNE-Python package was used while some custom-built scripts were also developed to calculate the explained variance and add the SEEG electrodes in the GUI as seen Fig. 5.16. It was found that sLORETA and eLORETA explained the highest variance in all subjects and were used accordingly as the inverse modelling approach.

Figure 5.16 shows the location of the phasic and tonic clustered sources based on the method described in Section 4.8 superimposed on the GUI. The phasic and tonic sources are shown in red and blue, respectively. It can be seen that at around 30 ms the reconstructed activity is attributed to areas such as the postcentral gyrus, posterior parietal cortex and supramarginal. The time-courses of phasic and tonic sources shown at the bottom plot of Fig. 5.16 has a strong peak at around 30 ms, the time associated with the afferent somatosensory signals reaches SI. Figure 5.17 shows the activation maps from different views of the brain. Since right median nerve stimulation was performed for this subject, the source modelling accurately reconstructs activity on the left hemisphere near the somatosensory cortex at around 30ms.

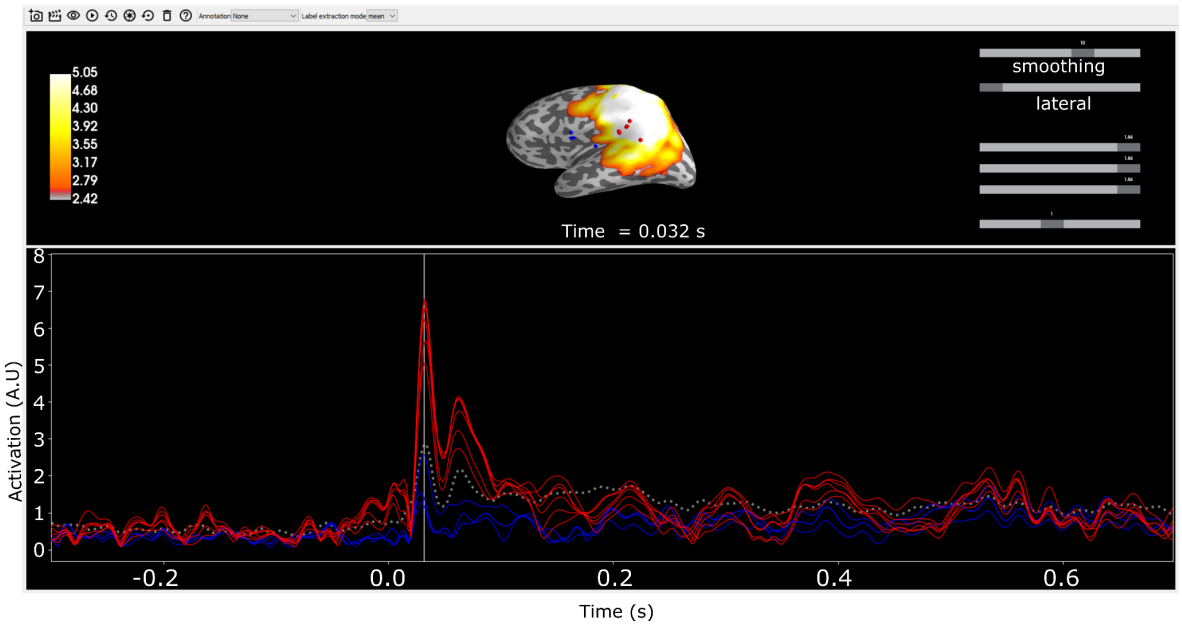

Figure 5.16. Source modelling GUI with (top) superimposed phasic and tonic sources on an inflated brain and (bottom) the reconstructed time-source of the sources. The phasic and tonic sources are colour-coded with red and blue, respectively. The brain activation at time 32 ms after stimulation is illustrated covering several neural areas including the postcentral gyrus, posterior parietal cortex and supramarginal gyrus for sub-06.

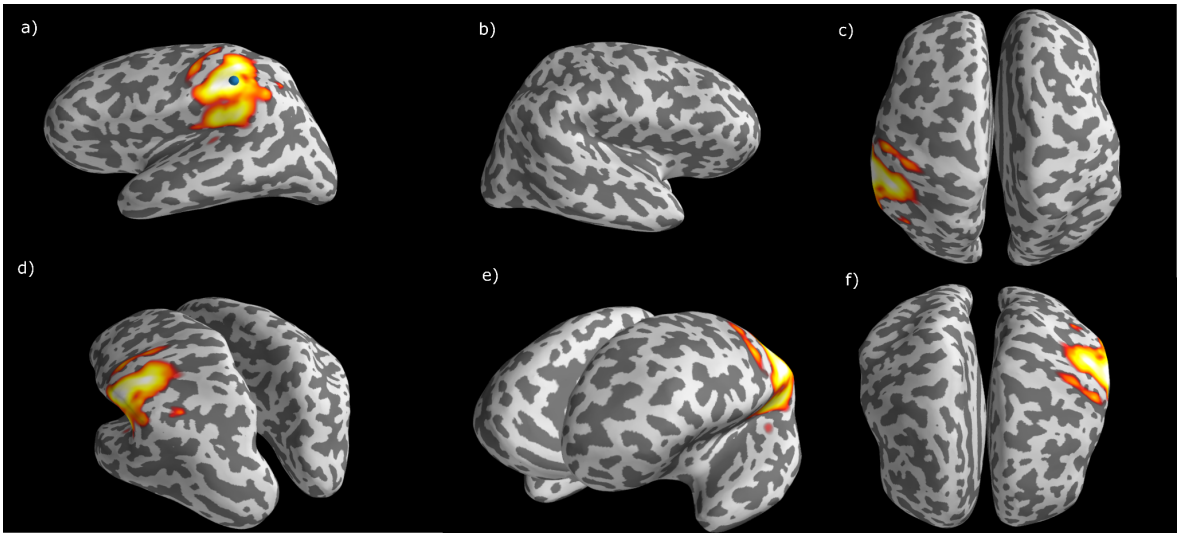

Figure 5.17. Different views of the activation maps at around 30 ms following right median nerve stimulation: a) right and b) left lateral, c) axial, d) parietal, e) frontal, and f) dorsal views.

Furthermore, activation maps of the left hemisphere at three different time bins are indicated in Fig. 5.18. The color range is dynamically adjusted from frame to frame using the MNE-Python package. At the median nerve stimulation time instance, no activation is present which supports that the interstimulus period of 1 s was enough for the slow somatosensory to unfold and not contaminate the following trials. In the second frame of 20-30 ms, the activity peaks in primary sensory areas are observed while in the second frame the activity spreads to the dorsal premotor area and posterior parietal cortex suggesting the activation of multiple neural areas following somatosensory stimuli.

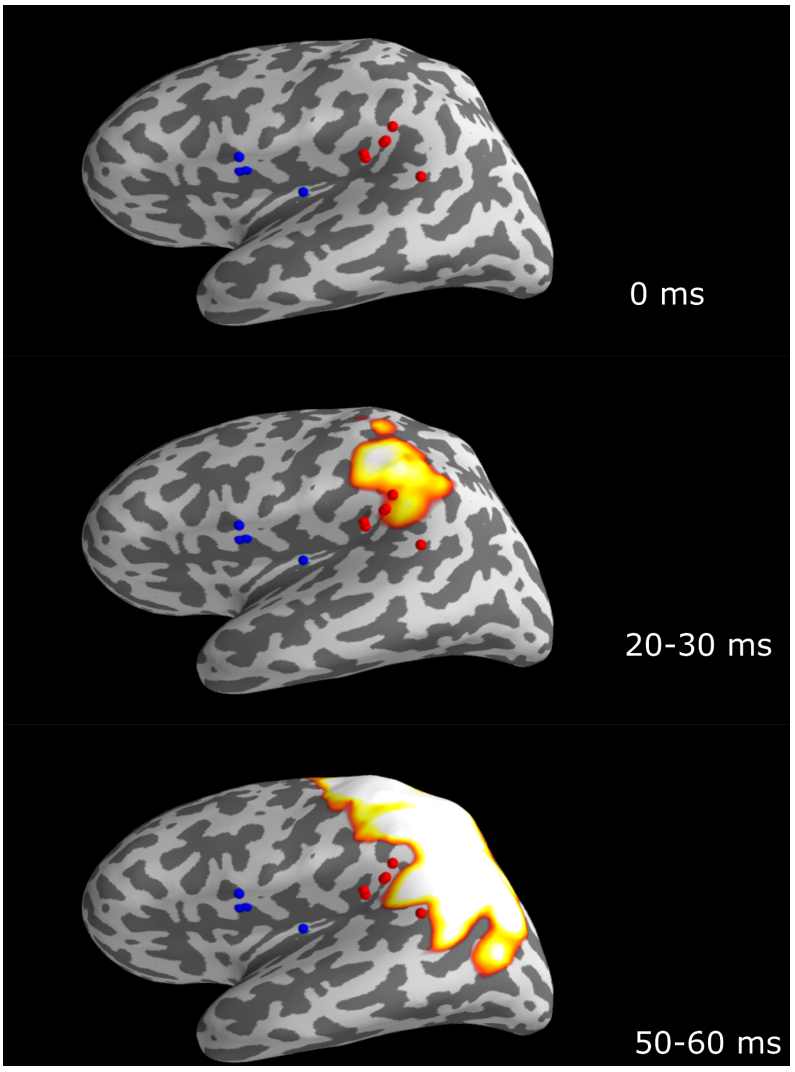

Figure 5.18. Activation maps following right median nerve stimulation at time instances: 0 ms, 20-30 ms and 50-60 ms.

5.5. Reconstructed sources exhibit distinct time-frequency characteristics

Existing studies have shown that somatosensory processing is served by a wide network of neural areas. Certain areas such as SI are responsive early after the presence of a stimulus, while others potentially involved in integration and perception of the stimulus such as SII become active later. An intracranial study analyzed SEEG recordings to cluster the intracranial SEPs (iSEPs) based on their gamma profile into early (i.e., phasic) and late (i.e. tonic) responses [4]. Motivated by this finding, we hypothesized that the same behaviour can be observed by reconstructed sources from EEG signals. Following source modelling, the time course of the reconstructed sources was not showing a clear distinction between phasic and tonic-clustered areas. To this end, time-frequency (TF) analysis was employed to analyze the spatiotemporal dynamics of the reconstructed sources. Figures 5.19 and 5.20 show the results of the TF analysis which proves that somatosensory areas exhibit phasic and tonic, respectively, as seen from the EEG recordings.

This first finding of this thesis suggests that EEG contains information about intracranial activity and may assist practitioners to infer information about the neural dynamics which up to date were only observable with intracranial EEG.

It must be noted that this finding was possible due to the availability of the simultaneous recordings. On the one hand the intracranial signals were clustered into phasic and tonic to be used as ground truth to support our hypothesis. On the other hand, TF analysis of the EEG-based reconstructed sources were computed for the locations of the phasic and tonic sources. The TF analysis results agreed with the groundtruth SEEG data. Moreover, it is important to note that both phasic and tonic electrodes may contain a combination of early and later activation. For example, Figure 5.20 shows the time-frequency distribution of 4

tonic electrodes with significant activation after 100 ms. However, an early weaker activation is also present at around 30 ms which is the typical response of phasic electrodes. It is worth mentioning that during source modelling, the inverse solutions introduce some "spreading" of the estimated current, thus, the generalization of these results should be done conscientiously.

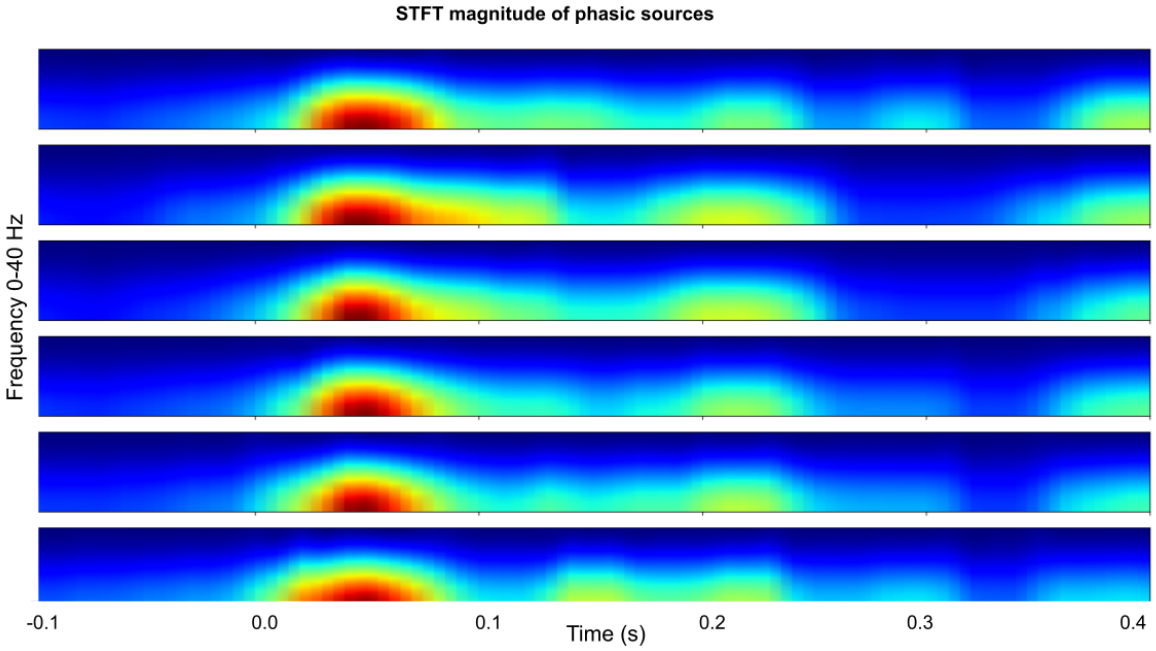

Figure 5.19. Time-frequency distribution for 6 phasic electrodes sampling the supramarginal area of a patient. The early activation of the estimated phasic sources can be seen at around 30 ms.

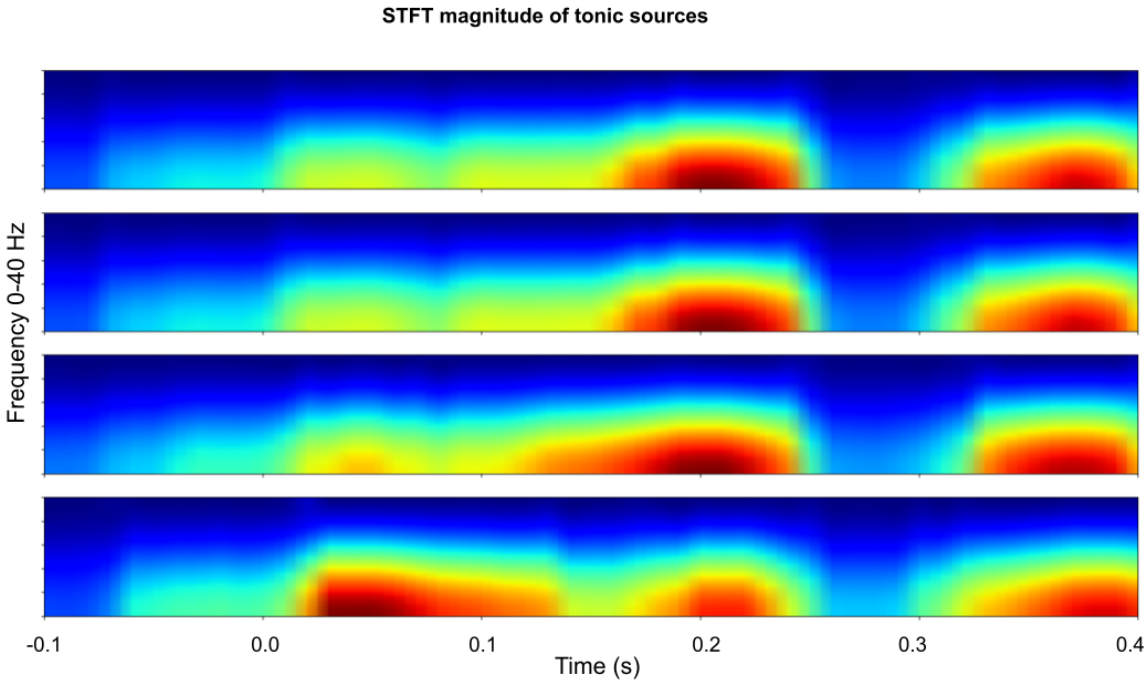

Figure 5.20. Time-frequency distribution for 4 tonic electrodes sampling the supramarginal area of a patient. The delayed strong activation of the estimated tonic sources can be seen at around 200 ms.

5.6. Intracranial activity can be predicted by extracranial signals.

After having shown that the time-frequency distribution of the reconstructed sources share similarities with the SEEG ground truth signals, the intracranial tonic activity was predicted using the multivariate temporal response function (mTFR) based on extracranial HD-EEG recordings. The mTFR method has been shown to successfully reconstruct the speech signal based on EEG recordings [17]. Figure 5.21 shows the preliminary results of the prediction for 4 patients and 4 different tonic electrodes. Given the SEEG recordings, a comparison between the predicted and groundtruth signals was possible. From the preliminary results, several remarks can be made:

- The predicted intracranial activity followed the dynamics of the real SEEG signals. This can be first visually inspected by looking at some distinct

features of the time-course of the two signals. Such features include the activity during the pre-stimulus interval which follows the same trend in both predicted and real signals as well as the close prediction of the maximum peak in predicted and real signals.

- There can be cases where discrepancies in the maximum peak are present. For example the bottom two graphs show that the predicted signal reaches its maximum around 100 ms later than the real signal. This result showcases that intracranial prediction based on HD-EEG may suffer from inherent limitations. For example, the volume conduction effect, the propagation delays and imperfections in simultaneous recordings setup can cause a delayed prediction of the intracranial activity. Moreover, high-frequency changes cannot be predicted accurately as seen in Fig. 5.21 (d), where the real signal is substantially more varying than the predicted one.
- Observing results from 8 patients and multiple electrodes, it becomes clear that the intracranial prediction accuracy depends on many factors. It is worth considering that the ground truth recordings comes from SEEG tonic electrodes which are typically limited based on the clinical needs. On the other hand, EEG signals record a mixture of activity from potentially many tonic areas, thus the performance of prediction may be limited. To fully assess the results, a more thorough investigation of the exact neural structures and their neural pathways is required at group level.

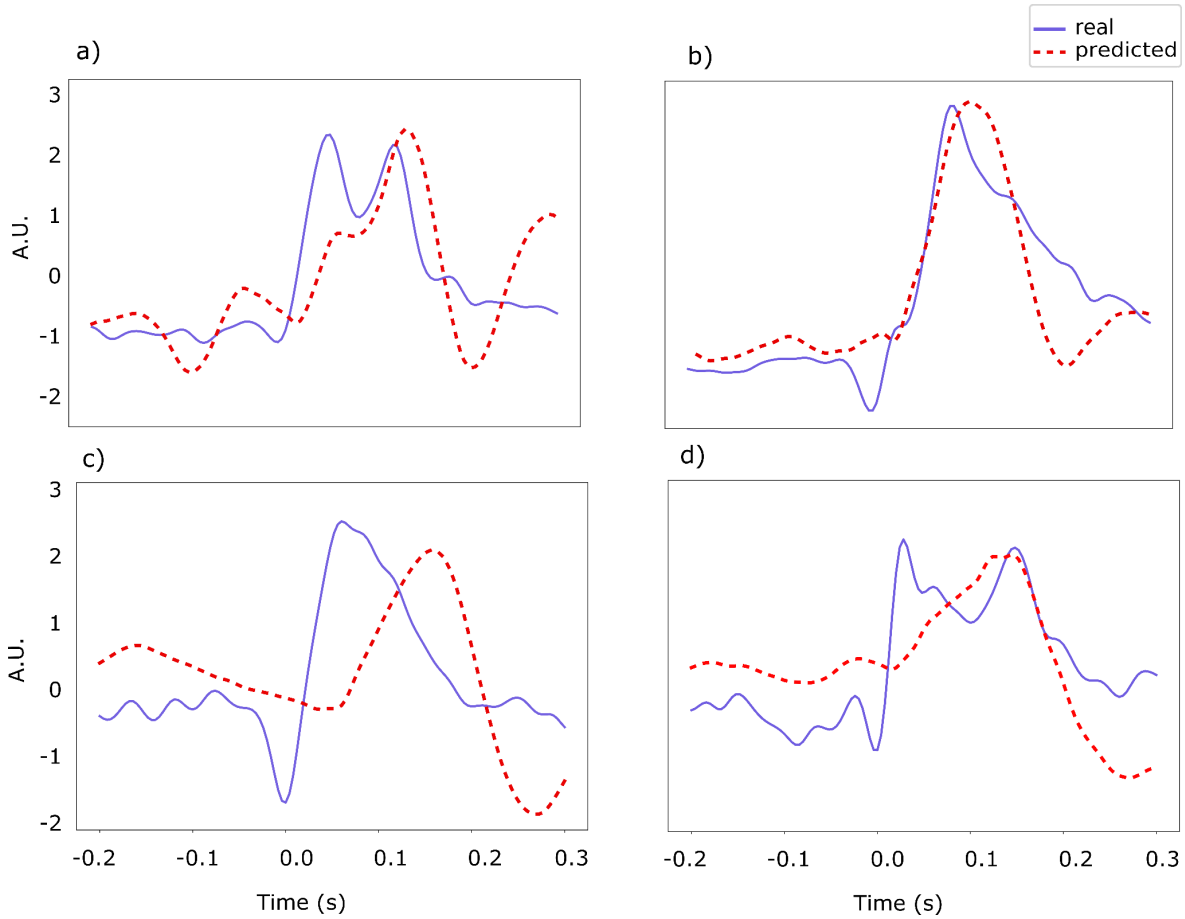

Figure 5.21. Prediction of intracranial tonic activity based on EEG recordings from 4 subjects: a) sub-06 with tonic electrodes in insula and premotor area, b) sub-08 with tonic electrodes in insula, postcentral and supramarginal area, c) sub-02 with tonic electrodes in superior parietal area and d) sub-04 with tonic electrodes in middle temporal and supramarginal area.

6. Conclusion

The somatosensory system is a complex system that enables the conscious perception of changes, such as vibration, pain, and pressure in the environment or inside the human body. To allow the processing, quantification and localization of the stimuli, distributed neural networks in the peripheral and central nervous system are employed. The somatosensory system has been extensively investigated in the last 50 years using electrophysiology techniques such as extracranial (i.e., M/EEG) and intracranial (i.e., ECoG/SEEG) recordings. A well studied approach to characterise normal and pathological behaviour of the somatosensory system is the evoked potentials. This approach involves multiple stimulations (e.g. acoustic clicks, pattern reversals, electrical stimulation) while recording the subject's brain response with a recording system such as an EEG. The idea behind evoked potentials is that repeated stimulation will cause the same response across trials. These responses can then be averaged to reveal a typical waveform with prominent peaks such as the P300. Additionally, during averaging the responses from multiple trials, the background noise is reduced since it is stochastic in nature and expected to vary between trials.

In this thesis, the simultaneous analysis of somatosensory evoked potentials (SEPs) using SEEG and high-density EEG (HD-EEG) was performed. The SEPs were recorded following stimulation of the median nerve from 8 patients that were undergoing pre-surgical evaluation for identification of the epileptogenic region with implanted SEEG electrodes. To the best of our knowledge, no prior study has examined somatosensory evoked potentials with simultaneous HD-EEG and SEEG modality. The work of this thesis was implemented in MNE, an open-source Python package for exploring, visualizing and analyzing neurophysiological data. The recorded signals were preprocessed using a

custom-designed pipeline that included filtering, visual inspection and artifact correction using ICA and Autoreject. Once the HD-EEG and SEEG signals were artifact-free, the following hypotheses were investigated as part of the thesis:

- Reconstructed signals from source modelling on the EEG recordings exhibit phasic and tonic behaviour depending on the location of the source (e.g., SI vs SII).
- Intracranial tonic activity can be predicted by extracranial recordings. The predicted intracranial activity is compared against the groundtruth activity provided by the SEEG recordings.

In summary, the following contributions were achieved through this thesis:

- Extensive literature review on state-of-the art findings related to somatosensory evoked responses following median nerve stimulation (*see* Chapter 3).
- Recommendation for future somatosensory evoked potentials studies using simultaneous EEG and SEEG recordings (*see* Section 5.1)
- Development of a preprocessing pipeline to clean simultaneous EEG and SEEG recordings from 8 epileptic patients (*see* Section 4.6 and Section 5.3).
- Source modelling implementation to reconstruct signal sources from HD-EEG signals for the available data (*see* Section 5.4).
- Development of custom-built scripts to evaluate results of source modelling (*see* Section 5.4)
- Showcase that reconstructed sources from EEG recordings exhibit distinct phasic and tonic behaviour which is area-dependent (*see* Section 5.5).
- Prediction of intracranial activity based on EEG recordings (*see* Section 5.6)

Ultimately, the research carried out in this thesis aimed to provide a mapping from extracranial to intracranial space by exploiting simultaneous intra- and extracranial recordings. Since SEEG recordings are rarely available, the findings of the thesis advance our understanding of the somatosensory system, thus

enhancing the clinical information in cases where intracranial invasive recordings are not available. The results of this work have led to a scientific poster, titled '*Scalp EEG prediction of intracranial high-frequency responses to median nerve stimulation: insights from simultaneous recordings*', Ezequiel Mikulan, Angelos Theocharis, Simone Russo, Flavia Maria Zauli, Ivana Sartori, Sara Parmigiani, Simone Sarasso, Maria Del Vecchio, Pietro Avanzini, Andrea Pigorini, Poster presented at the 4th International Brain Stimulation Conference. Charleston, USA.

Although the existing research has predominantly focused on understanding the contribution of the primary somatosensory area (SI) in the somatosensory processing [50], [62], [82], [83], [125], [126], more insights about the secondary somatosensory area (SII) and other neural areas [53], [80], [127] involved in somatosensation are required to gain a more complete picture of the distributed neural processing following somatosensory stimuli. Important neural areas that need to be further studied include the insula, motor and premotor cortex, supplementary motor area and superior and inferior parietal lobules. More specifically, future research could focus in the direction to understand why certain somatosensory areas involved later in somatosensory processing exhibit a characteristic tonic response. Lastly, preliminary results on prediction of intracranial activity based on HD-EEG showed promising results. However, it must be noted that such results were only possible due to the availability of simultaneous HD-EEG and groundtruth SEEG recordings. The preliminary prediction results need to be further examined to reveal more information about the potential to predict intracranial activity using non-invasive extracranial signals. The current results could potentially pave the way for studies on patients with somatosensory deficits even in cases where SEEG data is not available [53].

7. References

[1] D. L. Schomer and F. L. da Silva, *Niedermeyer's Electroencephalography: Basic Principles, Clinical Applications, and Related Fields*. Wolters Kluwer Health, 2012.

[2] D. R. Giblin, "Somatosensory evoked potentials in healthy subjects and in patients with lesions of the nervous system," *Ann. N. Y. Acad. Sci.*, vol. 112, no. 1, pp. 93–142, 1964, doi: 10.1111/j.1749-6632.1964.tb26744.x.

[3] C. Herff, D. J. Krusienski, and P. Kubben, "The Potential of Stereotactic-EEG for Brain-Computer Interfaces: Current Progress and Future Directions," *Front. Neurosci.*, vol. 14, p. 123, 2020, doi: 10.3389/fnins.2020.00123.

[4] P. Avanzini *et al.*, "Four-dimensional maps of the human somatosensory system," *Proc. Natl. Acad. Sci.*, vol. 113, no. 13, p. E1936, Mar. 2016, doi: 10.1073/pnas.1601889113.

[5] J. Jeong, "EEG dynamics in patients with Alzheimer's disease," *Clin. Neurophysiol.*, vol. 115, no. 7, pp. 1490–1505, Jul. 2004, doi: 10.1016/j.clinph.2004.01.001.

[6] R. Cassani, M. Estarellas, R. San-Martin, F. J. Fraga, and T. H. Falk, "Systematic review on resting-state EEG for Alzheimer's disease diagnosis and progression assessment," *Dis. Markers*, vol. 2018, 2018, doi: 10.1155/2018/5174815.

[7] C. X. Han, J. Wang, G. S. Yi, and Y. Q. Che, "Investigation of EEG abnormalities in the early stage of Parkinson's disease," *Cogn. Neurodyn.*, vol. 7, no. 4, pp. 351–359, Aug. 2013, doi: 10.1007/s11571-013-9247-z.

[8] D. Stoffers, J. L. W. Bosboom, J. B. Deijen, E. C. Wolters, H. W. Berendse, and C. J. Stam, "Slowing of oscillatory brain activity is a stable characteristic of Parkinson's disease without dementia," *Brain*, vol. 130, no. 7, pp. 1847–1860, Jul. 2007, doi: 10.1093/brain/awm034.

[9] S. J. M. Smith, "EEG in the diagnosis, classification, and management of patients with epilepsy," *Neurol. Pract.*, vol. 76, no. 2, pp. 2–7, Jun. 2005, doi: 10.1136/jnnp.2005.069245.

[10] C. Plummer, S. J. Vogrin, W. P. Woods, M. A. Murphy, M. J. Cook, and D. T. J. Liley, "Interictal and ictal source localization for epilepsy surgery using high-density EEG with MEG: a prospective long-term study," *Brain*, vol. 142, no. 4, pp. 932–951, Apr. 2019, doi: 10.1093/brain/awz015.

[11] M. Murphy *et al.*, "Propofol Anesthesia and Sleep: A High-Density EEG Study," *Sleep*, vol. 34, no. 3, pp. 283–291, Mar. 2011, doi: 10.1093/sleep/34.3.283.

[12] D. E. J. Linden, "The P300: Where in the brain is it produced and what does it tell us?," *Neuroscientist*, vol. 11, no. 6, pp. 563–576, Dec. 2005, doi: 10.1177/1073858405280524.

[13] G. Singh, "Somatosensory evoked potential monitoring," *J. Neuroanaesth. Crit. Care*, vol. 3, p. 97, Dec. 2016, doi: 10.4103/2348-0548.174745.

[14] R. Grech *et al.*, "Review on solving the inverse problem in EEG source analysis," *J. NeuroEngineering Rehabil.*, vol. 5, no. 1, p. 25, Nov. 2008, doi: 10.1186/1743-0003-5-25.

[15] H. Hallez *et al.*, "Review on solving the forward problem in EEG source analysis," *J. NeuroEngineering Rehabil.*, vol. 4, no. 1, p. 46, Nov. 2007, doi: 10.1186/1743-0003-4-46.

[16] A. Bruns, "Fourier-, Hilbert- and wavelet-based signal analysis: Are they really

different approaches?," *J. Neurosci. Methods*, vol. 137, no. 2, pp. 321–332, Aug. 2004, doi: 10.1016/j.jneumeth.2004.03.002.
[17] M. J. Crosse, G. M. Di Liberto, A. Bednar, and E. C. Lalor, "The Multivariate Temporal Response Function (mTRF) Toolbox: A MATLAB Toolbox for Relating Neural Signals to Continuous Stimuli," *Front. Hum. Neurosci.*, vol. 10, p. 604, 2016, doi: 10.3389/fnhum.2016.00604.
[18] A. L. Hodgkin and A. F. Huxley, "A quantitative description of membrane current and its application to conduction and excitation in nerve," *J. Physiol.*, vol. 117, no. 4, pp. 500–544, Aug. 1952, doi: 10.1113/jphysiol.1952.sp004764.
[19] C. C. Chen *et al.*, "Patch-clamp technique to characterize ion channels in enlarged individual endolysosomes," *Nat. Protoc.*, vol. 12, no. 8, pp. 1639–1658, Aug. 2017, doi: 10.1038/nprot.2017.036.
[20] M. P. Branco, Z. V. Freudenburg, E. J. Aarnoutse, M. G. Bleichner, M. J. Vansteensel, and N. F. Ramsey, "Decoding hand gestures from primary somatosensory cortex using high-density ECoG," *NeuroImage*, vol. 147, pp. 130–142, Feb. 2017, doi: 10.1016/j.neuroimage.2016.12.004.
[21] J. S. Ebersole, A. M. Husain, and D. R. Nordli, *Current practice of clinical electroencephalography*, 4th ed. Wolters Kluwer Health, 2014.
[22] G. H. Glover, "Overview of functional magnetic resonance imaging," *Neurosurg. Clin. N. Am.*, vol. 22, no. 2, pp. 133–139, Apr. 2011, doi: 10.1016/j.nec.2010.11.001.
[23] S. P. Singh, "Magnetoencephalography: Basic principles," *Ann. Indian Acad. Neurol.*, vol. 17, no. SUPPL. 1, pp. S107–S107, 2014, doi: 10.4103/0972-2327.128676.
[24] G. Buzsáki, C. A. Anastassiou, and C. Koch, "The origin of extracellular fields and currents — EEG, ECoG, LFP and spikes," *Nat. Rev. Neurosci.*, vol. 13, no. 6, pp. 407–420, Jun. 2012, doi: 10.1038/nrn3241.
[25] R. Oostenveld and P. Praamstra, "The five percent electrode system for high-resolution EEG and ERP measurements," *Clin. Neurophysiol.*, vol. 112, no. 4, pp. 713–719, Apr. 2001, doi: 10.1016/S1388-2457(00)00527-7.
[26] C. J. Chu, "High density EEG-What do we have to lose?," *Clin. Neurophysiol.*, vol. 126, no. 3, pp. 433–434, Mar. 2015, doi: 10.1016/j.clinph.2014.07.003.
[27] D. Yao, Y. Qin, S. Hu, L. Dong, M. L. Bringas Vega, and P. A. Valdés Sosa, "Which Reference Should We Use for EEG and ERP practice?," *Brain Topogr.*, vol. 32, no. 4, pp. 530–549, Jul. 2019, doi: 10.1007/s10548-019-00707-x.
[28] S. Hu, D. Yao, M. L. Bringas-Vega, Y. Qin, and P. A. Valdes-Sosa, "The Statistics of EEG Unipolar References: Derivations and Properties," *Brain Topogr.*, vol. 32, no. 4, pp. 696–703, Jul. 2019, doi: 10.1007/s10548-019-00706-y.
[29] S. J. Luck, *An Introduction to the Event-Related Potential Technique*. MIT Press, 2014. [Online]. Available: https://books.google.de/books?id=SzavAwAAQBAJ
[30] P. S. Reif, A. Strzelczyk, and F. Rosenow, "The history of invasive EEG evaluation in epilepsy patients," *Seizure*, vol. 41, pp. 191–195, Oct. 2016, doi: 10.1016/j.seizure.2016.04.006.
[31] R. A. Mak-McCully *et al.*, "Distribution, amplitude, incidence, co-occurrence, and propagation of human K-complexes in focal transcortical recordings," *eNeuro*, vol. 2, no. 4, 2015, doi: 10.1523/ENEURO.0028-15.2015.
[32] R. Matsumoto, T. Kunieda, and D. Nair, "Single pulse electrical stimulation to probe functional and pathological connectivity in epilepsy," *25th Anniv. Issue*, vol. 44, pp. 27–36, Jan. 2017, doi: 10.1016/j.seizure.2016.11.003.

[33] M. Cossu *et al.*, “Stereoelectroencephalography-guided radiofrequency thermocoagulation in the epileptogenic zone: A retrospective study on 89 cases,” *J. Neurosurg.*, vol. 123, no. 6, pp. 1358–1367, Dec. 2015, doi: 10.3171/2014.12.JNS141968.
[34] F. Cardinale *et al.*, “Stereoelectroencephalography: Surgical methodology, safety, and stereotactic application accuracy in 500 procedures,” *Neurosurgery*, vol. 72, no. 3, pp. 353–366, Mar. 2013, doi: 10.1227/NEU.0b013e31827d1161.
[35] K. Iida and H. Otsubo, “Stereoelectroencephalography: Indication and efficacy,” *Neurol. Med. Chir. (Tokyo)*, vol. 57, no. 8, pp. 375–385, 2017, doi: 10.2176/nmc.ra.2017-0008.
[36] J. Engel J., “Mesial temporal lobe epilepsy: What have we learned?,” *Neuroscientist*, vol. 7, no. 4, pp. 340–352, 2001, doi: 10.1177/107385840100700410.
[37] J. A. Obeso *et al.*, “The basal ganglia in Parkinson’s disease: Current concepts and unexplained observations,” *Ann. Neurol.*, vol. 64, no. SUPPL. 2, Dec. 2008, doi: 10.1002/ana.21481.
[38] G. Li *et al.*, “Optimal referencing for stereo-electroencephalographic (SEEG) recordings,” *NeuroImage*, vol. 183, pp. 327–335, Dec. 2018, doi: 10.1016/j.neuroimage.2018.08.020.
[39] D. Uher *et al.*, “Stereo-electroencephalography (SEEG) reference based on low-variance signals,” Jul. 2020, pp. 204–207. doi: 10.1109/EMBC44109.2020.9175734.
[40] D. A. Engemann and A. Gramfort, “Automated model selection in covariance estimation and spatial whitening of MEG and EEG signals,” *NeuroImage*, vol. 108, pp. 328–342, Mar. 2015, doi: 10.1016/j.neuroimage.2014.12.040.
[41] C. M. Michel and D. Brunet, “EEG Source Imaging: A Practical Review of the Analysis Steps,” *Front. Neurol.*, vol. 10, p. 325, 2019, doi: 10.3389/fneur.2019.00325.
[42] E. Mikulan *et al.*, “Simultaneous human intracerebral stimulation and HD-EEG, ground-truth for source localization methods,” *Sci. Data*, vol. 7, no. 1, pp. 1–8, Dec. 2020, doi: 10.1038/s41597-020-0467-x.
[43] T. Yamada, “Somatosensory Evoked Potentials,” in *Encyclopedia of the Neurological Sciences (Second Edition)*, M. J. Aminoff and R. B. Daroff, Eds. Oxford: Academic Press, 2014, pp. 230–238. doi: 10.1016/B978-0-12-385157-4.00544-3.
[44] G. Cruccu *et al.*, “Recommendations for the clinical use of somatosensory-evoked potentials.,” *Clin. Neurophysiol. Off. J. Int. Fed. Clin. Neurophysiol.*, vol. 119, no. 8, pp. 1705–1719, Aug. 2008, doi: 10.1016/j.clinph.2008.03.016.
[45] M. J. Aminoff and A. A. Eisen, “AAEM minimonograph 19: somatosensory evoked potentials.,” *Muscle Nerve*, vol. 21, no. 3, pp. 277–290, Mar. 1998, doi: 10.1002/(sici)1097-4598(199803)21:3<277::aid-mus1>3.0.co;2-7.
[46] I. Hashimoto, K. Yoshikawa, and M. Sasaki, “Latencies of peripheral nerve and cerebral evoked responses to air-puff and electrical stimuli.,” *Muscle Nerve*, vol. 13, no. 12, pp. 1099–1104, Dec. 1990, doi: 10.1002/mus.880131203.
[47] D. Purves *et al.*, Eds., “Neuroscience, 3rd ed.,” *Neurosci. 3rd Ed*, pp. xix, 773–xix, 773, 2004.
[48] S. B. Eickhoff, A. Schleicher, K. Zilles, and K. Amunts, “The human parietal operculum. I. Cytoarchitectonic mapping of subdivisions,” *Cereb. Cortex*, vol. 16, no. 2, pp. 254–267, Feb. 2006, doi: 10.1093/cercor/bhi105.
[49] J. H. Kaas, “Evolution of somatosensory and motor cortex in primates,” Nov. 2004, vol. 281, no. 1, pp. 1148–1156. doi: 10.1002/ar.a.20120.

[50] S. Geyer, A. Schleicher, and K. Zilles, “Areas 3a, 3b, and 1 of human primary somatosensory cortex: 1. Microstructural organization and interindividual variability,” *NeuroImage*, vol. 10, no. 1, pp. 63–83, Jul. 1999, doi: 10.1006/nimg.1999.0440.

[51] S. Geyer, T. Schormann, H. Mohlberg, and K. Zilles, “Areas 3a, 3b, and 1 of human primary somatosensory cortex. 2. Spatial normalization to standard anatomical space,” *NeuroImage*, vol. 11, no. 6 I, pp. 684–696, 2000, doi: 10.1006/nimg.2000.0548.

[52] S. Geyer, A. Schleiches, and K. Zilles, “The somatosensory cortex of human: Cytoarchitecture and regional distributions of receptor-binding sites,” *NeuroImage*, vol. 6, no. 1, pp. 27–45, Jul. 1997, doi: 10.1006/nimg.1997.0271.

[53] M. Del Vecchio *et al.*, “Tonic somatosensory responses and deficits of tactile awareness converge in the parietal operculum,” *Brain*, no. awab384, Oct. 2021, doi: 10.1093/brain/awab384.

[54] P. E. Roland, L. Eriksson, L. Widén, and S. Stone‐Elander, “Changes in Regional Cerebral Oxidative Metabolism Induced by Tactile Learning and Recognition in Man,” *Eur. J. Neurosci.*, vol. 1, no. 1, pp. 3–18, 1989, doi: 10.1111/j.1460-9568.1989.tb00769.x.

[55] A. Bodegård, S. Geyer, C. Grefkes, K. Zilles, and P. E. Roland, “Hierarchical processing of tactile shape in the human brain,” *Neuron*, vol. 31, no. 2, pp. 317–328, Aug. 2001, doi: 10.1016/S0896-6273(01)00362-2.

[56] E. Disbrow, T. Roberts, and L. Krubitzer, “Somatotopic organization of cortical fields in the lateral sulcus of Homo sapiens: evidence for SII and PV.,” *J. Comp. Neurol.*, vol. 418, no. 1, pp. 1–21, Feb. 2000, doi: 10.1002/(sici)1096-9861(20000228)418:1<1::aid-cne1>3.0.co;2-p.

[57] S. B. Eickhoff *et al.*, “Anatomical and functional connectivity of cytoarchitectonic areas within the human parietal operculum,” *J. Neurosci.*, vol. 30, no. 18, pp. 6409–6421, May 2010, doi: 10.1523/JNEUROSCI.5664-09.2010.

[58] J. R. Augustine, “Circuitry and functional aspects of the insular lobe in primates including humans.,” *Brain Res. Brain Res. Rev.*, vol. 22, no. 3, pp. 229–244, Oct. 1996, doi: 10.1016/s0165-0173(96)00011-2.

[59] T. Yamada, J. Kimura, J. T. Wilkinson, and R. Kayamori, “Short- and Long-Latency Median Somatosensory Evoked Potentials: Findings in Patients With Localized Neurological Lesions,” *Arch. Neurol.*, vol. 40, no. 4, pp. 215–220, Apr. 1983, doi: 10.1001/archneur.1983.04050040045007.

[60] “Guideline 9D: Guidelines on short-latency somatosensory evoked potentials.,” *J. Clin. Neurophysiol. Off. Publ. Am. Electroencephalogr. Soc.*, vol. 23, no. 2, pp. 168–179, Apr. 2006, doi: 10.1097/00004691-200604000-00013.

[61] T. Yamada, N. R. Graff-Radford, J. Kimura, Q. S. Dickins, and H. P. Adams, “Topographic analysis of somatosensory evoked potentials in patients with well-localized thalamic infarctions,” *J. Neurol. Sci.*, vol. 68, no. 1, pp. 31–46, Apr. 1985, doi: 10.1016/0022-510X(85)90048-6.

[62] T. Allison, G. McCarthy, C. C. Wood, T. M. Darcey, D. D. Spencer, and P. D. Williamson, “Human cortical potentials evoked by stimulation of the median nerve. I. Cytoarchitectonic areas generating short-latency activity,” *J. Neurophysiol.*, vol. 62, no. 3, pp. 694–710, 1989, doi: 10.1152/jn.1989.62.3.694.

[63] T. Allison, G. McCarthy, C. C. Wood, P. D. Williamson, and D. D. Spencer, “Human cortical potentials evoked by stimulation of the median nerve. II. Cytoarchitectonic areas generating long-latency activity,” *J. Neurophysiol.*, vol. 62, no. 3, pp. 711–722, 1989, doi: 10.1152/jn.1989.62.3.711.

[64] E. J. Colon and A. W. de Weerd, “Long-latency somatosensory evoked potentials.,” *J. Clin. Neurophysiol. Off. Publ. Am. Electroencephalogr. Soc.*, vol. 3, no. 4, pp. 279–296, Oct. 1986, doi: 10.1097/00004691-198610000-00001.

[65] L. B. Hinkley, L. A. Krubitzer, S. S. Nagarajan, and E. A. Disbrow, “Sensorimotor integration in S2, PV, and parietal rostroventral areas of the human Sylvian fissure,” *J. Neurophysiol.*, vol. 97, no. 2, pp. 1288–1297, Feb. 2007, doi: 10.1152/jn.00733.2006.

[66] S. Tsuji, H. Shibasaki, M. Kato, Y. Kuroiwa, and F. Shima, “Subcortical, thalamic and cortical somatosensory evoked potentials to median nerve stimulation,” *Electroencephalogr. Clin. Neurophysiol. Evoked Potentials*, vol. 59, no. 6, pp. 465–476, 1984, doi: 10.1016/0168-5597(84)90005-4.

[67] T. Yamada, “The anatomic and physiologic bases of median nerve somatosensory evoked potentials,” *Neurol. Clin.*, vol. 6, no. 4, pp. 705–733, Nov. 1988, doi: 10.1016/s0733-8619(18)30839-9.

[68] J. J. N. Van Der Walt, J. M. Thomas, and A. A. Figaji, “Intraoperative neurophysiological monitoring for the anaesthetist: Part 1: A review of the theory and practice of intraoperative neurophysiological monitoring,” *South. Afr. J. Anaesth. Analg.*, vol. 19, no. 3, pp. 139–144, 2013, doi: 10.1080/22201173.2013.10872913.

[69] T. B. Sloan and E. J. Heyer, “Anesthesia for intraoperative neurophysiologic monitoring of the spinal cord,” *J. Clin. Neurophysiol.*, vol. 19, no. 5, pp. 430–443, 2002, doi: 10.1097/00004691-200210000-00006.

[70] P. Walsh, N. Kane, and S. Butler, “The clinical role of evoked potentials.,” *J. Neurol. Neurosurg. Psychiatry*, vol. 76 Suppl 2, no. Suppl 2, pp. ii16-22, Jun. 2005, doi: 10.1136/jnnp.2005.068130.

[71] A. Ferretti *et al.*, “Cortical brain responses during passive nonpainful median nerve stimulation at low frequencies (0.5-4 Hz): An fMRI study,” *Hum. Brain Mapp.*, vol. 28, no. 7, pp. 645–653, Jul. 2007, doi: 10.1002/hbm.20292.

[72] G. Florence, J.-M. Guerit, and B. Gueguen, “Electroencephalography (EEG) and somatosensory evoked potentials (SEP) to prevent cerebral ischaemia in the operating room,” *Neurophysiol. Clin. Neurophysiol.*, vol. 34, no. 1, pp. 17–32, Feb. 2004, doi: 10.1016/j.neucli.2004.01.001.

[73] M. R. Nuwer, E. G. Dawson, L. G. Carlson, L. E. A. Kanim, and J. E. Sherman, “Somatosensory evoked potential spinal cord monitoring reduces neurologic deficits after scoliosis surgery: results of a large multicenter survey,” *Electroencephalogr. Clin. Neurophysiol. Evoked Potentials*, vol. 96, no. 1, pp. 6–11, 1995, doi: 10.1016/0013-4694(94)00235-D.

[74] A. Ihara *et al.*, “Neuromagnetic gamma-band activity in the primary and secondary somatosensory areas.,” *Neuroreport*, vol. 14, no. 2, pp. 273–277, Feb. 2003, doi: 10.1097/00001756-200302100-00024.

[75] J. Ruben, “Somatotopic Organization of Human Secondary Somatosensory Cortex,” *Cereb. Cortex*, vol. 11, no. 5, pp. 463–473, May 2001, doi: 10.1093/cercor/11.5.463.

[76] S. Thees, F. Blankenburg, B. Taskin, G. Curio, and A. Villringer, “Dipole source localization and fMRI of simultaneously recorded data applied to somatosensory categorization,” *NeuroImage*, vol. 18, no. 3, pp. 707–719, Mar. 2003, doi: 10.1016/S1053-8119(02)00054-X.

[77] A. Korvenoja *et al.*, “Activation of ipsilateral primary sensorimotor cortex by median nerve stimulation,” *NeuroReport*, vol. 6, no. 18, pp. 2589–2593, 1995, doi: 10.1097/00001756-199512150-00033.

[78] K. Whitehead, C. Papadelis, M. P. Laudiano-Dray, J. Meek, and L. Fabrizi, “The Emergence of Hierarchical Somatosensory Processing in Late Prematurity.,” *Cereb. Cortex N. Y. N 1991*, vol. 29, no. 5, pp. 2245–2260, May 2019, doi: 10.1093/cercor/bhz030.
[79] P. Manganotti *et al.*, “Steady-state activation in somatosensory cortex after changes in stimulus rate during median nerve stimulation,” *Magn. Reson. Imaging*, vol. 27, no. 9, pp. 1175–1186, Nov. 2009, doi: 10.1016/j.mri.2009.05.009.
[80] M. Del Vecchio *et al.*, “Ipsilateral somatosensory responses in humans: the tonic activity of SII and posterior insular cortex,” *Brain Struct. Funct.*, vol. 224, no. 1, pp. 9–18, Jan. 2019, doi: 10.1007/s00429-018-1754-6.
[81] Y. Iwamura, “Somatosensory association cortices,” *Int. Congr. Ser.*, vol. 1250, no. C, pp. 3–14, Oct. 2003, doi: 10.1016/S0531-5131(03)00971-3.
[82] J. E. Desmedt, Nguyen Tran Huy, and M. Bourguet, “The cognitive P40, N60 and P100 components of somatosensory evoked potentials and the earliest electrical signs of sensory processing in man,” *Electroencephalogr. Clin. Neurophysiol.*, vol. 56, no. 4, pp. 272–282, Oct. 1983, doi: 10.1016/0013-4694(83)90252-3.
[83] O. J. Arthurs, E. J. Williams, T. A. Carpenter, J. D. Pickard, and S. J. Boniface, “Linear coupling between functional magnetic resonance imaging and evoked potential amplitude in human somatosensory cortex,” *Neuroscience*, vol. 101, no. 4, pp. 803–806, Nov. 2000, doi: 10.1016/S0306-4522(00)00511-X.
[84] A. Gramfort *et al.*, “MEG and EEG data analysis with MNE-Python,” 2013, doi: 10.3389/fnins.2013.00267.
[85] A. Gramfort *et al.*, “MNE software for processing MEG and EEG data,” *NeuroImage*, vol. 86, pp. 446–460, 2014.
[86] A. Hyvärinen and E. Oja, “Independent component analysis: Algorithms and applications,” *Neural Netw.*, vol. 13, no. 4–5, pp. 411–430, 2000, doi: 10.1016/S0893-6080(00)00026-5.
[87] M. Jas, D. A. Engemann, Y. Bekhti, F. Raimondo, and A. Gramfort, “Autoreject: Automated artifact rejection for MEG and EEG data,” *NeuroImage*, vol. 159, pp. 417–429, Oct. 2017, doi: 10.1016/j.neuroimage.2017.06.030.
[88] M. Hämäläinen and R. Ilmoniemi, “Interpreting magnetic fields of the brain: minimum-norm estimates. Med Biol Eng Comput 32: 35-42,” *Med. Biol. Eng. Comput.*, vol. 32, pp. 35–42, Feb. 1994, doi: 10.1007/BF02512476.
[89] R. D. Pascual-Marqui, C. M. Michel, and D. Lehmann, “Low resolution electromagnetic tomography: a new method for localizing electrical activity in the brain,” *Int. J. Psychophysiol.*, vol. 18, no. 1, pp. 49–65, Oct. 1994, doi: 10.1016/0167-8760(84)90014-X.
[90] R. Pascual-Marqui, “Standardized low-resolution brain electromagnetic tomography (sLORETA): technical details,” *Methods Find Exp Clin Pharmacol*, vol. 24 Suppl D, pp. 5–12, 2002.
[91] R. D. Pascual-Marqui *et al.*, “Assessing interactions in the brain with exact low-resolution electromagnetic tomography,” *Philos. Trans. R. Soc. Math. Phys. Eng. Sci.*, vol. 369, no. 1952, pp. 3768–3784, Oct. 2011, doi: 10.1098/rsta.2011.0081.
[92] A. M. Dale *et al.*, “Dynamic statistical parametric mapping: Combining fMRI and MEG for high-resolution imaging of cortical activity,” *Neuron*, vol. 26, no. 1, pp. 55–67, 2000, doi: 10.1016/S0896-6273(00)81138-1.
[93] A. M. Dale, B. Fischl, and M. I. Sereno, “Cortical Surface-Based Analysis: I. Segmentation and Surface Reconstruction,” *NeuroImage*, vol. 9, no. 2, pp. 179–194,

Feb. 1999, doi: 10.1006/nimg.1998.0395.
[94] A. Fedorov *et al.*, "3D Slicer as an image computing platform for the Quantitative Imaging Network," *Quant. Imaging Cancer*, vol. 30, no. 9, pp. 1323–1341, Nov. 2012, doi: 10.1016/j.mri.2012.05.001.
[95] M. Narizzano *et al.*, "SEEG assistant: a 3DSlicer extension to support epilepsy surgery," *BMC Bioinformatics*, vol. 18, no. 1, p. 124, Feb. 2017, doi: 10.1186/s12859-017-1545-8.
[96] B. B. Avants, N. J. Tustison, G. Song, P. A. Cook, A. Klein, and J. C. Gee, "A reproducible evaluation of ANTs similarity metric performance in brain image registration," *NeuroImage*, vol. 54, no. 3, pp. 2033–2044, Feb. 2011, doi: 10.1016/j.neuroimage.2010.09.025.
[97] J.-Y. Chang, A. Pigorini, M. Massimini, G. Tononi, L. Nobili, and B. Van Veen, "Multivariate autoregressive models with exogenous inputs for intracerebral responses to direct electrical stimulation of the human brain," *Front. Hum. Neurosci.*, vol. 6, p. 317, 2012, doi: 10.3389/fnhum.2012.00317.
[98] P. Bloomfield, *Fourier Analysis of Time Series: An Introduction*. Wiley, 2004. [Online]. Available: https://books.google.de/books?id=zQsupRg5rrAC
[99] A. de Cheveigné and I. Nelken, "Filters: When, Why, and How (Not) to Use Them," *Neuron*, vol. 102, no. 2, pp. 280–293, Apr. 2019, doi: 10.1016/j.neuron.2019.02.039.
[100] G. A. Rousselet, "Does filtering preclude us from studying ERP time-courses?," *Front. Psychol.*, vol. 3, no. MAY, 2012, doi: 10.3389/fpsyg.2012.00131.
[101] D. J. Acunzo, G. MacKenzie, and M. C. W. van Rossum, "Systematic biases in early ERP and ERF components as a result of high-pass filtering," *J. Neurosci. Methods*, vol. 209, no. 1, pp. 212–218, Jul. 2012, doi: 10.1016/j.jneumeth.2012.06.011.
[102] B. Maess, E. Schröger, and A. Widmann, "High-pass filters and baseline correction in M/EEG analysis-continued discussion," *J. Neurosci. Methods*, vol. 266, pp. 171–172, Jun. 2016, doi: 10.1016/j.jneumeth.2016.01.016.
[103] D. Tanner, J. J. S. Norton, K. Morgan-Short, and S. J. Luck, "On high-pass filter artifacts (they're real) and baseline correction (it's a good idea) in ERP/ERMF analysis," *J. Neurosci. Methods*, vol. 266, pp. 166–170, Jun. 2016, doi: 10.1016/j.jneumeth.2016.01.002.
[104] D. Tanner, K. Morgan-Short, and S. J. Luck, "How inappropriate high-pass filters can produce artifactual effects and incorrect conclusions in ERP studies of language and cognition," *Psychophysiology*, vol. 52, no. 8, pp. 997–1009, 2015, doi: 10.1111/psyp.12437.
[105] A. Widmann, E. Schröger, and B. Maess, "Digital filter design for electrophysiological data - a practical approach," *J. Neurosci. Methods*, vol. 250, pp. 34–46, Jul. 2015, doi: 10.1016/j.jneumeth.2014.08.002.
[106] I. Dowding, S. Debener, K.-R. Müller, and M. Tangermann, *On the influence of high-pass filtering on ICA-based artifact reduction in EEG-ERP*, vol. 2015. 2015. doi: 10.1109/EMBC.2015.7319296.
[107] E. M. Whitham *et al.*, "Scalp electrical recording during paralysis: Quantitative evidence that EEG frequencies above 20Hz are contaminated by EMG," *Clin. Neurophysiol.*, vol. 118, no. 8, pp. 1877–1888, Aug. 2007, doi: 10.1016/j.clinph.2007.04.027.
[108] S. Muthukumaraswamy, "High-frequency brain activity and muscle artifacts in MEG/EEG: A review and recommendations," *Front. Hum. Neurosci.*, vol. 7, p. 138,

2013, doi: 10.3389/fnhum.2013.00138.
[109] S. Makeig, T.-P. Jung, A. J. Bell, and T. J. Sejnowski, “Independent Component Analysis of Electroencephalographic Data.”
[110] G. Tamburro, D. B. Stone, and S. Comani, “Automatic Removal of Cardiac Interference (ARCI): A New Approach for EEG Data,” *Front. Neurosci.*, vol. 13, p. 441, 2019, doi: 10.3389/fnins.2019.00441.
[111] M. K. Islam, A. Rastegarnia, and Z. Yang, “Methods for artifact detection and removal from scalp EEG: A review.,” *Neurophysiol. Clin. Clin. Neurophysiol.*, vol. 46, no. 4–5, pp. 287–305, Nov. 2016, doi: 10.1016/j.neucli.2016.07.002.
[112] J. P. Marques, J. Rebola, P. Figueiredo, A. Pinto, F. Sales, and M. Castelo-Branco, “ICA decomposition of EEG signal for fMRI processing in epilepsy.,” *Hum. Brain Mapp.*, vol. 30, no. 9, pp. 2986–2996, Sep. 2009, doi: 10.1002/hbm.20723.
[113] J. F. Gao, Y. Yang, P. Lin, P. Wang, and C. X. Zheng, “Automatic removal of eye-movement and blink artifacts from eeg signals,” *Brain Topogr.*, vol. 23, no. 1, pp. 105–114, Mar. 2010, doi: 10.1007/s10548-009-0131-4.
[114] C. A. Joyce, I. F. Gorodnitsky, and M. Kutas, “Automatic removal of eye movement and blink artifacts from EEG data using blind component separation,” *Psychophysiology*, vol. 41, no. 2, pp. 313–325, Mar. 2004, doi: 10.1111/j.1469-8986.2003.00141.x.
[115] F. Perrin, J. Pernier, O. Bertrand, and J. F. Echallier, “Spherical splines for scalp potential and current density mapping,” *Electroencephalogr. Clin. Neurophysiol.*, vol. 72, no. 2, pp. 184–187, Feb. 1989, doi: 10.1016/0013-4694(89)90180-6.
[116] J. C. Mosher, P. S. Lewis, and R. M. Leahy, “Multiple dipole modeling and localization from spatio-temporal MEG data,” *IEEE Trans. Biomed. Eng.*, vol. 39, no. 6, pp. 541–557, Jun. 1992, doi: 10.1109/10.141192.
[117] S. Baillet, “Toward functional imaging of cortical electrophysiology markovian models for the source estimation of magneto/electroencephalography and experimental assessments.,” Jul. 1998.
[118] R. D. Pascual-Marqui, “Review of methods for solving the EEG inverse problem,” *Int. J. Bioelectromagn.*, vol. 1, pp. 77–90, 1999.
[119] O. Ledoit and M. Wolf, “A well-conditioned estimator for large-dimensional covariance matrices,” *J. Multivar. Anal.*, vol. 88, no. 2, pp. 365–411, Feb. 2004, doi: 10.1016/S0047-259X(03)00096-4.
[120] D. Barber, *Bayesian reasoning and machine learning*. Cambridge University Press, 2012.
[121] F. Pizzo *et al.*, “Deep brain activities can be detected with magnetoencephalography.,” *Nat. Commun.*, vol. 10, no. 1, p. 971, Feb. 2019, doi: 10.1038/s41467-019-08665-5.
[122] S. Haufe *et al.*, “On the interpretation of weight vectors of linear models in multivariate neuroimaging,” *NeuroImage*, vol. 87, pp. 96–110, Feb. 2014, doi: 10.1016/j.neuroimage.2013.10.067.
[123] S. Ray and J. H. R. Maunsell, “Different Origins of Gamma Rhythm and High-Gamma Activity in Macaque Visual Cortex,” *PLoS Biol.*, vol. 9, 2011.
[124] J. Sarvas, “Basic mathematical and electromagnetic concepts of the biomagnetic inverse problem,” *Phys. Med. Biol.*, vol. 32, no. 1, pp. 11–22, Jan. 1987, doi: 10.1088/0031-9155/32/1/004.
[125] R. H. Chowdhury, J. I. Glaser, and L. E. Miller, “Area 2 of primary somatosensory cortex encodes kinematics of the whole arm,” *eLife*, vol. 9, p. e48198, Jan. 2020, doi:

10.7554/eLife.48198.
[126] M. Jafari *et al.*, “The human primary somatosensory cortex encodes imagined movement in the absence of sensory information,” *Commun. Biol.*, vol. 3, no. 1, p. 757, Dec. 2020, doi: 10.1038/s42003-020-01484-1.
[127] M. Del Vecchio and P. Avanzini, “La Recherche du Temps Perdu: Timing in Somatosensation. Commentary: Somatosensation in the Brain: A Theoretical Re-evaluation and a New Model,” *Front. Syst. Neurosci.*, vol. 14, pp. 529–541, Nov. 2020, doi: 10.3389/fnsys.2020.597755.